Modelling nitrogen emissions from soils fertilized with dairy slurry

Rick Hao Chen Li

Dissertação para a obtenção do Grau de Mestre em

Engenharia do Ambiente

Orientadores: Professora Maria do Rosário Cameira

Professor David Fangueiro

Júri:

Presidente: Doutor António José Guerreiro de Brito, Professor Associado com Agregação do Instituto Superior de Agronomia da Universidade de Lisboa;

Vogais: Doutora Maria do Rosário da Conceição Cameira, Professora Associada do Instituto Superior de Agronomia da Universidade de Lisboa;

Doutora Cláudia Saramago de Carvalho Marques dos Santos Cordovil, Professora Auxiliar do Instituto Superior de Agronomia da Universidade de Lisboa.

2016

Acknowledgments

Foremost, I want to express my sincere gratitude towards my advisors' support and guidance throughout my Master's thesis, Professor Maria do Rosário Cameira for her patience, motivation and enthusiasm. Modelling can be difficult, and most likely this would not have been possible if not by the continuous encouragement and many hours devoted to the model. Professor David Fangueiro for his patience, motivation and enthusiasm, and for providing field data necessary for this work. To reiterate, I am genuinely thankful for my advisors' help.

I would also like to thank Professor Fernanda Valente, of the Mathematics Department, for her continuous help and guidance regarding not only the statistical part used for the present study, but the thesis in general.

Finally, toward my family, friends and colleagues, I can only express my deepest gratitude for their support, friendship, encouragement and trust which all helped me go through another important phase of my professional and personal life.

Abstract

Diffuse nitrogen (N) emissions from agriculture have been increasing for the past decades constituting a major environmental problem. Instruments have been implemented during the last years such as legislations, technologies and measures to reduce emissions, but the diversity of the cropping systems allied with the complex diffuse N pathways resulted in an overall inefficiency of these instruments. As such, a holistic approach is needed, being the system modelling one important tool for that.

The Root Zone Water Quality Model was tested for a sandy soil (Haplic Arenosol) and a sandy loam soil (Haplic Cambisol), cultivated with winter oats (*Avena Sativa L.*) fertilized with dairy slurry. Field data was collected at Horto de Química Agrícola of the Instituto Superior de Agronomia in Lisbon, consisting of soil water, temperatures and drainage from 2014 to 2016. Data from previous studies (2012 to 2014) relative to nitrate leaching and N_2O emissions was also used. The model was then used for scenario analysis.

For the winter oats in the sandy soil, the model predicted soil water and drainage with efficiencies of 86 and 94 % respectively, while for nitrate fluxes below the root zone and the N_2O emissions to the atmosphere efficiency was 89 and 93% respectively. For the sandy loam system, the calibrated model yielded efficiencies of 87, 94, 62, 76 and 85%, for the control variables. Scenario analysis showed the occurrence of pollution swapping as the hydrologic year changed from very dry to wet, decreasing the N lost through gaseous emissions. As to the temperature scenarios results show that for this type of production systems, the most unfavourable climate change scenario was A1B1 (+4ºC) may produce an increase of 25 and 18 % in the N gas loss contributions for the sandy loam and the sandy soil respectively.

KEYWORDS: System modelling**;** RZWQM2; Diffuse pollution; N leaching; winter oats

Resumo

Emissões difusas de azoto da agricultura têm vindo a aumentar durante as últimas décadas, sendo um grande problema ambiental. Instrumento, como legislações, tecnologias e medidas de redução foram implementadas para reduzir estas emissões, contudo a grande variabilidade dos sistemas de cultura acoplado à complexidade das vias de emissão difusa do azoto tornaram estes ineficazes. Portanto uma abordagem holística é necessária, onde a modelação de sistemas integrados é uma importante ferramenta.

O Root Zone Water Quality Model foi testado para um solo arenoso (Haplic Arenosol) e um franco arenoso (Haplic Cambisol), cultivado com aveia (*Avena Sativa L.*) e fertilizado com chorume bovino. Os dados de campo foram recolhidos no Horto de Química Agrícola do Instituto Superior de Agronomia em Lisboa, como o teor de água, temperatura e drenagens de 2014 a 2016. Dados como a lixiviação de nitratos e emissão de N_2O de estudos anteriores também foram utilizados. O modelo foi utilizado para a análise de cenários.

Para o solo arenoso, o modelo previu os teores de água e drenagens com eficiências de 86 e 94% respetivamente, para os fluxos de nitratos abaixo da zona radicular e as emissões de N_2O para a atmosfera obteve-se eficiências de 89 e 93% respetivamente. No solo franco arenoso, o modelo calibrado devolveu eficiências de 87, 94, 62, 76 e 85% para as variáveis de controlo. A análise de cenários mostrou a ocorrência de *pollution swapping* à medida que o ano hidrológico mudou do muito seco para o húmido, com diminuição do azoto perdido através de emissões gasosas. Resultados dos cenários de temperatura revelam que para este sistema de produção, o cenário de alterações climáticas mais desfavorável é o A1F1 (+4ºC), onde se verificou um aumento de 25 e 18% na contribuição das perdas gasosas de azoto para os solos franco arenoso e arenoso, respetivamente.

PALAVRAS-CHAVES: Modelação de sistemas; RZWQM2; Poluição difusa; Lixiviação de azoto; Aveia

Resumo alargado

O azoto é um elemento que é essencial para a vida no planeta Terra, estando presente na constituição das proteínas, e ao mesmo tempo o mais comum no planeta. Embora a vasta maioria do azoto na Terra esteja "armazenado" na atmosfera na forma de gás (N_2), que é uma forma não diretamente assimilável pelas plantas, também se pode encontrar azoto no solo, sedimentos e rochas em formas orgânicas ou inorgânicas, pelo que é o nutriente que mais limita o crescimento vegetal.

Com a intensificação da produção de alimento desde o século XX até a atualidade, em resposta ao crescimento exponencial da população mundial durante o mesmo período, resultou numa intensificação da agricultura, e consequentemente num aumento da produção e utilização de água e fertilizantes a nível global. Este aumento levou a vários problemas ambientais, como a emissão de gases com efeito de estufa, contaminação dos corpos de água com nitratos e nitritos, e outros impactes negativos, em várias regiões do planeta, incluindo na Europa. Atualmente a agricultura é a principal atividade humana responsável poluição ambiental devido às emissões difusas do azoto.

Entretanto, vários instrumentos legais, tecnologias e medidas com o intuito de diminuir as emissões de azoto foram aplicadas e implementadas, mas dado à grande variedade dos sistemas de cultura que em conjunção com a complexidade das vias de emissões difusas do azoto deram origem a medidas reguladoras pouco eficazes para os diferentes tipos de sistemas de produção. Adicionalmente, vários estudos frisam o risco de ocorrer *"pollution swapping"* entre as várias vias de emissão do azoto, como por exemplo entre a lixiviação de nitratos e a emissão de amoníaco. Para se conseguir estudar as emissões difusas do azoto no sistema cultura-solo, é necessário uma abordagem holística desta problemática, incluindo a dinâmica do azoto e as práticas de gestão do azoto nos sistemas integrados cultura-solo-atmosfera.

Uma das ferramentas ideais para seguir este tipo de abordagem é a modelação dos sistemas integrados, onde o modelo consegue conciliar as interações entre os diferentes componentes de um sistema agrícola, pelo que os diferentes processos de transformação e transporte do N que ocorrem nos diversos compartimentos dos sistemas são considerados e relacionados com o regime hídrico do solo. O que foi efetuado no presente trabalho, através da utilização e avaliação do modelo RZWQM2.

O presente trabalho tem como principal objetivo modelar as emissões de azoto a partir de um sistema agrícola com a cultura de aveia, fertilizado com chorume bovino, calibrando e validando o modelo para um solo arenoso e solo franco arenoso com aplicação de chorume bruto com incorporação, assim como fazer uma comparação entre os dois solos, no que

concerne às respetivas emissões de nitrato e amoníaco, relacionando as diferenças com os respetivos regimes hídricos e temperaturas. Após finalizada a calibração e validação do modelo, e com este a simular os diversos processos relacionados com a água e azoto nos diversos compartimentos, com a precisão pretendida, utilizou-se o modelo para estimar os balanços de água e azoto, bem como as perdas de azoto para diferentes cenários relacionados com os anos hidrológicos e as alterações climáticas. Também foi efetuada uma simulação para se estimar os fluxos de nitratos lixiviados resultantes dos solos com aplicação de chorume de cinco tratamentos diferentes, com base nas drenagens simuladas e as concentrações medidas de nitratos na solução do solo, tendo sido efetuado a uma análise de variância dos resultados.

Foram instalados cinco lisímetros para cada tipo de solo (arenoso e franco arenoso), um para cada tratamento de chorume, perfazendo um total de dez lisímetros no Horto de Química Agrícola Boaventura Azevedo do Instituto Superior de Agronomia. Em cada lisímetro, colocaram-se aparelhos/equipamentos para medir os teores de água, temperatura, concentrações de nitratos e emissões de N_2O, que foram utilizados para o presente estudo. As medições das drenagens de água a 100 cm de profundidade foram efetuadas a partir de colheitas no interior de um túnel de acesso, diretamente abaixo dos lisímetros. Estas medições decorreram nas épocas húmidas de 2012 a 2016, com as emissões de azoto a serem recolhidas entre 2012 e 2014, enquanto que o teor de água, drenagem e temperatura do solo a serem coletados entre 2014-2016.

O modelo foi calibrado segundo um procedimento iterativo, em que se selecionaram alguns parâmetros sujeitos a serem alterados até o modelo conseguir resultados semelhantes aos medidos em 2014-2015, para as variáveis de controlo teor de água, drenagem, temperatura, emissões de nitratos e amoníaco. Os parâmetros escolhidos foram o teor de água a 10 kPa (capacidade de campo), a condutividade hidráulica saturada, os coeficientes relativos à partição da matéria orgânica e os parâmetros relativos às transformações do N. Sendo posteriormente validado com dados independentes de 2012-2013 2013-2014 e 2015-2016 para as mesmas variáveis.

No final do processo de modelação, o modelo mostrou-se apto a simular os diferentes processos relacionados com a água e azoto no solo com a precisão pretendida, tendo em conta os diferentes resultados para a avaliação da qualidade do modelo, como a eficiência de modelação (EF), que no geral foi elevada para as variáveis consideradas, também o erro médio quadrático (RMSE) foi determinado, com resultados razoáveis. Ambos EF e RMSE resultantes do presente trabalho estão em conformidade com os valores obtidos por outros autores. Verificou-se ainda, que a qualidade de modelação foi melhor para o solo arenoso aquando comparado com o solo franco arenoso.

O modelo foi então utilizado para simular os balanços de água e azoto para diferentes cenários relacionados com diferentes anos hidrológicos (muito seco, seco, médio e húmido) e de alterações climáticas (aumento da temperatura média em 1.8 ou 4.0 ºC).

No que toca aos cenários dos anos hidrológicos, verificou-se que em média a contribuição da precipitação para a evapotranspiração é 42% superior para o solo franco arenoso do que o solo arenoso, por outro lado a contribuição da precipitação na drenagem é 12.5% menor. Sendo que as maiores diferenças ocorrem nos cenários mais secos enquanto que nos cenários mais húmidos que estes, o aumento na quantidade de precipitação consegue "mascarar ", até certo ponto, as diferenças hidráulicas entre os dois solos.

O solo arenoso possui valores de azoto lixiviado maiores que o solo franco arenoso sendo que estes valores aumentam com o aumento da quantidade de precipitação dos quatro cenários, embora o contrário se verifique para o azoto perdido em forma de gás, constituindo um caso de *pollution swapping*. As variações dos balanços de água e azoto pelos anos hidrológicos revelam que o solo franco arenoso é mais sensível às variações de humidade dos diferentes anos hidrológicos.

Para as previsões relacionadas com as alterações climáticas, o cenário com o maior incremento na temperatura média, acréscimo de 4 ºC, provocou um aumento de 25 e 18% em perdas gasosas de azoto para o solo franco arenoso e solo arenoso, respetivamente. Neste caso, também se verifica uma situação de *pollution swapping*, com o aumento de perdas gasosas de azoto, que são compensadas pela diminuição das perdas de azoto por lixiviação.

Em relação às estimativas de fluxo de nitratos para os diferentes tratamentos de chorume, e posterior análise de variância, verificaram-se diferenças estatisticamente significativas entre tratamentos, onde estas foram maiores para o solo arenoso. Concluiu-se que as diferenças entre tratamentos aumenta com o aumento da quantidade de precipitação.

TABLE OF CONTENTS

1. Introduction 1
2. Literature review 3
   2.1 Diffuse pollution and nitrogen emissions 3
   2.2 Nitrogen pathways and processes 4
      2.2.1 The importance of soil water 4
      2.2.2 Forms and transformations of N in the soil 5
   2.3 Environmental and health impacts related to nitrogen 13
   2.4 Dairy cattle slurry 14
   2.5 Modelling of integrated systems 15
      2.5.1 RZWQM2 15
      2.5.2 Modelling process 20
   2.6 Statistical analysis of nitrate leaching fluxes 21
3. Materials and methods 22
   3.1 Field experiments 22
      3.1.1 Experimental site 22
      3.1.2 Experimental design 25
      3.1.3 Installed equipment and measurements 26
   3.2 Modelling 30
      3.2.1 Parameterization 30
      3.2.2 Calibration 36
      3.2.3 Validation 37
      3.2.4 Goodness of fit – Evaluation of the calibration and validation procedure 37
   3.3 Model application 39
      3.3.1 Prediction scenarios 39
      3.3.2 Determination of nitrate leaching and slurry treatment comparison 39
4. Results and discussion 40
   4.1 Model calibration 40
      4.1.1 Sandy soil 40
      4.1.2 Sandy loam soil 46
   4.2 Model validation 53
      4.2.1 Sandy soil 53
      4.2.2 Sandy loam soil 56
   4.3 Model applications 59
      4.3.1 Water and N balances 60
      4.3.2 Nitrate leaching fluxes 65
5. Conclusions 74

References
Appendices
1 Nitrogen cascade model
2 Nitrate flux means comparison tables for sandy and sandy loam soils

LIST OF FIGURES

Figure 2.1 – Nitrogen cycle in the crop-soil system (adapted from Cameron, 1992). 5
Figure 2.2 – Nitrification and denitrification, with both N_2O formation pathways (adapted from Koon et al., 2009). 9
Figure 2.3 – Calculation sequence utilized by RZWQM2 (adapted from Ahuja et al., 2000a). 15
Figure 2.4 – Diagram of residue and soil organic matter pools in RZWQM2 (Adapted from Cameira *et al*., 2007). 18
Figure 3.1 – Drainage lysimeters existing at Horto facilities (Adapted from Martins, 2014). (Letters designate the slurry treatments as described in 3.1.2) 22
Figure 3.2 – Lysimeters: a) top view with bare soil; b) top view with oats crop; c) access tunnel beneath the lysimeters before recuperation; d) access tunnel cleaned and in use.....23
Figure 3.3 - Monthly mean maximum and minimum temperatures and monthly precipitation during the study period, with the 30 years' average (1951-1980), collected from the meteorological station of Tapada da Ajuda. 24
Figure 3.4 - Representation of the lysimeters used for this work, with the slurry treatments and both soils. (Adapted from Martins, 2014) 25
Figure 3.5 - a) Reflectometers installed in lysimeters for the measurement of SWC; b) Lysimeter with both chambers for the measurement of NH_3 volatilization (round) and N_2O (square). 29
Figure 3.6 – General view of the installed equipment. 29
Figure 3.7 – Simple modelling procedure overview (adapted from Ma *et al*., 2012). 30
Figure 3.8 - Graphical representation of the simulation domain and boundary conditions.....31
Figure 4.1 - Hydraulic properties of the sandy soil described by the Brooks and Corey functions before (BC) and after (AC) calibration: a) Water retention; b) Saturated hydraulic conductivity. 40
Figure 4.2 - Simulated versus measured values for: a) soil water content at 25 cm and b) drainage at 100 cm. Sandy soil, 2014-2015 crop season (calibration). (FC_{10} is the soil water content at field capacity at 10 kPa.) 41

Figure 4.3 - Simulated versus measured values for the soil temperature at the depth of 25 cm. Sandy soil, 2014-2015 crop season (calibration). 42
Figure 4.4 - Simulated versus measured values of: a) NO_3^- flux at the depth of 70 cm; b) N_2O emissions at soil surface. c) Water filled pore space. Sandy soil, 2014-2015 crop season (calibration). 43
Figure 4.5 - Simulated versus measured values correlation comparison for: a) soil water content; b) drainage; c) nitrate leaching and d) N_2O flux to the atmosphere. Sandy soil, 2014-2015 (calibration).....45
Figure 4.6 - Hydraulic properties of the sandy loam soil described by the Brooks and Corey functions before (BC) and after (AC) calibration: a) Water retention; b) Saturated hydraulic conductivity. 47
Figure 4.7 - Simulated versus measured values for: a) soil water content at 20 cm and b) drainage at 100 cm. Sandy loam soil, 2014-2015 crop season (calibration). (FC10 is the soil water content at field capacity at 10 kPa.) 48
Figure 4.8 - Simulated versus measured values for the soil temperature at the depth of 25 cm. Sandy loam soil, 2014-2015 crop season (calibration). 48
Figure 4.9 - Simulated versus measured values of: a) NO_3^- flux at the depth of 70 cm; b) N_2O emissions at soil surface. c) Water filled pore space. Sandy loam soil, 2014-2015 crop season (calibration). 50
Figure 4.10 - Simulated versus measured values correlation comparison for: a) soil water content; b) drainage; c) nitrate leaching and d) N2O flux to the atmosphere. Sandy loam soil, 2014-2015 (calibration).....52
Figure 4.11 - Simulated versus measured values for: a) soil water content at 25 cm and b) drainage at 100 cm. Sandy soil, 2015-2016 crop season (validation). (FC10 is the soil water content at field capacity at 10 kPa.).....53
Figure 4.12 - Simulated versus measured values for the soil temperature at the depth of 25 cm. Sandy soil, 2015-2016 crop season (validation).....54
Figure 4.13 - Simulated versus measured values of: a) NO_3^- flux at the depth of 70 cm; b) N_2O emissions at soil surface. c) Water filled pore space. Sandy loam soil, 2012-2013 and 2013-2014 crop seasons (validation).....55
Figure 4.14 - Simulated versus measured values for: a) soil water content at 20 cm and b) drainage at 100 cm. Sandy loam soil, 2015-2016 crop season (validation). (FC10 is the soil water content at field capacity at 10 kPa). 56
Figure 4.15 - Simulated versus measured values for the soil temperature at the depth of 20 cm. Sandy loam soil, 2015-2016 crop season (validation). 57

Figure 4.16 - Simulated versus measured values of: a) NO_3^- flux at the depth of 70 cm; b) N_2O emissions at soil surface. c) Water filled pore space. Sandy loam soil, 2012-2013 and 2013-2014 crop seasons (validation). 57
Figure 4.17 - N output from crop-soil system comparison for sandy soil (top) and sandy loam soil (bottom), in the different precipitation scenarios: a) very dry; b) dry; c) medium and d) wet. 62
Figure 4.18 – N_2O and NH_3 variation for all hydrological years, in comparison with Vdy in the a) sandy soil and b) sandy loam soil (VDy – very dry; Dy – dry; M – medium; W – wet; N2O – N_2O emission losses; NH3 – NH_3 volatilization losses). 62
Figure 4.19 – Contribution of nitrification and denitrification for the total N_2O emission for: a) sandy soil and b) sandy loam soil. (VDy – very dry; Dy – dry; M – medium; W – wet; N2O Nit - N_2O resulting from nitrification process and N2O Denit - N_2O resulting from denitrification process). 63
Figure 4.20 – Variation in N_{gas} losses during the temperature scenarios. Sandy and sandy loam soils. 63
Figure 4.21 – Variation of NH_3 volatilization during the temperature scenarios, in comparison with M scenario. Sandy and sandy loam soils. 64
Figure 4.22 – Contribution of nitrification and denitrification for the total N_2O emission for: a) sandy soil and b) sandy loam soil. (N2O Nit - N_2O resulting from nitrification and N2O Denit - N_2O resulting from denitrification). 65
Figure 4.23 - N output from crop-soil system comparison for sandy soil (top) and sandy loam soil (bottom), in the different temperature scenarios: a) M; b) B1 and c) A1F1. 65
Figure 4.24 – Drainage fluxes at 70 cm depth, average for all slurry treatment in the SS. 66
Figure 4.25 - Nitrate flux means comparison between slurry treatments of the sandy soil, for the (a) 2012-2013, (b) 2013-2014 and (c) 2014-2015 crop seasons. 69
Figure 4.26 - Drainage fluxes at 70 cm depth, average for all slurry treatment in the SLS. 70
Figure 4.27 - Nitrate flux means comparison between slurry treatments of the SLS, for the (a) 2012-2013, (b) 2013-2014 and (c) 2014-2015 crop seasons. 71

LIST OF TABLES

Table 3.1 - Main soil physical properties....23
Table 3.2 - Measurement dates and equipment utilized for relevant variables....26
Table 3.3 – Temporal domain for each crop season and correspondent modelling phase....31
Table 3.4 – Model input data and respective sources....32
Table 3.5 - Parameterization of the basic soil physical properties....32
Table 3.6 - Parameterization of the Brooks and Corey hydraulic functions....33
Table 3.7 - Nitrogen nutrient efficiency factors and reaction rates parameterization....33
Table 3.8 - Plant and crop parameterization....34
Table 3.9 - Crop management events for each crop season, in both sandy and sandy loam soils....34
Table 3.10 - Dairy cattle slurry characterization....34
Table 3.11 - Thermal properties of soil constituents (after de Vries, 1963)....35
Table 3.12 - Soil water content and temperature initial conditions for each crop season....35
Table 3.13 - Selected parameters for calibration and respective control data....36
Table 3.14 - Initial residue state, microorganism and inorganic N profile after wizard and 10 year equilibration, for both soils....37
Table 4.1 - Initial and calibrated values of the selected soil hydraulic parameters. Sandy soil....40
Table 4.2- Initial and calibrated values for the OM partitioning and for N related parameters. Sandy soil, 2014-2015 crop season (calibration)....43
Table 4.3 - Goodness of fit analysis for the soil water content at 25 cm, water drainage at 100 cm depth and soil temperature at 25 cm depth, before (BC) and after (AC) model calibration. Sandy soil (2014-2015)....44
Table 4.4 - Goodness of fit analysis for NO_3^- and N_2O emissions after model calibration. Sandy soil (2014-2015)....46
Table 4.5 - Initial and calibrated values of the selected soil hydraulic parameters, for the sandy soil loam soil....46
Table 4.6 - Initial and calibrated values for the OM partitioning and for N related parameters. Sandy loam soil, 2014-2015 crop season (calibration)....49
Table 4.7 - Goodness of fit analysis for the soil water content at 25 cm, water drainage at 100 cm depth and soil temperature at 25 cm depth, before (BC) and after (AC) model calibration. Sandy loam soil (2014-2015)....51
Table 4.8 - Goodness of fit analysis for NO_3^- and N_2O emissions after calibration. Sandy loam soil (2014-2015)....52

Table 4.9 - Goodness of fit analysis for the validation of WWC at 25 cm, D at 100 cm depth and T at 25 cm (2015-2016) and the NO_3^- flux and N_2O emission flux (2012-2013 and 2013-2014). Sandy soil.....55
Table 4.10 - Goodness of fit analysis for the validation of soil water content, water drainage at 100 cm depth and temperature (2015-2016 crop season) and the NO_3^- flux and N_2O emission flux (2012-2013 and 2013-2014 crop seasons). Sandy loam soil.....58
Table 4.11 – Soil water balance for the precipitation scenarios. Sandy and sandy loam soils (04/11 to 22/04),.....60
Table 4.12 – Nitrogen balance for precipitation scenarios. Sandy and sandy loam soils, 2013-2014 crop season.....61

LIST OF ACRONYMS

A1F1	IPCC climate change scenario, increase of 4ºC in average temperature
ANOVA	Analysis of variance
AOB	Ammoniaoxidising bacteria
AWSM	Acidified whole slurry mobilization application
AWSS	Acidified whole slurry surface application
B1	IPCC climate change scenario, increase of 1.8ºC in average temperature
CAP	Common Agricultural Policy
CTR	Control
Dy	Dry
EU	European Union
FAO	Food and Agriculture Organization
IPCC	Intergovernmental Panel on Climate Change
IPPC	Integrated Pollution Prevention and Control
KW	Kruskal-Wallis
M	Medium
ND	Nitrates Directive
NEC	National Emission Ceilings
OMNI	Organic Matter/Nitrogen model
ppb	Parts per billion
RZWQM2	Root Zone Water Quality Model
SLS	Sandy loam soil
SS	Sandy soil
UK	United Kingdom
USDA	United States Department of Agriculture
UWWD	Urban Waste Water Treatment Directive
VDy	Very dry
W	Wet
WFD	Water Framework Directive
WSI	Whole slurry injection application
WSM	Whole slurry mobilization application

LIST OF SYMBOLS

Symbol	Physical variable
C/N	Carbon to nitrogen relation
CEC	Cation exchange capacity
CO_2	Carbon dioxide
K(h)	Hydraulic conductivity function
LAI	Leaf area index
LPW	Litres of pore water
N	Nitrogen
N_2	Dinitrogen gas
N_2O	Nitrous oxide
NH_3	Ammonia
NH4+	Ammonium
$N\text{-}NH_4^+$	Ammonium as nitrogen
$N\text{-}NO_3^-$	Nitrate as nitrogen
NO	Nitric oxide
NO_3^-	Nitrate
pH	Power of Hydrogen
$\theta(h)$	Water retention function

LIST OF PHYSICAL VARIABLES

Physical variables	Physical name	SI Units
A2	Pore size distribution index	dim
Aero	Aerobic heterotrophs	org g^{-1}
AET	Actual evapotranspiration	mm
Anae	Anaerobic heterotrophs	org g^{-1}
aNH4	Autotroph converting nitrified NH to autotroph biomass-N	frac
Auto	Autotrophs	org g^{-1}
BD	Bulk density	g cm^{-3}
BM	Biomass converting organic matter uptake	frac
C_0, C_1	Reflectometers calibration coefficients	dim
C1	Saturated hydraulic conductivity	cm h^{-1}
C2	Second intercept on conductivity curve	dim
Cv	Volumetric heat capacity	J mm^{-3} $^oC^{-1}$
D	Soil water drainage	mm d^{-1}
DENIT	Denitrification constant	d^{-1}
$DENIT_{OM}$	Denitrification rate converting to anaerobic organic matter decay rate	dim
EC	Electrical conductivity	µS cm-1
EF	Modelling efficiency	%
FH	Fast soil humus	µg C g^{-1}
FR	Fast residue	µg C g^{-1}
h	Soil water matrix pressure	cm
IH	Intermediate soil humus	µg C g^{-1}
Kc	Thermal conductivity	J mm^{-3} h^{-1} $^oC^{-1}$
kNH_3	NH3 volatilization constant	km d^{-1}
K_s	Saturated hydraulic conductivity	cm h^{-1}
MSD	Mean standard deviation of observations	*
n	Total number of observations	#
N2	Second exponent for conductivity curve	dim
N_2N_2O	Denitrification efficiency factor	frac
N_{fert}	Total N input from fertilization	kg ha^{-1}
N_{fert}	N input from fertilization	kg ha^{-1}
N_{gas}	N lost in the gaseous form	kg ha^{-1}
NIT	Nitrification constant	mol LPW^{-1} d^{-1}
NIT_{N2O}	N2O fraction from nitrification constant	frac
N_{leach}	N lost from drainage	kg ha^{-1}
N_{uptk}	N uptake by the plant	kg ha^{-1}
Õ	Measured mean	*
O_k	kth observed value	*
OM%	Organic matter percentage in slurry	%
OW	Amount of organic matter in the slurry	kg ha^{-1}

p	Reflectometers signal travel time	µs
P	Precipitation	mm
P_k	kth simulated value	*
R2	Coefficient of determination	frac
RMSE	Root mean square error of simulations	*
S1	Bubbling pressure	cm
S2	Bubbling pressure	cm
SD_k	Standard deviation for kth level	*
Sf_N	Final stored mineral N in the soil	kg ha^{-1}
SH	Slow soil humus	µg C g^{-1}
Si_N	Initial stored mineral N in the soil	kg ha^{-1}
$S_{N\text{-}NH4+}$	Amount of ammonium in the slurry	kg ha^{-1}
SR	Slow residue	µg C g^{-1}
SWC	Soil water content in the soil	cm^3 cm^{-3}
T	Soil temperature	ºC
T_{max}	Monthly mean maximum temperature	ºC
T_{min}	Monthly mean minimum temperature	ºC
VHC	Dry volume heat capacity	J mm^{-3} C^{-1}
WFPS	Water filled pore space	%
y_k	kth measured value	*
$\hat{y}_k$	kth predicted value	*
$\bar{y}$	Measured mean	*
ΔS_N	Variation of the mineral N stored in the soil,	kg ha^{-1}
ϕ	Porosity	cm^3 cm^{-3}
φN_2O	Nitrous oxide emissions flux	kg ha^{-1}
φNO_3^-	Nitrate leaching flux	kg ha^{-1}
θ	Soil water content in the soil	cm^3 cm^{-3}
θ_{10}	Soil water content at 10 kPa (Field capacity)	cm^3 cm^{-3}
θ_{15}	Soil water content at 33 kPa (Field capacity)	cm^3 cm^{-3}
θ_{33}	Soil water content at 1500 kPa (Wilting point)	cm^3 cm^{-3}
θr	Residual water content	cm^3 cm^{-3}
θs	Water content at saturation	cm^3 cm^{-3}

(*) The physical variables with * have the same units as the studied variables.

1. Introduction

During the 20th and 21st centuries, a large increase in food and animal feed production occurred, as a response to the increasing human population in the world, and consequent food demand. This lead to the intensification of agriculture in many regions of the globe, with the increased use of resources namely water and fertilizers over the past 50 years (Smil, 2000; 2001).

In some world regions, including Europe, the agriculture intensification led to numerous environmental problems, directly or indirectly affecting human health, such as greenhouse gases emission, water bodies' contamination with nitrates and other ecosystem vulnerabilities. (Mosier *et al*., 2004; Tedesco, 2013). Agriculture is actually seen as one of the main N pollution sources through the diffuse emission of ammonia (NH_3) and nitrous oxide (N_2O) to air and nitrate (NO_3^-) to surface and ground waters (Oenema *et al*., 2011).

The legislation, technologies and measures to reduce N emissions exist, but the diversity of the cropping systems and the complex diffuse N pathways have resulted in regulatory obligations, which are not equally efficient for different type of production system (Cameira & Mota, 2016). Also, as recent studies have highlighted (Stevens & Quinton, 2009; Agostini *et al*., 2010) there is the danger of pollution swapping between NO_3^- leaching and N_2O and NH_3 gaseous losses, which requires a holistic approach to the diffuse pollution issue, including the N dynamics and management in the soil-plant-atmosphere systems.

One important tool for the application of this integrated or holistic approach is the use of system modelling, where the interactions between the different components of an agricultural system are considered. Thus, the different N transport and transformation processes occurring at the different compartments are accounted for and related with the water regime of the soil. This constitutes the modelling approach used in the present work, through the evaluation and application of the RZWQM2 model.

The present study, which was developed under the scope of scientific Project PTDC/AGRPRO/119428/2010, had the general objective of modelling the N emissions from a winter oat crop fertilized with dairy cattle slurry. More particularly it was intended to:

- Calibrate and validate the RZWQM2 model for a sandy soil and a sandy loam soil under a whole slurry application followed by incorporation;
- Make a comparative analysis between both soils with respect to both path losses for NO_3^- leaching and N_2O emissions to the atmosphere;
- Conceptually relate the different types of losses with the soil water regimes and temperatures;

- Analyse different scenarios to predict the N losses under different hydrological years and a climatic change perspective using a 30 years' data series;
- Estimate the nitrate fluxes (φNO_3^-) under different slurry treatments using the predicted soil water and drainage and the measured nitrate concentration in the soil solution. Perform an analysis of variance to find differences between treatments' effect in the NO_3^- leaching flux.

The current work is divided in 5 chapters. In chapter 2, the literature review, the relevance of the study is justified and the theoretical bases needed to understand the results are presented. Chapter 3 describes the materials and methods used for data collection and treatment and the methodology for the modelling procedure. Chapter 4 presents the results obtained for model calibration and validation as well as the ones relative to scenario analysis under a climatic change perspective. The results of the variance analysis applied to the nitrate leaching for the different slurry treatments are also presented. Finally, Chapter 5 summarizes the main conclusions of the present work and presents some consideration about the future perspectives for further studying this subject.

The collection of climate related variables was done, in the Meteorological Station of Tapada da Ajuda, and the sampling of NO_3^- concentration in the soil solution and N_2O emissions during the autumn/winter seasons from 2012 to 2014) were not performed by the author of the present work, as they were done by colleagues. The soil water content (SWC) and soil temperature (T) measurements as well as the water drainage (D) collection under the lysimeters were performed by the author during the autumn/winter season of 2015-2016, as well as all of the modelling work.

2. Literature review

This chapter presents the theoretical aspects necessary for the understanding the type of problem studied in this work and the information necessary to interpret the results.

2.1 Diffuse pollution and nitrogen emissions

Diffuse or non-point source pollution refers to both water and air pollution caused by a variety of activities that have no specific point of discharge. In addition, the long-range transport ability and multiple sources of the pollutant contribute to the diffuse nature of the process. The management of diffuse pollution is complex and requires the careful analysis and understanding of various processes (WMO, 2013).

Agriculture is one of the main N diffuse pollution sources. N loss through gaseous emissions, primarily in dinitrogen gas (N_2), N_2O and NH_3, is one of the most significant loss of N from the crop-soil system (Chen *et al*., 2014). N_2O not only contributes to climate change, it has a large radioactive-forcing potential with long-term warming potential 298 times greater than carbon dioxide (CO_2), but it also induces the depletion of the ozone layer (Cameron *et al*., 2013). Approximately 62% of total global N_2O emissions are attributed to agricultural soils and non-agricultural land (Thomson *et al*., 2012).

There are several sources of N_2O emissions from agricultural soils, e.g. the application of synthetic fertilizers, manure/slurry and other organic fertilizers, biological fixation by the crops and the mineralization of crop residues. Following a methodology revision (Moisier *et al*., 1998), by request of OECD/IPCC/IEA three types of emissions are considered: (i) direct emissions; (ii) emissions from animal production; and (iii) indirect emissions (Mosier *et al*., 1998). However, only direct and indirect emissions of N_2O are within scope of the present study.

Direct emissions include those where N_2O is emitted directly into the atmosphere from the soils, with agriculture appearing as a major contributor, mostly through biogenic production of N_2O, i.e. nitrification and denitrification processes (IPCC, 1995a; Bouwman *et al*., 1995; Parton *et al*., 1996).

Indirect emissions are due to: (a) the transport process that N suffer, from the soil-plant system into ground and surface waters through deep drainage and surface runoff; or (b) emissions as NH_3 or nitrogen oxides (NO_x) posteriorly suffering deposition elsewhere, inducing N_2O production (Smith *et al*., 1997).

2.2 Nitrogen pathways and processes

To choose the mitigation practice more suitable for each production system it is necessary first to identify the main path for the N losses (e.g. leaching or gas loss) for that system as well as the most important N transformations (e.g. nitrification, denitrification, volatilization).

2.2.1 The importance of soil water

2.2.1.1 Soil water and the N losses

Most of the cases of N loss from farming practices are caused by its transport with excess of water over and/or through the agricultural soil (Carpenter, 2008). This physical process is called convective transport or N leaching). On the other hand, the soil moisture will influence the biological and chemical reactions that determine the N form present in the soil and consequently the N available for the plant (see section 2.2.2).

As such, controlling the water flow from the agricultural field to the surface and ground waters is one of the most important practices to reduce N loss and pollution. The influence of soil moisture in the N related processes and transport is within the scope of the present study and shall be further discussed below.

The soil physical properties (such as bulk density, porosity, soil texture), the soil hydraulic properties consisting in the soil water retention curve and the soil hydraulic conductivity curve, and the basic chemical properties (e.g. pH, and organic matter (OM) content) are important to understand a given N-related process. In fact, both the water transport flux and soil water content (SWC) depend heavily in the soil hydraulic/hydrodynamic and, to some extent in the chemical properties. Only knowing these soil properties that it is possible to assess/evaluate and predict the N impact in the environment, devising a suitable mitigation measure.

2.2.1.2 Soil water balance

In order to determine the amount of water (W) in the soil at any given moment of time and to minimize the excess of drainage, the following water balance equation is used:

$$W = \Delta S + Irr + P - AET - D - Ro \quad [2.1]$$

where ΔS is the variation of stored water in the soil (initial-final), P is the precipitation, Irr is irrigation, AET is the actual evapotranspiration, D is the drainage, Ro is runoff. All terms are in mm. Both P and Irr are water input terms, while D, AET and RO are water outputs/ from the soil. D it is the most important N loss pathway (N leaching) especially for the rainy seasons as it is not possible to control precipitation. For the spring/summer seasons, if irrigation is well designed and managed, N leaching can be minimized. D occurs when the stored water in the

soil is higher than the field capacity, yielding higher values for coarser soils and lower for finer texture soils.

2.2.2 Forms and transformations of N in the soil

N is subject to process of many natures in the crop-soil system, related to storage, transformations and transport. As a result, N can be found in many forms in the soil, being the four major forms: (i) organic matter (OM), as plant material, fungi and humus; (ii) soil organisms and microorganisms; (iii) ammonium ions (NH_4^+) adsorbed to clay minerals and OM and; (iv) mineral N forms in the soil solution, including NH_4^+, NO_3^- and nitrite (NO_2^-) in low concentrations. All the transformations and forms of N in an agricultural system are illustrated in Figure 2.1. The preferred forms of nitrogen for plant absorption are NH_4^+ and NO_3^- (Cameron *et al*., 2013). While the atmosphere is the largest reservoir of N (Schlesinger, 1991), most of this N is in the molecular form (N_2), which is not directly available to most plants. Over 90% of the N in most soils is in organic form (Stevenson, 1982).

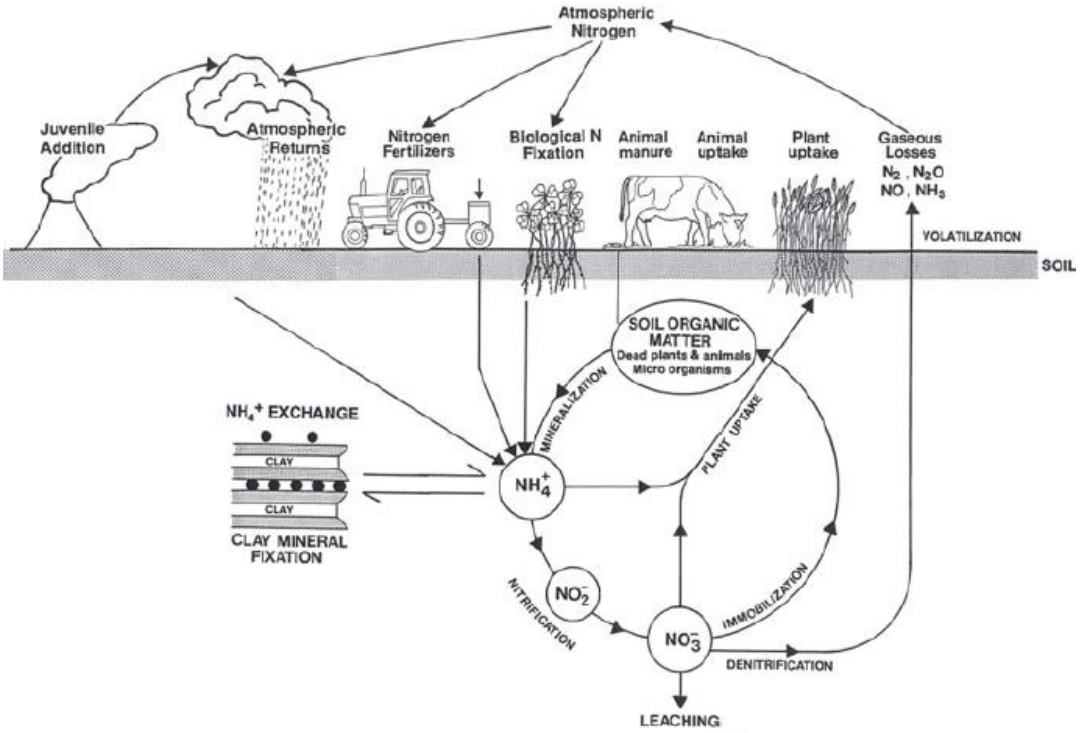

Figure 2.1 – Nitrogen cycle in the crop-soil system (adapted from Cameron, 1992).

2.2.2.1 Nitrogen fixation

Fixation is the conversion of molecular N, present in the atmosphere, into biologically available forms (Boyer *et al*., 2002), that may be incorporated in organic materials by specific microorganisms (Nicolardot *et al*., 1997). Biologically, this conversion is conducted by aerobic or anaerobic microorganisms. The most relevant factors affecting this process are:

Soil moisture: The microorganism primarily responsible for this process (cyanobacteria) are only physiologically active when wet (Nash, 1996). Soil water is necessary for C fixation by the cyanobacteria, because N fixation depends upon products of photosynthesis, which by turn requires water (Belnap, 2001).

Soil temperature: N fixation is also controlled by soil temperature, with most soil cyanobacteria being capable of N fixation between -5 and 30 ºC, whereas optimum temperature for this activity ranges from 20 to 30 ºC. Out of this range the N fixation rate rapidly declines (Belnap, 2001).

pH: Microorganism growth and N fixation in soil is increased at pH 7 or above (Dubois & Kapustka, 1983). However, some decline in the microbial activity has been found at pH 8-10 (Granhall, 1973).

Other: High concentration of aluminium (Al) and/or manganese (Mn) in the soil inhibit the activity of N fixing bacteria (Carranca, 2000).

2.2.2.2 N mineralization

According to Crohn (2004), mineralization consists in the conversion or degradation of the organic N into mineral N forms, performed by the microorganisms that need of the organic N as energy source. It is a two-step process, with the initial step known as aminization, which consists of the decomposition of complex proteins/nitrogenous contained in the organic substances, present in the soil, into simpler material like amino acids, amines and amides, alongside CO_2 and energy:

$$\text{Organic matter} \longrightarrow RNH_2 + CO_2 + \text{Energy} \qquad [2.2]$$

where RNH_2 are the amines and amino acids, and CO_2 is carbon dioxide

The resulting amino groups may be used by the microorganisms in the soil to form their own structure or further converted in simpler compounds of NH_3, which is the end-product alongside energy and sometimes CO_2, of the second-phase of this process, ammonification:

$$\text{RNH}_2 + \text{H}_2\text{O} \longrightarrow \text{ROH} + \text{Energy} \qquad [2.3]$$

where ROH is an alcohol functional group.

Based on Scheppers & Mosier (1991) rule of thumb to estimate the annual N mineralization is to consider that it should be around 20 kg ha^{-1} $year^{-1}$ per each 1% of soil endogenous OM, for the top 30 cm. Mineralization depends of environmental factors affecting microbial growth and activity:

Moisture: Based on Killham *et al*., (1993), water availability in the soil not only seems to have a positive effect on microbial growth and nutrition, but it also increases the ability of a microorganism to reach the substrate, consequently increasing N mineralization rate. Meanwhile low soil moisture induces negative effects in the N mineralization rate, due to increasing osmotic pressure, which in turn increases the energy required for osmoregulation of the microorganisms (Harris, 1981). The optimum range of moisture for mineralization is between field capacity and 40% of field capacity (Campbell & Biederbeck 1982).

Temperature: Increases in this state variable have a positive effect in the N mineralization rate (Zak *et al*., 1999), being the optimum range of temperature between 25 and 35 ºC (Honeycutt and Metcalf, 1994).

pH: The optimal pH for soil biomass growth has been established near neutrality, with mineralization being restricted at low pH levels (Appel & Mengel, 1990).

Salinity: A high salt content in the soil solution has been reported as having a negative effect in biomass growth, and consequently in N mineralization (Laura, 1977), which is related to the required osmoregulation of the microbial tissues in these conditions.

C/N relation: According to Tisdale *et al*. (1985), the C/N relation of any substance applied to the soil will affect the mineralization rate. If C/N is between 20:1 and 30:1, the mineral N will be released at an equilibrated rate, in relation to plant uptake rate. Above 30:1, more immobilization is verified during the initial stages of the decomposition process due to the lack of mineral N in the substance; Below 20:1 the release rate of mineral N from the substance is too fast and the loss potential increases (Bengtsson, 2003).

2.2.2.3 Fertilization

Different forms of N can be added into the soil, directly and indirectly, through fertilization and/or soil melioration applications. In the case of fertilization, where the applied substance supplies relevant nutrients directly to the plant, the majority of N-based fertilisers derive from NH_3, which is synthetized with the widely used industrial N fixation process of Haber-Bosch, where N_2 is fixed chemically, at high temperature and pressure, producing NH_3. Whereas the soil improvers, that indirectly help the plant growth by enhancing the soil quality, which indirectly helps the plant growth, are generally organic materials, such as animal manures and green composts.

2.2.2.4 Plant uptake

The preferred N forms for plant uptake are NH_4^+ and NO_3^-, while NO_2^- and other simple organic compounds may be absorbed too, but only in small quantities (Nacry *et al*., 2013). Generally,

plants absorb NO_3^- predominantly, as in well aerated and neutral pH soils, this is the N form present in highest concentrations (Tisdale *et al*., 1985).

2.2.2.5 N volatilization

This process, involving physical, chemical and biological factors, consist in the loss of N from the soil-crop system through the surface layer in the form of NH_3, which results from the accumulation of N-NH_4^+ in soils with high soil moisture.

$$NH_4^+ + OH \longleftrightarrow NH_3 + H_2O \quad [2.4]$$

This process is influenced by the following factors:

Temperature: NH_3 volatilization increases with temperature, as observed by Ball & Keeney (1979), with the optimum range being from 25-30 ºC (Sommer *et al*., 1991). Nonetheless, a few studies have shown that the amount of N lost via volatilization may not be different at low versus high temperature, since volatilization may continue for longer at low temperatures (e.g. Harper *et al*., 1987). Nonetheless, the initial volatilization is slow for temperatures below 15ºC (Sommer *et al*., 1991).

pH: Higher pH tend to lose more NH_3 gas (Sommer *et al*. 2004), though neutral or acid pH soils may also loose significant amounts when urea or animal urine are applied (Black *et al*., 1985a,b), i.e. higher pH promote NH_3 volatilization.

$NH4^+$ concentration: Generally, a high concentration of NH_4^+ in the soil solution induces a high potential emission rate of NH_3 gas. Therefore, the application of N fertilizers in this form and animal dejects (slurry and/or urine) can significantly enhance the NH_3 emission rate. The NH_4^+ concentration in the soil depends of several factors like nitrification rate, plant uptake rate, denitrification rate and immobilization rate, all of which reduce the NH_4^+ concentration (Cameron *et al*., 2013).

Moisture: Soil moisture influences the concentration of NH_3/ NH_4^+ in the soil solution, with low values inducing higher concentrations and thus promoting higher NH_3 volatilization (Cameron *et al*., 2013). Nonetheless, Al-Kanani *et al*. (1991) found that at very low SWC, the rate of NH_3 emission will be slow. In situations where there is a significant input of water through rainfall or irrigation the NH_3 volatilization can be reduced, because the water transports the N far from the soil surface where the concentration of NH_4^+ is kept low (Black *et al*., 1987).

Other: The mechanism of soil cation exchange (CEC) helps in storing NH_4^+ in the soil thus, concentration in the soil solution. Additionally, CEC helps to buffer against pH changes, i.e. it high CEC implies lower NH_3 volatilization potential and low CEC implies higher potential (Cameron *et al*., 2013).

The potential risk of ammonia volatilization from urea fertiliser can represent between 0% and 65% of the N applied, depending on soil and climatic conditions (Bishop & Manning, 2010). Whereas, the greatest risk of NH_3 volatilization occur with the use of ammonium bicarbonate, urea and ammonium hydroxide based fertilizers (Whitehead & Rastrick, 1990). Volatilization losses from poultry manure and dairy slurry was found to be 9-20 % and 14-35% of total N applied respectively (Miola *et al*. 2014; Sadeghpour *et al*. 2015).

2.2.2.6 Nitrification

According to Mosier *et al*. (1998) nitrification consists of the aerobic microbial oxidation of NH_4^+ into NO_3^-, via NH_2OH (hydroxylamine), as shown below:

$$NH_4^+ \longrightarrow NH_2OH \longrightarrow NO_2^- \longrightarrow NO_3^- \qquad [2.5]$$

This process may be divided in 2 phases, conducted by the activity of two different autotrophic bacteria. Firstly, the oxidation of NH_4^+ to NO_2^- is due to soil ammonia-oxidising bacteria (AOB), such as *Nitrosospira* and *Nitrosomonas* (Prosser, 2007). The second phase, the oxidation of NO_2^- to NO_3^- is conducted by *Nitrobacter*, characterized as occurring very rapidly which makes NO_2^- accumulation in the soil somewhat rare. The nitrification process described above is detailed in Figure 2.2, showing that the oxidation of NH_4^+ can also produce N_2O (Cameron *et al*., 2013):

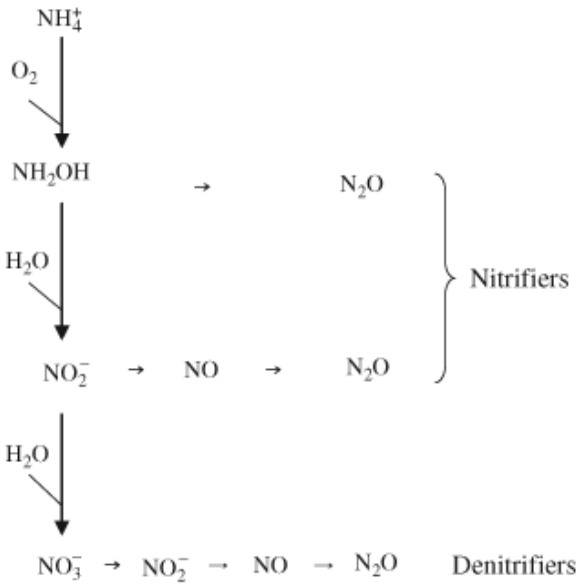

Figure 2.2 – Nitrification and denitrification, with both N_2O formation pathways (adapted from Koon et al., 2009).

The production of N_2O from NH_4^+ and NH_2OH, an intermediary compound, is possible thanks to the activity of AOB, such as *Nitrosospira* and *Nitrosomonas* (Zaman *et al*., 2009). The main factors that affect the nitrification process in the soil are:

Temperature: Nitrification intensifies as temperature increases, with the optimum soil temperature for nitrifying bacteria being between 25 and 30ºC (Haynes *et al*., 1986). Nonetheless, nitrification still occurs at temperatures below 5ºC, but the rates is significantly slower than at higher temperatures (Cameron *et al*., 2013).

pH: The bacteria responsible for this process normally operate at pH ranges from 5.5-8, with the optimum soil pH range being from 4.5 to 7.5 (Haynes *et al*., 1986).

Moisture and aeration: As the soil gets wetter, i.e. more prone to anaerobic conditions, nitrification rate decreases, as these microorganisms are typically aerobic. Nitrification rate is also significantly slower when the soil is dry, although it still can occur at wilting point (-1500 kPa) (Monaghan & Barraclough, 1992).

The maximum nitrification rate occurs around soil moisture content at field capacity (-10 kPa) (Haynes *et al*., 1986).

Ammonium concentration: As shown in the reaction equation [2.5], the whole process of nitrification is dependent of the NH_4^+ available in the soil, however high concentration of NH_4^+/ NH_3 can restrict the activity of *Nictrobacter* (Monaghan & Barraclough, 1992).

2.2.2.7 Denitrification

Denitrification is a reductive process, which mainly occurs in poorly drained soils where there are anaerobic soil conditions, low oxygen availability and low redox conditions (Dobbie & Smith, 2001; Bateman & Baggs, 2005). This permits facultative anaerobic bacteria to use NO_3^-, instead of O_2, as the final electron acceptor during respiration with NO_3^- being reduced, producing NO_2^-, nitric oxide (NO), N_2O and finally N_2, which can escape from microbial cells to the soil atmosphere (Cameron *et al*., 2013), reaction that is shown below:

$$NO_3^- \longrightarrow NO_2^- \longrightarrow NO \longrightarrow N_2O \longrightarrow N_2 \qquad [2.6]$$

The main factors that affect denitrification are:

Temperature: Ryden (1986) and Dobbie & Smith (2001) show that the denitrification rate increases with temperature. For example, the denitrification rate increased by 10-times in a grassland when the temperature increased from 10ºC to 20ºC (de Klein & van Logtestijn, 1996).

pH: Haynes & Sherlock (1986) states that acid soils with pH lower than 5.0 have lower denitrification rates than agricultural soils with a typical pH around 6.0, taking into account that the N_2O/N_2+N_2O ratio increases with acidity (Thomson *et al*., 2012).

Moisture and aeration: The soil moisture content has a big influence in the denitrification rate. When soil moisture content is greater than field capacity, a significant increase in the potential denitrification is verified (Moisier *et al*., 1986). A high soil moisture is associated with anaerobic

conditions, meaning that there is a larger water filled pore space (WFPS), with denitrification greatly increasing as WFPS increases (Rabot *et al*., 2015). More specifically, once WFPS exceeds 0.6 (60%) of the soil pore space, denitrification starts to intensify rapidly (Dobbie *et al*. 1999).

Nitrate and ammonium availability: The availability of N (NH_4^+ and NO_3^-) in the soil has a big influence upon the denitrification rate, with emissions generally increasing due to increases in mineral N in the soil (Saggar *et al*., 2009). It is worth noting that the anthropologic input of N, through N fertilizer and animal excreta application, often increases the availability of mineral-N in the soil, which can induce very large denitrification rates in the appropriate conditions (de Klein et al., 2001).

Carbon in the soil: Increases in the amount of readily available organic C, from the application of organic waste or animal manure, stimulates the denitrification process (Di & Cameron, 2003), since it is widely established that there is a strong relationship between readily available organic C in the soil and the denitrification rate (Burford & Bremner, 1975).

2.2.2.8 N Leaching

Leaching is the process through which N is lost from the soil root zone to ground and surface waters. It can be described by a combination of three physical processes: convection, diffusion and hydrodynamic dispersion (Hillel, 1998). The convective transport occurs due to the mass flow of water through the soil during drainage events after precipitation and/or irrigation (Cameira & Mota, 2016). It is calculated by modified form of Darcy's law.

$$\varphi NO_3^- = D\, C_{NO3} = -C_{NO3}\left(K\frac{dH}{dx}\right) \qquad [2.7]$$

where φNO_3^- is the convective NO_3^- flux, C_{NO3} is the N-NO_3^- concentration, D is the water flux or drainage, K is the hydraulic conductivity and dH/dx is the hydraulic gradient.

This implies uniform displacement of the band of NO_3^-, which in reality, the band of NO_3^- tends to spread throughout the profile because of the processes of diffusion and hydrodynamic dispersion. The diffusive transport results from a concentration gradient between the band of NO_3^- and the surrounding soil, there is a diffusive flux of NO_3^- from the band of NO_3^- into the surrounding soil, described by Fick's law.

$$J_d = -D_S\frac{dc}{dx} \qquad [2.8]$$

where J_d is the rate of diffusion, D_S is the diffusion coefficient of the NO_3^- in the soil which depends on the soil moisture content and dc/dx is the NO_3^- concentration gradient.

Hydrodynamic dispersion is due to (a) non-uniformity of the flow velocity within a single pore; (b) large variations in pore size in the soil, which causes a range of pore water velocities and (c) the 'tortuosity' of soil pores produces a range of flow path lengths. Thus, combining the three mechanisms, φNO_3^-, is given by the convection-dispersion equation, which is used by the process based mathematical models that simulate the leaching process:

$$\frac{\partial c}{\partial t} = -D_a \frac{\partial^2 c}{\partial x^2} - U \frac{\partial c}{\partial x} \qquad [2.9]$$

where D_a is the apparent diffusion coefficient which represents the sum of molecular diffusion and hydrodynamic dispersion.

The form of N most susceptible to leaching is the NO_3^-, since as it is negatively charge it will not be retained in the CEC. On the other hand it is very soluble in water and is the mineral form found in higher concentrations in the soil (Countinho-Mendes, 1989). The NO_3^- in the soil is produced by the nitrification process. The amount of leached NO_3^- depends on one hand upon the concentration of NO_3^- in the soil (which in turn, strongly depends on the amount of applied N, the nitrification and denitrification rates), and on the other hand it depends upon the amount of drainage that occurs through the soil which will carry the NO_3^- (convective transport). Nonetheless, there are other soil factors that also affect NO_3^- leaching and are far more difficult to describe mathematically because of their transient nature and complexity:

Climate: N losses through NO_3^- leaching are usually higher in late-autumn, winter and early-spring months, when plant uptake of N is low because of cooler conditions and drainage is high due to rainfall inputs exceeding evapotranspiration demands (Wild & Cameron, 1980). Whereas a dry summer may result in an accumulation of NO_3^- in the soil since no drainage occurred, this NO_3^- can be leached over the upcoming winter. Furthermore, the rewetting of the soil after a dry summer can cause a big and sudden increase in mineralization and thus originating more N leaching (Scholefield *et al*., 1993).

Soil properties: Soil texture and structure affects N losses through leaching, as it influences the water movement in the soil. NO_3^- leaching is generally greater in more poorly structured sandy soils than from clay soils, alongside a greater denitrification potential in clay soils. Macrospores created by the living beings in the soil or the wetting and drying cycles, induce a quicker leaching of NO_3^- through the soil profile (Cameron *et al*., 2013).

Others: Irrigation during summer does not generally cause leaching, unless excessive amounts of water are applied causing drainage events. This is because irrigation increases plant growth, and consequently plant N uptake, reducing the potential for NO_3^- leaching losses (Cameron *et al*., 2013). Concerning fertilization, the amount of application, date of application,

and frequency/rate of application have a large influence in the NO_3^- leaching, after fertilization application. The same factors are verified in the organic manures and waste application, with the addition of manure type. The efficiency of fertilization is an important factor to consider when dealing with NO_3^- leaching, as it will dictate the amount of available N that is not recovered by crops, to be lost through leaching, and other process. Jenkinson (2001) found that when N fertiliser is applied at rates that match cereal plant demand, there is no residual mineral fertiliser-N left in the soil at harvest.

2.2.2.9 N budget in the soil

In order to determine the amount of mineral-N in the soil at any time, Wild & Cameron (1980) and Di & Cameron (2002*a)* recommend the following N balance equation based on the N cycle:

$$N = N_p + N_b + N_{fert} + N_{min} - N_{uptk} - N_{gas} - N_{leach} - N_i - N_e \qquad [2.10]$$

where p is the N provided by precipitation and dry deposition, b is biological fixation, fert is fertilizer more urine and dung/slurry, min is mineralization, uptk is plant uptake, gas is gaseous losses, I is immobilization, leach is leaching loss and e is erosion and surface runoff.

2.3 Environmental and health impacts related to nitrogen

Inputs of N in the soil causes a “cascading” effect and a broad range of changes, which have effect/impacts on humans and ecosystems in many ways all over the world (Galloway & Cowling, 2002). Adapting the “cascade model” in Appendix 1, it illustrates the multiple effects N has in the environment, alongside the complexity in reducing one emission pathway without considering the total N supply (Erisman *et al*., 2005).

The most common impacts associated to agriculture are related with the contamination of surface and ground waters with NO_3^-, and atmospheric air with NH_3 and greenhouse gases. These losses of N in the soil have a negative impact on the environment, and consequently on humans. The potential negative impacts are: drinking water contamination, acidification and eutrophication of natural ecosystems, soil fertility reduction, and ozone layer depletion (Cameron *et al*., 2013).

Acidification consists of the alteration/reduction of the pH of a natural ecosystem, and consequent yielding acid reaction pH, is generally caused by NH_3 volatilization, with agriculture accounting about 50% of all the worldwide volatized NH_3 (Sommer *et al*., 2004).

NO_3^- leaching is also responsible for the drinking water supplies contamination, originating complications related to pregnancy, concretely methaemoglobinaemia in babies, where affected infants develop a peculiar blue-grey skin colour which can progress rapidly into causing coma and death, if not diagnosed and treated appropriately (Knobeloch *et al*., 2000);

high concentrations of NO_3^- in drinking water have also been linked to cancer and heart diseases by Grizzetti *et al*. (2011), whom estimated that 50 % of European population live in areas where N_2O concentration exceeded 5.6 mg $N\text{-}NO_3^-$ L^{-1} and roughly 20% in areas where it exceeds the recommended level of 11.3 mg $N\text{-}NO_3^-$ L^{-1}, varying between countries.

Eutrophication is caused by the excessive presence of macronutrients (N and P) in surface waters. They can be derived from leaching and surface runoff, and/or indirectly from the volatized NH_3 that is posteriorly deposited, in water bodies which may result in algae blooms and loss of fish (Smith & Schindler, 2009).

Concerning the depletion of the ozone layer caused by N gas emissions, primarily N_2 and N_2O, additionally the emissions of N_2O gas also contribute to climate change, due to the denitrification process, even though these emissions already are a significant loss of N from the soil. The concentration of N_20 increased in about 18.5%, from the preindustrial period to the present times, that is, from 270 parts per billion (ppb) to roughly 320 ppb (IPCC, 2007). Approximately 62% of total global N_2O emissions are due to emissions from agricultural soils (4.2 Tg N $year^{-1}$) and non-agricultural land (6 Tg N $year^{-1}$) (Thomson *et al*., 2012).

2.4 Dairy cattle slurry

The increase and intensification of livestock farming in the recent years, originated a large animal density, i.e. larger number of animal heads per farm, consequently a large increase in animal excreta production, including slurry (Rocha, 2007). Slurry production is associated with intensive cattle farm, often being dairy cattle (Cordovil, 2004). Slurry is a mix of animal dejects (faeces and urine) with water that was utilized to it, which may contain animal food and/or bedding (Portaria nº 631/2009 de 9 de Junho do Ministério do Ambiente, 2009).

As this type of effluent generally has high amounts of organic matter and nutrients, especially N, phosphorus and potassium (Bakhsh *et al*., 2005), it can become a potential pollutant or a reutilized waste, depending of its management during storage ad field application supplying OM and nutrients to the crop-soil system, where it may reduce the dependence on artificial fertilizers (Amaro *et al*., 2006).

Nonetheless, the effect of slurry acidification on N_2O emissions is still fairly uncertain (Petersen & Sommer, 2011), with many studies (Velthof & Oenema, 1993; Fangueiro *et al.*, 2010c) being inconclusive regarding its effects on nitrous oxide emissions. The only certain fact, is that by acidifying the slurry, it slows the nitrification process down, consequently postponing the N_2O emissions in soils applied with treated slurry, when compared to the soils with untreated slurry (Chadwick *et al*., 2011).

Nevertheless, as recent studies have highlighted (Stevens & Quinton, 2009; Agostini *et al*., 2010) there is the danger of pollution swapping between N_2O and NH_3 gaseous losses and

NO_3^- leaching, which requires a holistic approach to the diffuse pollution issue, including the N dynamics and management in the soil-plant-atmosphere systems. One important tool to follow this approach is the integrated modelling of systems (Cameira & Mota, 2016).

2.5 Modelling of integrated systems

2.5.1 RZWQM2

The model used in the present study was the Root Zone Water Quality Model (RZWQM2), which was developed by the USDA – Agricultural Research Service (Ahuja *et al*., 2000). It is considered a research-level model containing physical, chemical, and biological processes for simulating agricultural management effects on soil processes, crop production, and water quality (Ma *et al*., 2011). As such, its main use is to study the processes that affect the water quality in agricultural scenarios, assessing the associated environmental impact in the soil layer, result of different management practices (Tedesco, 2013).

The simplified processes and execution time steps in RZWQM2 are shown in Figure 2.3, where DSSAT is the V4.0 crop growth model (Jones *et al*., 2003; Hoogenboom *et al*., 1994, 2004) and SHAW is the Simultaneous Heat and Water energy balance model (Flerchinger *et al*., 2000; Kozak *et al*., 2007).

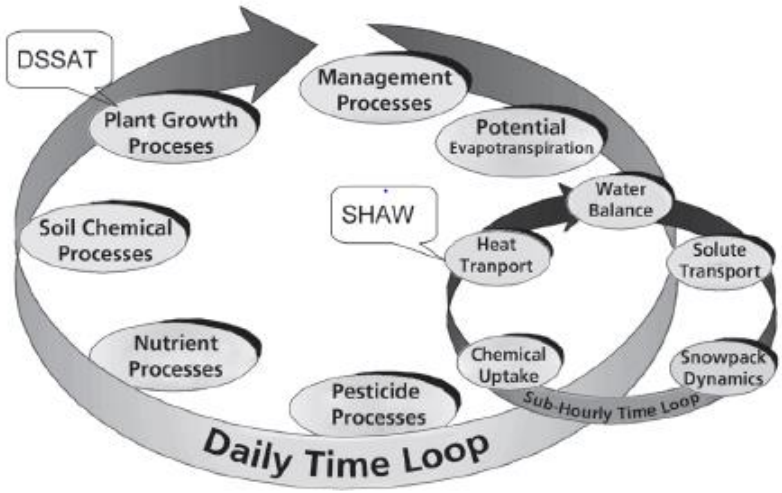

Figure 2.3 – Calculation sequence utilized by RZWQM2 (adapted from Ahuja et al., 2000a).

As shown above, RZWQM2 consists of seven main components/modules: i) soil water module; ii) heat and chemical transport module; iii) nutrient module; iv) plant growth module; v) soil chemical processes module; vi) evapotranspiration module; and vii) pesticides plus management module (Ma *et al*., 2011). Only the processes of calculation for the components of interest for the present study, alongside its theoretical assumptions are shown below.

2.5.1.1 Soil water component

Sub-modules of macrospore flow and transport, alongside sub-modules of infiltration and redistribution in the soil matrix are included in the soil water component, with the matrix soil hydraulic properties being described in the model by the functional forms suggested by Brooks and Corey with slight modifications (Brooks & Corey, 1964; Ahuja *et al*., 2000b). The soil water content versus soil water pressure head relation or soil water retention curve is expressed by:

$$\theta(h) = \theta_S - A\,|h| \qquad 0 < |h| < |h_{b1}| \qquad [2.11]$$

$$\theta(h) = \theta_r - B\,|h|^{-\lambda} \qquad |h| \geq |h_{b1}| \qquad [2.12]$$

where θ is the soil water content ($cm^3\ cm^{-3}$), h is the soil water pressure head (cm), θ_s is the saturated water content, θ_r the residual content, h_{b1}, A, B and l are parameters derived from best fitting of experimental data.

The hydraulic conductivity versus soil water pressure head relation is expressed by:

$$K(h) = K_S\,|h|^{-N1} \qquad 0 < |h| < |h_{b2}| \qquad [2.13]$$

$$K(h) = C\,|h|^{-N2} \qquad |h| \geq |h_{b2}| \qquad [2.14]$$

where K is the hydraulic conductivity ($cm\ h^{-1}$), h is the soil water pressure head (cm), K_s is the field saturated hydraulic conductivity and h_{b2}, N_1, N_2 and C are parameters derived from experimental data.

In situations where there are no enough field data in order to determine all the parameters for the Brooks-Corey equation, the model is able to estimate these parameters based in other properties that are easy to measure and sample, such as the soil texture, soil bulk density and field water capacity at 33 kPa (Ahuja *et al*., 1999).

The Green-Ampt equation is used to determine the infiltration rate in the soil matrix during a precipitation or irrigation event. Between successive events, the soil water is redistributed by a mass conservative, finite-difference numerical solution of the Richards' equation (Green & Ampt, 1911; Celia *et al*., 1990):

$$\frac{\partial\theta}{\partial t} = \frac{\partial}{\partial z}\left[K(h,z)\frac{\partial h}{\partial z} - K(h,z)\right] - S(h,z) \qquad [2.15]$$

where θ is the volumetric water content ($cm^3\ cm^{-3}$), t is time (h), z is the soil depth (cm), h is the pressure head (L), K is the unsaturated hydraulic conductivity ($cm\ h^{-1}$), expressed as function of h and z, and S is the root water uptake ($cm\ h^{-1}$) given by Nimah & Hanks (1973):

$$S(t,z) = \frac{\left[H_{rs} + (R_{res.z}) - h(z,t) - h_o(z,t)\right] R_a(z)\, K(h)}{x_r\, \Delta z} \qquad [2.16]$$

where H_{rs} is the water pressure head in the roots at the crown level (L); R_{res} is the root resistance (TL^{-1}) assumed constant and equal to 1.05 and $R_{res.z}$ the term introducing the gravity and head losses in H_{rs}; h(z,t) is the average soil water pressure head at the depth z; h_o is the osmotic pressure head (L); x_r is the distance between the roots and the point where h(z,t) was considered, assumed to be equal to unity (L); Δz is soil depth increment (L) and; $R_a(z)$ is the proportion of active roots in the depth increment Δz obtained from the crop growth model.

The surface boundary condition for the Richards' equation is an evaporative flux until the surface pressure head falls below a minimum value (-20,000 cm) at which time a constant head condition is used, whereas the bottom boundary condition can be specified as a unit gradient, a constant or a variable flux, or a constant pressure head (Cameira *et al*., 2005).

2.5.1.2 Evapotranspiration component

The calculation of evapotranspiration (ET) is based in a dual surface version of Penman-Monteith equation (Monteith, 1965), which is the Shuttleworth & Wallace model for ET (Shuttleworth & Wallace, 1985), extended to include evaporation from residue-covered soils with the form in the following way:

$$\lambda ET = CC(PM_c) + CS(PM_S) + CR(PM_r) \qquad [2.17]$$

where λET is the total flux of latent heat above the canopy (J); CC, CS and CR are coefficients based upon the fractions of area covered by the canopy, bare soil and residue, respectively, and the correspondent aerodynamic and surface resistances; and PM_c, PM_s and PM_r are the Penman–Monteith equations applied to the canopy, bare soil and residues, respectively.

2.5.1.3 Plant growth component

RZWQM2 only has a conceptual growth model for maize, soy and potato crops. For most crops, which includes the winter oats from the present study, it only present simplified empiric models, such as Quickplant and Quicktree (for orchards), in order to introduce a sink for water and N in the soil, while simulating as the crop is present in the crop-soil system. The user must input values for the maximum plant height and root depth, maximum leaf area index (LAI), the potential N uptake, and plant growth length, among other parameters. Quickplant assumes that the maximum values for each parameter occur exactly in the middle of the crop cycle, estimating the daily values, based in a triangular distribution, of parameters that are inputs for other sub-models (Tedesco, 2013).

2.5.1.4 Nutrient component

Organic Matter/Nitrogen (OMNI) cycling is a state-of-the-art model for C and N cycling in soil systems, combining many features such as crop residue and soil OM pools found in existing models, adding basic principles of chemical rate process theory, soil microbial growth, and environmental interactions. OMNI simulates all the major pathways illustrated in the flow diagram of the soil carbon-nitrogen cycle shown in Figure 2.4. This includes the processes of mineralization-immobilization of crop residues, manure, and other organic wastes; mineralization of soil humus fractions; inter-pool transfers of C and N; denitrification; gaseous losses of NH_3; nitrification of NH_4^+ producing NO_3^-; production and consumption of CH_4 and CO_2, and microbial biomass (MBM) growth and death (Shaffer *et al*., 2000).

The model divides OM into five pools, consisting in slow and fast pools for crop residues; and fast, medium, and slow soil humus pools, while there are three microbial pools, including aerobic heterotrophs, autotrophs, and anaerobic heterotrophs, which mediate the transfer and decomposition of the five organic pools (Shaffer *et al*., 2000a).

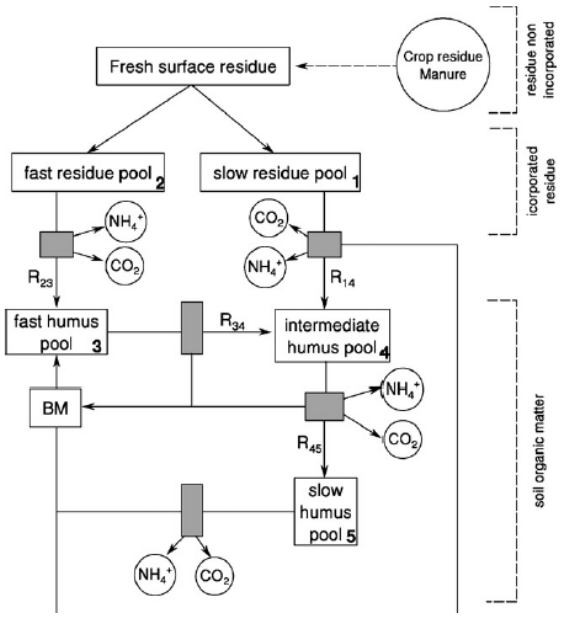

Figure 2.4 – Diagram of residue and soil organic matter pools in RZWQM2 (Adapted from Cameira *et al*., 2007).

Aerobic decay of the OM pools to NH_4 by heterotrophs is assumed to be a first-order reaction with its constant as a function of soil temperature, soil moisture, soil pH, and microbial population, with the resulting ammonium being nitrified into NO_3^- by autotrophs. Meanwhile, under anaerobic conditions, NO_3^- might be denitrified to N_2O and N_2 by anaerobic heterotrophs, in a first-order reaction. With the water filled pore space (WFPS) determining the aeration conditions for a give situation (Ma *et al*., 2012).

According to Shaffer *et al*. (2000), the basic form of decay rate equation is the same for all five organic pools, with the only difference being in the values of user-supplied rate coefficients.

These equations are all of first order regarding the C substrate source and are given by the following equation:

$$r_{dec,i} = K_{dec,i} \times s_i \quad [2.18]$$

where i is the organic pool index, $r_{dec,I}$ the substrate decomposition rate in µg C g^{-1} soil day^{-1}, $K_{dec,I}$ the first order rate coefficient for decay in day^{-1} and s_i the concentration of C substrate in µg C g^{-1} soil. These type of reaction is all due to the aerobic action of heterotrophic fungi and bacteria.

Followed by the nitrification, which is described by both a zero and first order rate equations based on the content of NH_4^+ in OMNI:

$$r_{nit0} = -K0_{nit} \times s_{12} \times \gamma_1 \quad [2.19]$$

$$r_{nit1} = -K1_{nit} \times s_{12} \times \gamma_1 \quad [2.20]$$

where $r_{nit\ 1}$ is the first order nitrification rate in moles NH_4.LPW^{-1} day^{-1}, $r_{nit\ 0}$ the zero order nitrification rate in moles NH_4 LPW^{-1}.day^{-1}, $K1_{nit}$ the first order rate coefficient for nitrification in moles LPW^{-1} day^{-1}; $K0_{nit}$ the zero order rate coefficient for nitrification in moles LPW^{-1} day^{-1}, s_{12} the concentration of NH_4^+ ions in moles LPW^{-1} and γ_1 the activity coefficient for monovalent ion. Note that LPW stands for litres pore water, and both $K1_{nit}$ and $K0_{nit}$ were calibrated during the modelling procedure.

For the denitrification process, it is described by the following equation:

$$r_{den} = -K_{den} \times s_{11} \times \gamma_1 \quad [2.21]$$

.where r_{den} is the first order denitrification rate in moles NO_3^- LPW^{-1} day^{-1}, K_{den} the first order rate coefficient for denitrification in day^{-1} (which was calibrated during the modelling procedure) s_{11} the concentration of NO_3^- ions in moles LPW^{-1} and γ_1 the activity coefficient for monovalent ion. As NO_3^- is diminished by the process, the rate r_{den} is presented as negative.

NH_3 volatilization is modelled based on partial pressure gradient of NH_3 in the soil (P_{NH3}) and air (P'_{NH3}):

$$r_v = -K_v\ T_f \left(P_{NH3} - P'_{NH3}\right) C_{NH4} \quad [2.22]$$

Where r_v is the ammonia volatilization rate (moles NH_4 LPW^{-1} day^{-1}), K_v is a volatilization constant (km day^{-1}), affected by wind speed and soil depth; T_f a temperature factor; C_{NH4} is the NH_4^+ concentration in the soil.

2.5.1.5 N_2O emissions during nitrification and denitrification process

N_2O is produced as intermediate and/or by-products due to incomplete pathways of nitrification and denitrification (Parton *et al*., 2001). The following algorithms are simplified process models,

where N_2O is estimated based on the nitrification and denitrification rates, as function of SWC, T and soil N-NO_3^- levels

N_2O from nitrification, in NOE model is estimated as:

$$N_2O_{\_nit} = Fr_{N2O\_Nit\_NOE} \times F_{SW\_Nit\_NOE} \times R_{nit} \quad [2.23]$$

$$F_{SW\_Nit\_NOE} = \frac{0.4 \times WFPS - 1.04}{WFPS - 1.04} \quad [2.24]$$

where $Fr_{N2O\_Nit\_NOE}$ is the fraction of nitrification for N_2O emissions and R_{nit} is the nitrification constant rate (which were calibrated during the modelling procedure), $F_{SW\_Nit\_NOE}$ is the soil water factor for the oxygen availability effect on N_2O during nitrification (Khalil et al., 2004).

N_2O from denitrification, in Daycent model as following (Del Grosso *et al*., 2000):

$$N_2O_{\_den} = Fr_{N2O\_Den\_DAYCENT} \times R_{den} \quad [2.25]$$

$$F_{N2O\_Den\_DAYCENT} = \frac{1}{1 + R_{NO\_N2O} + R_{N2\_N2O}} \quad [2.26]$$

$$R_{NO\_N2O} = 4 + \frac{9 \times \tan^{-1}\left(0.75 \times \pi \times \left(10 \times D_g - 1.86\right)\right)}{\pi} \quad [2.27]$$

$$R_{N2\_N2O} = \max\left(0.16k1, k1 \times \exp\left(\frac{-0.8[NO3]}{[co2]}\right)\right) \times \max\left(0.1, 0.015 \times WFPS \times 100 - 0.32\right) \quad [2.28]$$

$$k1 = \max\left(1.5, 38.4 - 350 \times D_g\right) \quad [2.29]$$

where $Fr_{N2O\_Den\_DAYCENT}$ is the fraction of denitrification for N2O emissions; R_{NO_N2O} is the ratio of NO to N_2O; R_{N2_N2O} is the ratio of N_2 to N_2O; [NO3] is the soil nitrate concentration; D_g is the gas diffusivity in the soil R_{den} is the denitrification constant rate (which was calibrated during the modelling procedure) and WFPS is the water filled pore space

2.5.2 Modelling process

The whole process of modelling is divided in parameterization, calibration and validation. With the first step being the parameterization which consists in the input of data in the model for an initial run, that in most cases, it will no yield good results for the simulation, when comparing the simulated to the observed data of the chosen dataset. Thus, calibration and validation are required. The objective of modelling in RZQWM2 is to create a tool capable of predicting and simulating, at a reasonable level, the water, N and plant growth components under many different conditions.

According to Ma *et al*.(2012) it is recommended that the simulation of the calibrated model provides overall reasonable simulation results for all the system components, and not only those which the user has measured data to compare and assess the quality of the given component of the said data. Hence, the user must check all the outputs in order to guarantee a good calibration and consequently and good model/simulation. The goodness of the calibration and validation processes must be evaluated not only through visual analysis but also by the calculation of statistical indicators.

2.6 Statistical analysis of nitrate leaching fluxes

The Kruskal – Wallis test is a one-way parametric form of variance analysis, when the ANOVA assumptions are not met by the data, namely the normality and homoscedasticity ones. Normality distributed data should follow a trending line, when plotted (Q-Q, etc.), while homoscedasticity means that the variance of each group present in the data must be equal, thus scattering homogeneously when plotted (Kruskal & Wallis, 1952; Pohlert, 2014).

For this study, the data failed in the homoscedasticity and normality assumption, meaning that all the results from a one-way ANOVA would not be reliable nor robust. Which is why a non-parametric variance analysis was applied in order to test the null hypothesis (Pohlert, 2014):

$$H_0 : \mu_1 = \mu_2 = ... = \mu_K \quad [2.30]$$

where μ are the group means and k the number of groups/kth group. However, in the scenario that the Kruskal – Wallis test returns a significant value that defies the null hypothesis, we accept the alternative hypothesis (H_1), which means that there are at least 2 means that are significantly different between them. The formula for the KW test statistics is shown below:

$$H = \frac{12}{n(n+1)} \sum_{i=1}^{k} \frac{R_i^2}{n_i} - 3(n+1) \quad [2.31]$$

where n_i (i=1, 2, …, k) is the sample sizes for each k groups, i.e. samples in the data; R_i is the sum of the ranks for each group i.

Additionally, it approximates a chi-square distribution with k-1 degrees of freedom when the null hypothesis is accepted. In order for this approximation to be valid, each of the n_i should be at least 5. Finally, the decision regarding the null hypothesis is done in the following way:

- When $H < X^2_{k-1,\alpha}$ or when p-value > α, we accept H_0, meaning that there are no statistically significant differences between the group means;
- When $H > X^2_{k-1,\alpha}$ or when p-value < α, we reject H_0, while accepting H_1, meaning that there are statistically significant differences between the group means, however we need to run post hoc test as a follow-up.

3. Materials and methods

This chapter describes the field experiments that produced the data used in this work, namely the experimental design and the equipment used. Also included is a description of the methodologies related to the modelling processes for each phase and the goodness of fit calculations. Finally, the elaboration of scenarios to exemplify model applications is described. A part of these experiments was performed during the previous years of 2012-2015 under the scientific Project reference PTDC/AGRPRO/119428/2010. During this period data collection was not performed by the author of the present work. The data collection during the 2015-2014 season was already performed in the scope of the present thesis.

3.1 Field experiments

3.1.1 Experimental site

The experimental work was conducted at the Horto de Química Agrícola Boaventura Azevedo located in Instituto Superior de Agronomia, Technical University of Lisbon, in Tapada da Ajuda, district of Lisbon, Portugal (38º4'' N, 9º10' W, 62 m above sea level). Among the diverse equipment and structures present in this facility, the present study used the drainage lysimeters to mimic a crop-soil system. A total of 32 lysimeters are present in Horto, as shown in Figure 3.1.

Sandy loam soil															
17	18 B	19 A	20 D	21 C	22 E	23 D	24 A	25 B	26 E	27 C	28 B	29 C	30 E	31 B	32 D
First block						Second block					Third block				
1	2 A	3 C	4 E	5 B	6 D	7 C	8 A	9 D	10 B	11 E	12 C	13 E	14 A	15 D	16 B
Sandy soil															

Figure 3.1 – Drainage lysimeters existing at Horto facilities (Adapted from Martins, 2014). (Letters designate the slurry treatments as described in 3.1.2)

The experiment was installed in 2 types of soils both classified as light textured, a sandy soil (SS), Haplic Arenosol, and a sandy loam soil (SLS), Haplic Cambisol, each type occupying 16 lysimeters. SS was collected in the Pegões area (near Lisbon) and the SLS in the center of Portugal (Castelo Branco) selected physical properties of the soils are shown in Table 3.1. The sandy soil has a coarser texture when compared to the sandy loam soil, being this difference reflected in the water that both soil can retain at 33 and 1500 kPa of both soils. Concerning the chemical properties, SS has a pH of 7.30 (neutral), electric conductivity (EC) of 105.63 µS cm^{-1} and OM content of 0.82% (low), while the SLS had a slightly lower pH of 6.57 (slightly acid), higher EC of 132.00 µS cm^{-1} and OM at 1.48% (low/medium). According to LQARS (2005), for

these pH values the N availability to the plants will is maximized since microbes' activity is not negatively affected. Both soils are also considered as no saline.

Table 3.1 - Main soil physical properties

Soil type	Depth	BD	Coarse sand	Fine sand	Silt	Clay	θ_{33}	θ_{15}	ϕ
	cm	g cm^{-3}	%				cm^{-3} cm^{-3}		
Sandy	0-10	1.48	70.7	17.0	9.7	2.6	0.108	0.020	0.440
	30-40	1.41	70.7	17.0	9.7	2.6	0.108	0.021	0.467
Sandy loam	0-10	1.44	19.2	55.8	15.0	10.0	0.142	0.057	0.456
	30-40	1.48	19.2	55.8	15.0	10.0	0.132	0.056	0.442

where BD is the soil bulk density, θ_{33} is the field capacity at 33 kPa, θ_{15} is the field capacity at 1500 kPa and ϕ is the soil porosity.

Directly beneath the lysimeters, there is an access tunnel that allows the collection of the water drained from each lysimeter (Figure 3.2).

Figure 3.2 – Lysimeters: a) top view with bare soil; b) top view with oats crop; c) access tunnel beneath the lysimeters before recuperation; d) access tunnel cleaned and in use.

The study area presents typical Mediterranean climate conditions, characterized by a temperate climate, with dry to very dry summers and wet to very wet winters. Figure 3.3 shows monthly rainfall and mean maximum and minimum temperatures collected in the Meteorological Station of Tapada da Ajuda for the period from 2012 to 2015. Solar radiation,

wind speed, and relative humidity were also collected in the same station. The 30 year's average for the period of 1951-1980 was added in the Figure for further interpretation.

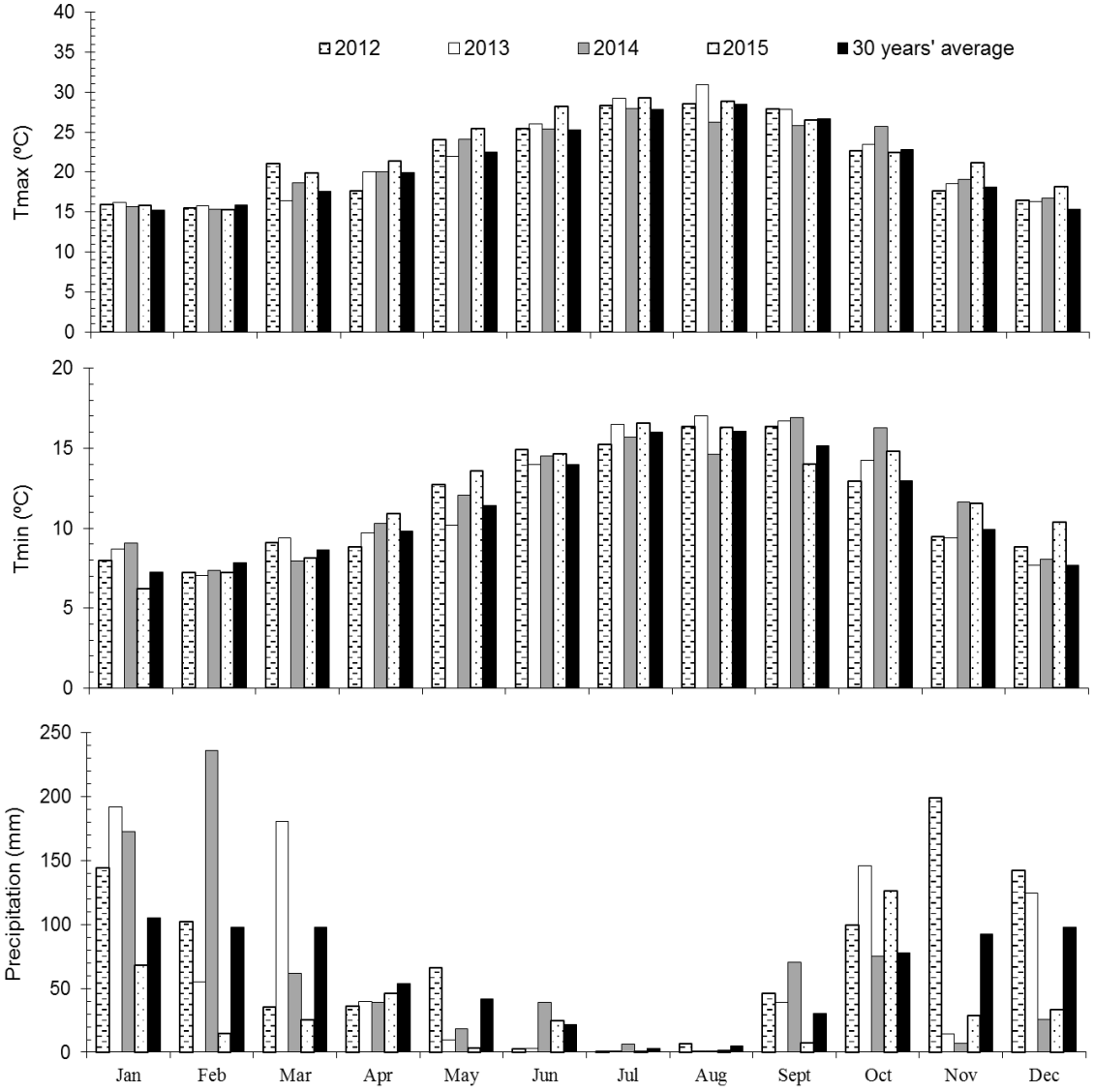

Figure 3.3 - Monthly mean maximum and minimum temperatures and monthly precipitation during the study period, with the 30 years' average (1951-1980), collected from the meteorological station of Tapada da Ajuda.

The monthly mean maximum and minimum temperatures present values of similar magnitude as the 30 year's correspondent average, meaning that the temperature probably has a small influence on the different results found among the studied years. Precipitation shows a large variability from year to year and in relation with the 30 year's average. The years of 2012, 2013 and 2014 present larger volumes of rainfall than the 30 year's average (724 mm), in particular during the autumn-winter season (October-March). Among the studied years, 2013 was the one with the highest amount (2015 mm), followed by 2014 (1809 mm) and finally 2012 (1125 mm). The year 2015 presents a total precipitation very similar (725 mm) to the 30 year's average, but with a different distribution within the year. These differences in water inputs

through precipitation will probably be an important cause for the inter-annual differences in both water and N related results.

3.1.2 Experimental design

Each lysimeter has an area of 1 square meter and a volume of 1 cubic meter (1x1x1 m). The lysimeters were planted with a spring-winter crop sequence, being the spring crop drip irrigated and the winter crop rain fed. Common oat (*Avena Sativa L.*) was selected as the winter study crop, an annual cereal whose erect stems may reach 40-150 cm long possessing cauline leaves. For Mediterranean regions, it is primarily sown during the autumn-winter season, especially during November and it is rain fed. The planting density was of 140 kg ha^{-1}, with a row spacing of 20 cm and a planting depth of 4 cm. The oat crop was preceded by a maize crop during the spring-summer season.

The only nutrients source applied to the lysimeters was cattle slurry, where five different treatments were considered:

A) Control (CTR): no slurry was applied for control purposes;
B) Whole slurry injection application (WSI): the whole slurry was injected in the soil;
C) Whole slurry mobilization application (WSM): the whole slurry was applied and incorporated in the soil;
D) Acidified whole slurry mobilization application (AWSM): the whole slurry was subject of an acidification treatment prior to its application in the lysimeter, where it was incorporated;
E) Acidified whole slurry surface application (AWSS): the whole slurry was subject of an acidification treatment prior to its superficial application in the lysimeter.

Each slurry treatment had 3 replications, as shown in Figure 3.1, however only 5 lysimeters for each soil type were fully equipped (Figure 3.4).

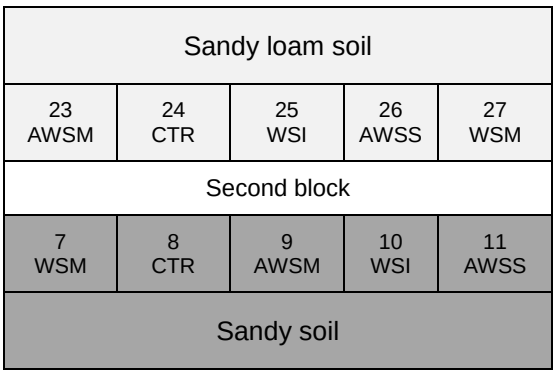

Figure 3.4 - Representation of the lysimeters used for this work, with the slurry treatments and both soils. (Adapted from Martins, 2014)

In the scope of the present thesis, modelling was performed only for treatment C) which consisted in the application of the whole slurry followed by incorporation in the soil. However,

data regarding NO_3^- in the soil solution was collected for all treatments and replications and was used to calculate NO_3^- leaching. The results were then compared statistically in order to identify significant differences between slurry treatments.

3.1.3 Installed equipment and measurements

The measured variables are shown in Table 3.2, where each variable is listed alongside the date of sampling/measurement and equipment utilized for the measuring. The table lines with an a) in the first column refer to equipment's that were installed at the beginning of the project PTDC/AGRPRO/119428/2010 without any input of the author. The measurements made with these equipment were also performed by other people. The remaining lines refer to equipment installed after 2004, especially for this work.

Table 3.2 - Measurement dates and equipment utilized for relevant variables

	Variable	Measuring equipment	Lysimeters	Measurement dates
a	Soil properties	see 3.1.3.1	Randomly	Start of crop seasons
b	Soil water	Water reflectometers	All in Fig 3.4	Continuously: 2014 to 2016
b	Drainage	Volumetric beakers	All in Fig 3.4	**2014:** 08, 18, 28/11, 08, 18, 28/12; **2015:** 10, 20, 31/01, 10, 20/02, 02/03, 14, 28 /12; **2016:** 04, 12, 19, 28/01, 05, 08, 15, 25/02
a	NH_3 volatilization	NH_3 trap (Kokkonen *et al*., 2006)	All in Fig 3.1, except #1 and #17	During 9 days after slurry application
a	N_2O emission	Accumulation box	All in Fig 3.1, except #1 and #17	2012-2013: 05/11 to 13/03; 2013-2014: 12/11 to 07/03; 2014-2015: 05/11 to 05/01. (*)
a	NO_3^- in soil solution	Porous capsules	All in Fig 3.1, except #1 and #17	During crop seasons of 2012-2013, 2013-2014 and 2014-2015 (**)
b	Soil temperature	Thermometers	# 7 and # 27	Continuously 2014 to 2016
a	Meteorology	Meteorological station	-	Continuously 2012 to 2015

b	Precipitation	Rain gauge	-	Continuously 2014 to 2015
	Crop parameters	-	# 7 and # 27	End of the crop seasons

(*) Some measurements were average estimations between samples).
(**) **2012-2013:** 08, 12, 15, 19-21, 23, 26, 27, 29, 30/11, 03, 05-07, 13, 14, 16, 18, 19, 23, 26, 28, 31/12, 02, 08, 09, 11, 14, 17, 18, 21, 22, 24, 26, 28/01, 13, 25/02 and 05-08, 11, 13/03; **2013-2014:** 25/11, 13, 30/12, 07, 13, 17, 21, 29/01, 06, 10, 14, 17, 21/02 and 03, 07/04; **2014-2015:** 07, 10, 14, 18, 21, 26/11, 21/01 and 05/02.

3.1.3.1 Soil characterization

For the particle size distribution, wilting point, pH and OM, soil samples were collected with a shovel and stored in plastic bags. For the soil water content at field capacity and bulk density, a non-destructive method of soil sampling was used, where the soil is sampled in metallic cylinders so that it maintains its original structure.

3.1.3.2 Slurry characterization

The slurry was characterized through the measurement of the following properties in samples collected from a dairy farm in Palmela: pH; total N, determined as described in Horneck & Miller (1998); dry matter and organic matter, determined as described in Fangueiro *et al*. (2012a); microelements, determined as described in Lakanen & Ervio (1971). In order to parameterize the slurry for the modelling activity, it was necessary to determine the amount of $N\text{-}NH_4^+$ and organic waste (OW) contained in the amount of slurry applied in each crop season, equations [3.1] and [3.2]:

$$S_{N-NH_4^+} = \left[N - NH_4^+\right] \times SLR \qquad [3.1]$$

where $S_{N\text{-}NH4+}$ is the ammonium contained in the applied slurry (kg ha^{-1}), $[N\text{-}NH_4^+]$ is the measured concentration of $N\text{-}NH_4^+$ in the slurry (kg kg^{-1}) and SLR is the amount of applied slurry (kg ha^{-1});

$$OW = \frac{OM_{\%}}{100} \times SLR \qquad [3.2]$$

where OW is the amount of organic matter in the applied slurry (kg ha^{-1}), $OM_{\%}$ is the measured percentage of organic matter in the slurry and SLR is the amount of applied slurry (kg ha^{-1}).

3.1.3.3 Soil water content

Soil water content (SWC) was measured at the depths of 20 and 25 cm, in the SLS and SS respectively, using water content reflectometers (CS616 and CS625 from Campbell Scientific, Inc.), which were installed in 10 lysimeters (Figure 3.5a). This probes make and indirect measurement of the SWC, since they measure the travel time of the electromagnetic pulse that propagates between the probes' rods. The pulse velocity depends on the dielectric

permittivity of the material around. The propagation time decreases as water content in the soil increases, due to the polarization of water molecules, which increases the consumption of time, and thus retarding the propagation velocity time. This signal is then reflected from the rod ends, travelling back to the probe head, triggering the next pulse (Rhoades *et al*., 1989). This period of travel is converted in volumetric water content by the linear calibration equation:

$$SWC = C_0 + C_1 \times p \quad [3.3]$$

where SWC is the volumetric water content in the soil ($cm^3\ cm^{-3}$); C_0 and C1 are calibration coefficients that must be determined for the soil in study; and p is the signal travel time in µs.

The probes were calibrated by relating the p readings and volumetric water contents of the soil measured in soil samples collected at the time of each p reading. Thus, specific parameters were determined for each soil yielding the following values: SS, C_0 is equal to -0.4677 and C_1 is 0.0307; SLS, C_0 is equal to -0.475 and C_1 is 0.028.

3.1.3.4 Drainage

Drainage water (D) from the lysimeters was measured in the access tunnel directly beneath them. The water was collected in buckets during a known period of time. Then the collected volume was measured using 2 litre beakers. The measurement frequency depended on the climatological conditions in the previous days, being this sampling/measuring performed mainly after rainfall events (Table 3.2).

3.1.3.5 Nitrates in soil solution

Nitrate in the soil solution was monitored in 3 replications of each slurry treatment by measuring the $N\text{-}NO_3^-$ concentration in the solution collected by porous capsules installed at a depth of 70 cm. A suction of 60 and 70 kPa was created in the capsules, for the SS and SLS, respectively, 24 hours prior to rainfall (Carneiro *et al*, 2012). The collection was performed immediately after rainfall and frozen for posterior analysis in laboratory, where $N\text{-}NO_3^-$ was measured using a molecular absorption spectrophotometry with segmented flow autoanalyzer, according to the methodology described in Mulvaney (1996).

3.1.3.6 NH_3 volatilization and N_2O emissions

NH_3 emissions were measured over periods of a few days (depending on the year) after the application of manure, using a system of continuous flux in a solution of phosphoric acid (H_3PO4) (0.05 M). In each lysimeter a closed small circular chamber was randomly placed (Figure 3.5b), covering an area of approximately 0.035 m^2. For the measurement of N_2O emissions, a square camera was also placed, buried 5 cm into the ground to ensure gas

accumulation. Details about the measurements and associated calculations are provided in Martins (2014).

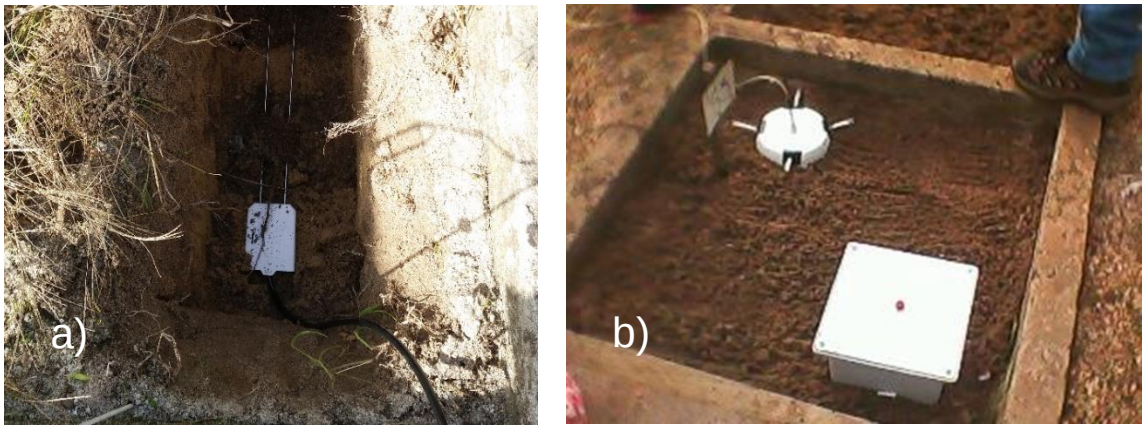

Figure 3.5 - a) Reflectometers installed in lysimeters for the measurement of SWC; b) Lysimeter with both chambers for the measurement of NH_3 volatilization (round) and N_2O (square).

3.1.3.7 Other measurements

Soil temperature (T) was continuously monitored after 2014 using 2 thermometers (107 temperature probes from Campbell Scientific) installed at the same depth as the soil water reflectometers (20-25 cm). The precipitation was both measured in the Meteorological Station of Tapada da Ajuda, and in Horto facilities, utilizing a 0.5 mm capacity rain gauge (W5720 Casella, London, UK) in order to detect variations due to the existence of a metallic net used as the facility´s roof. Some crop parameters were periodically measured in the lysimeter with the slurry treatment C, which was the one that was going to be modelled, including plant density, plant height and rooting depth. At harvest, the plant biomass was evaluated as well its N content. The reflectometers, thermometers and rain gauge were all connected to a data logger (CR10 from Campbell Scientific LTD).

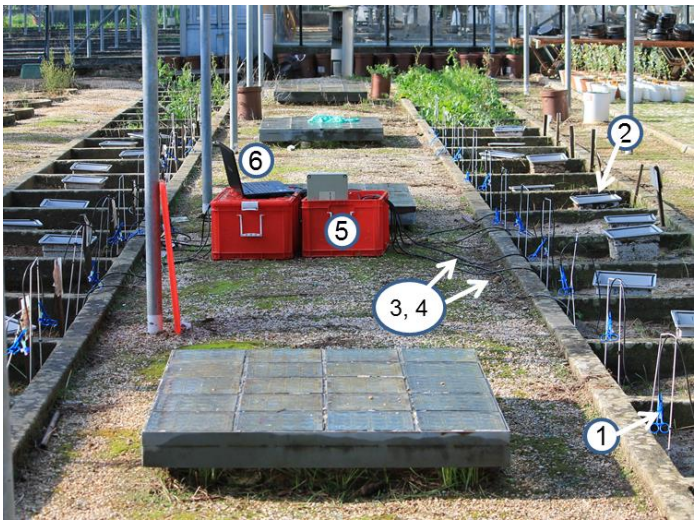

1 – Porous capsule for NO_3^- in soil solution;
2 – N_2O chamber;
3 – Cable for the soil water probe;
4 – Cable for the soil temperature probe;
5 – Data logger;
6 – Laptop for data collection

Figure 3.6 – General view of the installed equipment.

3.2 Modelling

As mentioned in Chapter 2, models must undergo the procedures of parameterization, calibration and validation before being considered adequate to be applied as a prediction tools. The whole process of modelling applied for the present study is described below, including the methodology for each phase. A flowchart that shows an overview of the modelling procedure utilized in the present study is shown in Figure 3.7.

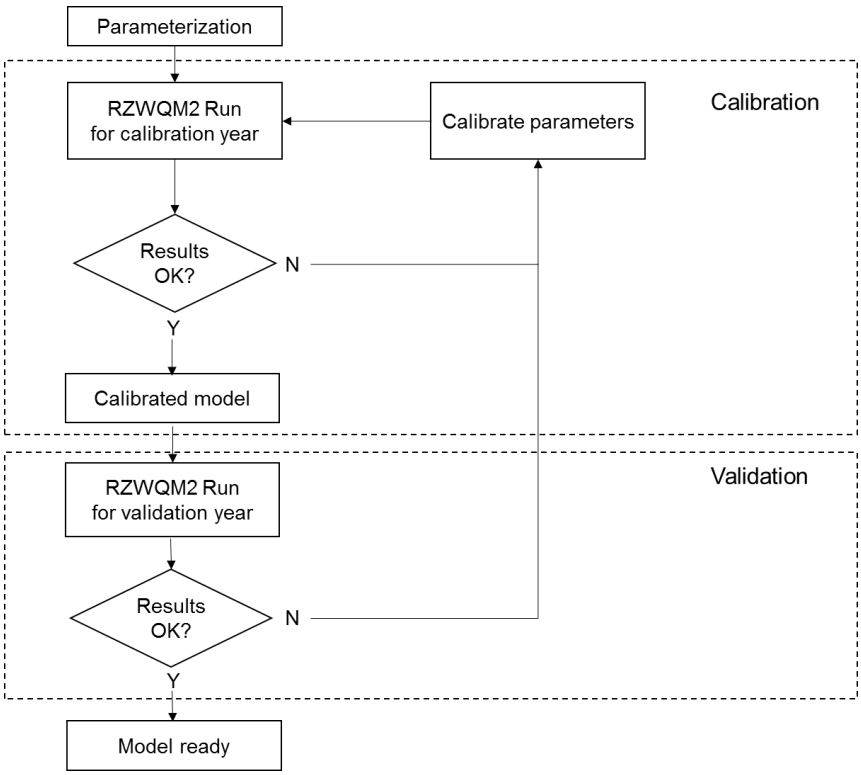

Figure 3.7 – Simple modelling procedure overview (adapted from Ma *et al*., 2012).

3.2.1 Parameterization

The parameterization of the systems to be modelled, which are an oat crop in a sandy soil and an oat crop in a sandy loam soil, both amended with whole cattle slurry applied and incorporated in the soil (treatment C), is presented next including system definition and parameter sources.

3.2.1.1 Simulation domain and boundary conditions

The simulations were performed in field lysimeters, each with a surface of one square meter and a depth of one meter. As shown in Figure 3.8, the simulation domain is one-dimensional, it is limited at the bottom by the depth of 100 cm, coincident with the bottom of the lysimeters and at the top it follows the crop high, from 50 to 60 cm at maximum growth. The boundary conditions are then the evapotranspiration flux at the top of the crop canopy and the unit gradient flow at the bottom of the lysimeters.

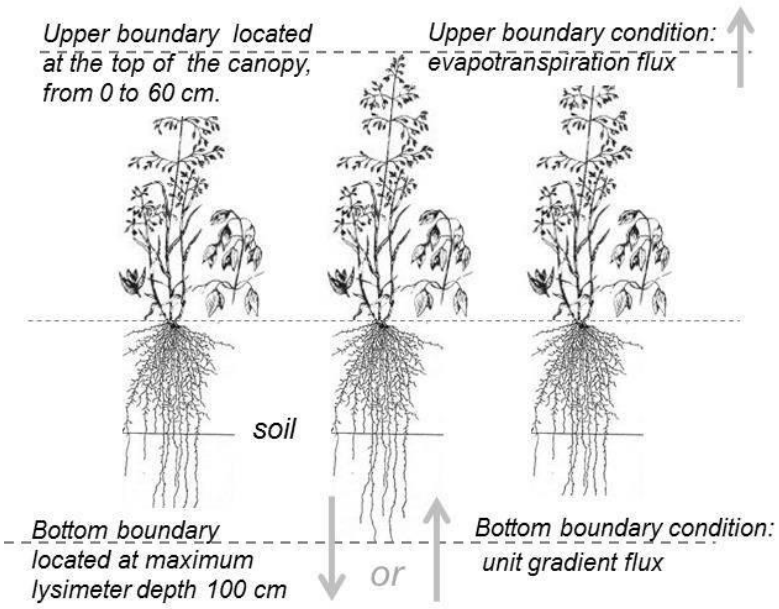

Figure 3.8 - Graphical representation of the simulation domain and boundary conditions.

For each crop season, the time domain corresponded to the period starting one week before the slurry application and one day after crop harvest, as shown in Table 3.3.

Table 3.3 – Temporal domain for each crop season and correspondent modelling phase

Crop season	Modelling phase	Simulation periods		Simulation length (days)
		Start	End	
2012-2013	Validation	28/10/2012	15/03/2013	138
2013-2014	Validation	04/11/2013	22/04/2014	169
2014-2015	Parameterization and Calibration	28/10/2014	22/04/2015	176
2015-2016	Validation	15/11/2015	12/03/2016	117

3.2.1.2 Parameterization data sources

Table 3.4 shows the different sources for the data (measured, estimated and/or literature), used for the present study, where estimated data means that it was calculated using measured properties.

The meteorological parameterization was done with the daily data collected in the meteorological station and the precipitation recorded in Horto. The file xxx.met contains the data series for temperatures, relative humidity and wind speed. The file xxx.brk contains the precipitation data organized in breakpoints, that is as a form of a hyetograph. The breakpoint calculation considered events with an average duration of 600-800 minutes and precipitation depth between 0.05 mm and 0.7 mm.

Table 3.4 – Model input data and respective sources

Module Parameter	Data source
Soil water	
Soil texture, bulk density, field capacity at 30 kPa, $\theta_{1/3}$, and wilting point, θ_{15},	Measured
Porosity, field capacity at 10 kPa $\theta_{1/10}$	Estimated
Saturated hydraulic conductivity, K_{sat}	Literature
Meteorological data	
Maximum and minimum temperatures, precipitation, solar radiation, wind speed and relative humidity	Measured
Crop and management practices	
Leaf area index	Estimated
Planting density, rows spacing, crop height and depth of roots	Measured
Soil organic matter and N	
Organic matter in the soil and slurry and C/N of slurry	Measured
Organic pools partitioning and interpool coefficients	Estimated
N transformation reaction rates	Literature

3.2.1.3 Soil physical properties

According to the experimental soil characterization two layers were defined for modelling, the first one from 0 to 50 cm and the second from 50 to 100 cm deep. Table 3.5 shows the input data regarding the soil physical properties.

Table 3.5 - Parameterization of the basic soil physical properties

Soil type	Horizon	Bulk density	Porosity	Mineral fraction		
	cm	g cm^{-3}	cm^3 cm^{-3}	Sand	Silt	Clay
Sandy	50	1.48	0.442	0.88	0.09	0.03
Sandy	100	1.41	0.468	0.88	0.09	0.03
Sandy loam	50	1.44	0.457	0.70	0.20	0.10
Sandy loam	100	1.48	0.442	0.70	0.20	0.10

Using the basic soil properties (particle size distribution, bulk density and water at the pressure of 33 kPa), the model estimated the Brooks and Corey parameters describing the two functions describing the hydraulic properties which are h(θ) and k(θ) (Eq [2.11]-[2.14]). The extended similar media approach was utilized to derive the Brooks and Corey parameters for the soil

water retention function (Warrick *et al*., 1977; Ahuja *et al*., 1985). The average parameters for the sandy and sandy loam textural classes (Rawls *et al*., 1982) were used to represent the reference h(θ) curve from which the new scaled curve parameters were obtained. Given the measured K_{sat} and the estimated h(θ) functions, the unsaturated conductivity/suction relationship, K(h) was estimated by the approximate capillary-bundle approach of Capmbell (1974). The estimated parameters are shown in Table 3.6.

Table 3.6 - Parameterization of the Brooks and Corey hydraulic functions

Layer (cm)	S_2	A_2	N_2	C_1	θ_R	θ_S	FC_{33}	FC_{10}	FC_{15}	S_1	C_2
Sandy soil											
0-50	7.1	0.592	3.776	21	0.020	0.442	0.063	0.108	0.025	7.1	34922
50-100	6.4	0.592	3.776	21	0.020	0.468	0.063	0.108	0.025	6.4	23698
Sandy loam soil											
0-50	14.3	0.322	2.966	2.59	0.041	0.457	0.192	0.263	0.085	14.3	6854
50-100	16.0	0.322	2.966	2.59	0.041	0.442	0.192	0.263	0.085	16.0	9637

where S_2 is the bubbling pressure (cm), A_2 is the pore size dist. index, N_2 is the 2nd exponent for conductivity curve, C_1 is the saturated conductivity (cm h^{-1}), θ_R is the residual water content, θ_S is the saturated water content, FC_{33} is the 33 kPa field capacity, FC_{10} is the 10 KPa field capacity, FC_{15} is the 15 bar field capacity, S_1 is the bubbling pressure (cm), C_2 is the 2nd intercept on conductivity curve, N_1 is the 1st exponent for conductivity curve and A_1 is a constant water retention curve.

3.2.1.4 Soil organic matter, C and N

The constitution of each OM pool, including residues, humus and microbes, was estimated according with the procedure advised by the model authors. The initial soil organic C pools was set based on measured soil OM content at each depth using the wizard provided in RZWQM2, followed by a long time running of the model for a 10 years' period under the current management practices and climate in order to equilibrate the pools (Ma *et al*., 2011). At this phase of the process, default values were used for the parameters influencing the N transformations in the soil, such as efficiency factors and reaction rate constants for the diverse N related process equations are shown in Table 3.7

Table 3.7 - Nitrogen nutrient efficiency factors and reaction rates parameterization

Efficiency factors				Reaction rates			
BM	NH_4	N_2N_2O	$DENIT_{OM}$	NH_3	NIT	NIT_{N2O}	DENIT
frac	frac	frac	frac	km d^{-1}	Moles LPW^{-1} d^{-1}	frac	d^{-1}
0.267	0.01	0.133	0.1	1000	1.00E-09	0.0016	1.00E-13

where BM is the biomass converting decayed organic matter uptake, NH_4 is the autotroph converting nitrified NH_4 to autotroph biomass-N, N_2N_2O is the denitrification efficiency factor where the remainder goes off as N_2 and N_2O, $DENIT_{OM}$ is the denitrification rate converting to anaerobic organic matter decay rate, NH_3 is the NH_3 volatilization constant, NIT is the nitrification constant, NIT_{N2O} is the N_2O fraction from nitrification process constant and DENIT is the denitrification constant. (LPW is litres of pore water and frac stands for fractional)

3.2.1.5 Crop characteristics and management

The most relevant plant related parameters are shown in Table 3.8. The values for each parameter were kept constant for all of the seasons, except the duration of the crop season with the values of 119, 152, 160 and 100 days for the seasons between 2012 and 2016. Additionally, Table 3.9 presents the dates for the crop management practices for each season. The properties of the dairy cattle slurry applied in each crop season (except 2015-2016) is shown in Table 3.10. The slurry was applied at soil surface followed by a slight incorporation.

Table 3.8 - Plant and crop parameterization

Planting density	Max crop height	Max depth of roots	Max LAI	Minimum leaf stomatal resistance
Plants ha^{-1}	cm	cm		s m^{-1}
250000	60	100	3.7	200

Table 3.9 - Crop management events for each crop season, in both sandy and sandy loam soils

Crop season	Slurry application	Seeding	Harvest
2012-2013	05/11/2012	15/11/2012	14/03/2013
2013-2014	12/11/2013	20/11/2013	21/04/2014
2014-2015	04/11/2014	12/11/2014	21/04/2013
2015-2016	23/11/2015	04/12/2015	12/03/2016

Table 3.10 - Dairy cattle slurry characterization

Crop season	NH_4-N^+	Organic waste	C/N Organic waste	Fraction C in waste
	kg ha^{-1}	kg ha^{-1}		
2012-2013	38.3	1382.1	16	0.4
2013-2014	34.7	1588.6	16	0.4
2014-2015	29.4	2074.5	15	0.4

As the C/N of the slurry for all the crop season is below 20, N mineralization rate of the slurry is higher than the N uptake of the crop, and thus it represents a potential N pollution source.

3.2.1.6 Soil thermal properties

In order to determine the soil thermal properties, the model follows the equation described in de Vries (1963), as shown below:

$$VHC = c_s x_s + c_{om} x_{om} + c_w x_w + c_a x_a \quad [3.4]$$

where VHC is the dry volume heat capacity (J mm^{-3} C^{-1}); c and x are the volumetric heat capacity and the volume fraction of soil constituents: solid minerals (subscript s), organic

matter (OM), water (w) and air (a). The contribution of air to soil heat capacity is generally neglected. It is noted that $x_s + x_{om} = 1 - f$ (porosity). Average volume fraction of solids (x_s) usually ranges from 0.45 to 0.65. This, coupled with soil organic matter volume fractions ranging from 0 to 0.05, yields typical soil dry volumetric heat capacities in the range of 0.001 to 0.0014 J mm^{-3} C^{-1}. Table 3.11 shows the typical average values of c_s and c_{om} (Ahuja *et al*., 2000a). Since both soil present a coarse texture, the model calculates the value of 0.00111 J mm^{-3} C^{-1} for the dry volumetric heat capacity.

Table 3.11 - Thermal properties of soil constituents (after de Vries, 1963)

Soil constituent	Density	Volumetric heat capacity, C_v	Thermal conductivity, K_c
	g cm^{-3}	J mm^{-3} C^{-1}	J mm^{-1} h^{-1} C^{-1}
Quartz	2.66	0.0020	31.7
Other minerals (average)	2.65	0.0020	10.4
Organic matter	0.7-1.3	0.0025	0.9

3.2.1.7 Initial conditions

In order for the model to solve the differential equations describing the several processes it is necessary to describe the initial state of each soil horizon, concerning the SWC, T, N and OM. The initial SWC for the 2014-2015 and 2015-2016 crop seasons was measured in field for the top layer, while for the bottom layer and the remaining seasons, it was estimated as a percentage of the field capacity accordingly to the rainfall events during the days prior to the start of the simulation. Table 3.12 shows the initial SWC and T for both soils and layers.

Table 3.12 - Soil water content and temperature initial conditions for each crop season

Crop season	Layer (cm)	Sandy soil		Sandy loam soil	
		θ (cm^3 cm^{-3})	Temperature (ºC)	θ (cm^3 cm^{-3})	Temperature (ºC)
2012-2013	0-50	0.112	15.9	0.192	15.4
	50-100	0.112	19.0	0.242	19.0
2013-2014	0-50	0.112	15.9	0.192	15.4
	50-100	0.112	19.0	0.242	19.0
2014-2015	0-50	0.122	13.0	0.230	15.4
	50-100	0.122	13.0	0.230	19.0
2015-2016	0-50	0.127	15.9	0.260	15.4
	50-100	0.127	19.0	0.260	19.0

3.2.2 Calibration

Due to measurement uncertainty, use of literature parameters and spatial variability of measured properties, simulation models require calibration. The parameters selected for calibration are the ones for which the model shows higher sensitivity. According to Ma *et al*. (2011), as the measured data available for this study was the SWC, that is influenced the most by the soil water retention curve and K_{sat}, the recommended parameters to adjust are the SWC at 33 kPa (θ_{33}), and 1500 kPa (θ_{15}) and $K_{sat.}$ These parameters were adjusted by an iterative process of trial-and-error procedure (Figure 3.7), where the parameters were changed in a conceptually correct manner, until the model yielded acceptable estimations of the variables for which there was field measurements (control variables). Table 3.13 shows the parameters that were selected for calibration and the correspondent control variables.

Table 3.13 - Selected parameters for calibration and respective control data

Process	Selected parameters	Control variables
Soil hydraulic properties	$\theta_{1/3}$ and K_{sat}	Soil water content (SWC) at 20 and 25 cm depth
		Drainage (D) at 100 cm depth
C/N related properties	Interpool coefficients and organic pool partitioning	Mineralization rate of the soil
N component	N reaction rates	NO_3^- flux (φNO_3^-) at 70 cm depth
		N_2O emission (φN_2O) from the soil

Based in Scheppers & Mosier (1991), the expected yearly N mineralization of a soil should be roughly 20 kg ha^{-1} $year^{-1}$ per each 1% of soil endogenous OM, for the top 30 cm layer. As the SS and SLS presented 0.82 % and 1.48 % OM, respectively, the estimated mineralization rate for the simulation length, which calibration aimed to simulated, was of 7.9 and 14.3 kg ha^{-1} during the simulation length in 2014-2015 crop season for SS and SLS, respectively.

To accomplish this, the OM was partitioned between the humus pools in the following way: 14% in fast pool, 6% in intermediate pool and 80% in slow humus pool. Finally, these partitioning values were inputted in the initial residue initialization wizard, and then equilibrated, during 10 years, with the following conditions:

- Minimum and maximum air temperature of 8 and 32ºC, respectively;
- Corn culture with a total N uptake of 170 kg ha^{-1}, uptake start at 132 and a length of 74;
- 2 wet cycles starting in January;
- 0.8 and 0.2 fractional root distribution for layer 1 and 2, respectively.

The resulting initial residue profile for each soil is shown below in Table 3.14, while the interpool exchanges coefficients were calibrated in order to yield good simulation results, which will be discussed further in the present document. Calibration was performed using field data for the 2014-2015 period, since this was the crop season with the greatest diversity of variables measured regarding soil water and N losses.

Table 3.14 - Initial residue state, microorganism and inorganic N profile after wizard and 10 year equilibration, for both soils

SR	FR	FH	IH	SH	Aero	Auto	Anae	Urea-N	NO_3-N	NH_4-N
µg-C g^{-1}					#orgs g^{-1}			µg-N g^{-1}		
Sandy soil										
89.7	0	73.4	472.5	4588.2	135578	7575	19372	0	0.85	0.0017
0.5	0	87.2	90.9	431.1	9917	736	335	0	0	0
Sandy loam soil										
45.3	0	52.1	147.7	7202.3	175091	14991	18028	0	1.325	0.017
0.5	0	68.4	35	426.6	13390	1024	305	0	0.1	0.001

where the first row corresponds to the first layer (0-50cm) and the second row the second layer (50-100cm); SR is slow residue; FR is fast residue; FH is fast humus; IH is intermediate humus; SH is slow humus; Aero is aerobic heterotrophs; Auto is autotrophs and Anae is anaerobic heterotrophs.

3.2.3 Validation

After attaining a satisfactory calibration, it is necessary to confirm that the calibrated model is able to simulate, within the desired range of accuracy, different boundary conditions using independent datasets as control variables. The model was then run using SWC and drainage data measured during 2015-2016 season. NO_3^- fluxes at 70 cm depth and the N_2O emissions measured during 2012-2013 and 2013-2014 seasons were used as the control variables since this kind of data was not available for the 2015-2016 season.

3.2.4 Goodness of fit – Evaluation of the calibration and validation procedure

The goodness of fit of the model simulations, for both water and N components was evaluated using two type of methods:

Graphical analysis, where the plots of the simulated values versus the observed values (either calibration or validation) are presented, assessing if the model was well fit visually. This is a qualitative procedure, thus, somehow subjective, but still able to provide an idea of the goodness of fit of a given simulation;

Statistical/Quantitative analysis, where the quality of the model is quantified through the use of statistical indicators, and then its quality assessed. The statistics used in this work were the following:

The root mean square error of the simulations, given by:

$$RMSE = \left(\sum_{k=1}^{n} \left(P_k - O_k \right)^2 / n \right)^{0.5} \quad [3.5]$$

where RMSE is the root mean squared error, n is the total number of observations, k is the k^{th} observation/data, P_k are the simulated value and O_k are the measured value.

The mean standard deviation of the measured data, calculated as:

$$MSD = \frac{\sum_{k=1}^{n} SD_k}{n} \quad [3.6]$$

where MSD is the mean standard deviation, n is the total number of observations/, k is the k^{th} observation/data and SD_k are the standard deviations for each level of k.

The modelling efficiency (Loague & Green, 1991; Legates & McCabe, 1999) calculated as:

$$EF = \left(\sum_{k=1}^{n} \left(O_k - \overline{O} \right)^2 - \sum_{k=1}^{n} \left(P_k - O_k \right)^2 \right) \Big/ \sum_{k=1}^{n} \left(O_k - \overline{O} \right)^2 \quad [3.7]$$

where EF is the modelling efficiency, n is the total number of observations/data, k is the k^{th} observation/data, O_k are the measured value, $\bar{O}$ is the measured values mean and P_k are the predicted values.

The coefficient of determination, as follow:

$$R^2 = \left(\sum_{k=1}^{n} \left(\hat{y}_k - \bar{y} \right)^2 \right) \Big/ \sum_{k=1}^{n} \left(y_k - \bar{y} \right)^2 \quad [3.8]$$

where R^2 is the determination coefficient; n is the total number of observations/data; k is the k^{th} observation/data; $\hat{y}$ is the k^{th} predicted value; $\bar{y}$ is the mean of the measured values and y_k is the k^{th} measured value.

RMSE reflects the magnitude of the difference between measured and simulated results (Ma *et al*., 2011). According to Cameira *et al*. (2005), a good calibration is met when RMSE of the simulated values is lower than MSD of the measured data. EF measures the deviation between the predicted values and the measured data, varying from minus infinity to 1, with higher values indicating a better agreement. EF=0 indicates that the measured mean is as good a predictor as the model while negative EF values indicate that the observed mean is a better predictor than the model (Wilcox *et al*., 1990). R^2 describes the proportion of the total variance in the observed data that can be predicted by the model (Legates & McCabe, 1999). Ranging from 0 to 1, with higher values indicating a better agreement, nonetheless the use of this indicator can be misleading as this indicator is oversensitive to outliers, leading to a bias towards extreme values, meaning that it should only be used as a complementary indicator. For soil

water and N-related calibrated predictions the expected minimum values for EF and R^2 are 0.7 and 0.8 respectively (Ma *et al*., 2011).

3.3 Model application

3.3.1 Prediction scenarios

Once the model was capable of simulating the studied system with the desired accuracy, it was used to predict the water and N balances and main pathways for losses of six scenarios. The first four intended to show the influence of the hydrological year upon the water balance and the N losses. Based upon a 30 years (1951-1980) series of meteorological data and using the cumulative frequency analysis, the wet, average, dry and very dry years were selected corresponding to 80, 50, 20 and 10% probability of non-exceedance. Then, the meteorological data for those years was used to simulate the effect of the current management practices upon the water and N processes. The other two scenarios were based upon the projected values of average temperature increase released by IPCC (2001; 2007a; Melo e Abreu & Pereira, 2010).

3.3.2 Determination of nitrate leaching and slurry treatment comparison

Based on the $N\text{-}NO_3^-$ concentrations measured in the soil solution collected in the porous capsules, for all of the slurry treatments, the NO_3^- leaching flux was calculated using the D estimated by the calibrated and validated RZWQM2 model, using equation [3.9].

$$\varphi NO_3^- = D \times C_{NO3} \times 0.01 \qquad [3.9]$$

where φNO_3^- is the nitrate flux in kg ha^{-1}, C_{NO3} is the concentration of nitrate as N measured in the capsules at 70 cm depth in mg L^{-1} and D is the drainage obtained from the model at 70 cm depth in L m^{-2}

φNO_3^- for all slurry treatments was calculated and statistically analysed and compared. An equal number of data was selected, 5 for each treatment for the 3 crop seasons. For the KW test to yield meaningful and valid results at least a sample size of 5 is needed (Pohlert, 2014).The criteria for this selection was days that were meaningful in the NO_3^- drainage process, representing different phases of the leaching cycle. All statistical analysis plus graphs were conducted with the RStudio software (Version 0.99.892 – © 2009-2016 RStudio, Inc.) and/or in spreadsheets (Microsoft Office Excel 2013 for Windows). The effect of different slurry treatment on φNO_3^- was analysed by a mean value for each treatment at a significance level of 0.05, these calculations were done based on the fact that the data failed homoscedasticity and normality assumptions. A post hoc for KW, the Conover - Iman pairwise test (Pohlert, 2014) was applied on the days that yielded statistics that rejected H_0, in order to identify the treatments that had statistically significant differences between means of φNO_3^-.

4. Results and discussion

This chapter presents the results from the modelling procedure and its application, alongside an interpretation of the results.

4.1 Model calibration

4.1.1 Sandy soil

4.1.1.1 Soil water content, drainage and soil temperature

Table 4.1 shows the initial and calibrated values of saturated hydraulic conductivity (K_{sat}) and soil moisture at field capacity at 10 kPa (θ_{10}). The correspondent Brooks and Corey functions for soil water retention and hydraulic conductivity are presented in Figure 4.1. Field and laboratory measurements uncertainties of both K_{sat} and $\theta_{1/10}$, and the spatial heterogeneity of the soil properties justify the variations obtained with the calibration process.

Table 4.1 - Initial and calibrated values of the selected soil hydraulic parameters. Sandy soil

Parameter	Layer (cm)	Initial	Calibrated	Variation (%)
K_{sat}	0-50	21.0	13.5	-36
θ_{10}		0.107	0.097	-9
K_{sat}	50-100	21.0	25.0	19
θ_{10}		0.107	0.046	-57

where K_{sat} is the saturated hydraulic conductivity in cm hr^{-1}; and θ_{10} is the field capacity at 10 kPa in cm^3 cm^{-3}.

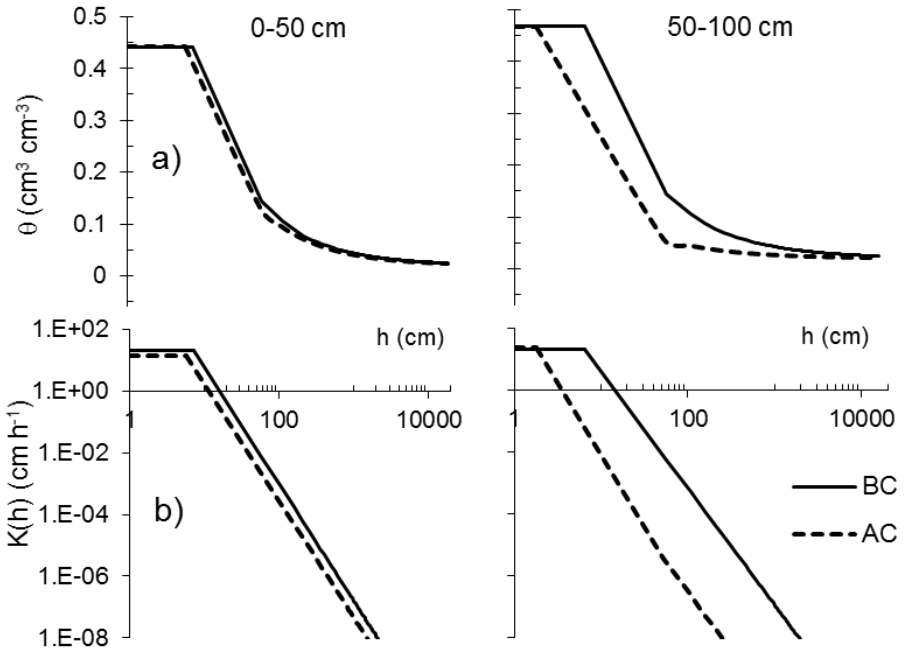

Figure 4.1 - Hydraulic properties of the sandy soil described by the Brooks and Corey functions before (BC) and after (AC) calibration: a) Water retention; b) Saturated hydraulic conductivity.

Figure 4.1 shows the typical hydraulic behaviour of a sandy soil, which is associated with a high saturated hydraulic conductivity with a very rapid decrease as pressure head (h) increases. A similar behaviour is also observed for the water retention curve. Both Table 4.1 and Figure 4.1 show that the calibration process did not change significantly the hydraulic properties of the surface layer. However, significant changes are observed for the 50-100 cm layer, for which the calibration led to less water retention and a higher conductivity at saturation, and lower unsaturated conductivities for the same pressure head value. Thus, the process accentuated the typical sandy soil behaviour. The control variables for the calibration of the hydraulic properties were the SWC and D time series.

Figure 4.2 shows the measured and simulated values for SWC at the depth of 25 cm, and for the water drainage (D) at the bottom of the profile (100 cm) after the calibration of the soil hydraulic properties for the 2014-2015 crop season. The precipitation (P) during the simulation period is also shown for further analysis. The X-axis represents the number of days after slurry application, where X= 0 marks the application day.

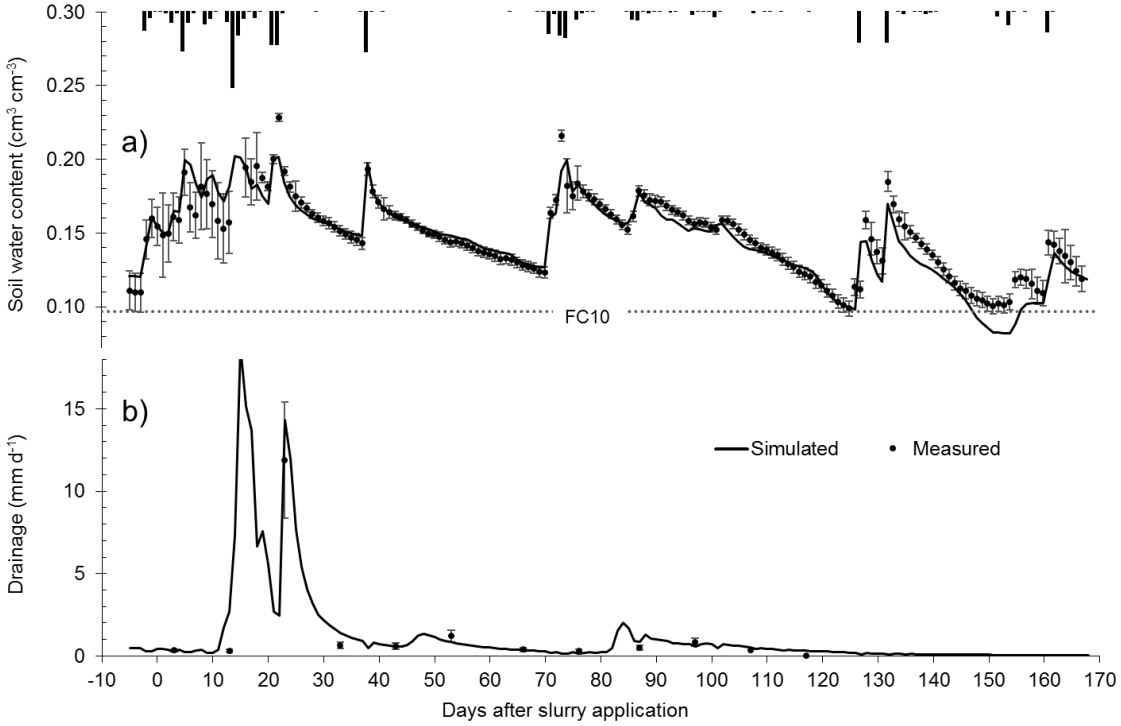

Figure 4.2 - Simulated versus measured values for: a) soil water content at 25 cm and b) drainage at 100 cm. Sandy soil, 2014-2015 crop season (calibration). (FC_{10} is the soil water content at field capacity at 10 kPa.)

Figure 4.2 describes the behaviour of a very permeable soil as the SS in this study, which is reflected by a rapid SWC and D responses to the precipitation inputs. The soil shows low to medium-low SWC (0.10 to 0.20 cm^3 cm^{-3}), not being optimum for N mineralization (Campbell & Biederbeck, 1982) and nitrification, except on the last days (Haynes et al., 1986), often with sharp variations due to rainfall events (Fig 4.2.a). During the precipitation days, the SWC at the depth of 25 cm rises abruptly above the FC_{10} line, meaning that D is occurring to the

underlying soil layers and eventually out of the profile. In fact, during the period between 10 and 30 days after slurry application there is a considerable amount of D (Fig 4.2.b) which introduces in this system the potential for NO_3^- leaching. Graphically there is a good fit between simulated and measured values for both SWC at the depth of 25 cm and D at the bottom of the profile. The model reproduced closely the variations of soil moisture as a result of precipitation and crop uptake, in both wetting and drying periods. Regarding D at 100 cm, the model closely predicted the peak in day 25 and the lower values in the remaining days on which D was measured at the bottom of the lysimeters.

Figure 4.3 shows the simulated and measured values for the T at the depth of 25 cm, after soil water calibration during the 2014-2015 crop season. The temperature range (approximately 8-22 ºC) is favourable for N mineralization (Stanford *et al*., 1973), NH_3 volatilization (Sommer *et al*., 1991) and denitrification (Dobbie & Smith, 2001), nonetheless it is not the optimum T for nitrification (Haynes *et al*., 1986). A reasonably good model fit to the measured T is observed, with the highest deviations occurring during the period from 10 to 80 days after slurry application, coinciding with the period of higher water dynamics in the soil. This may impact the simulation of the soil N transformations, as T is one of the abiotic factors entering the process equations.

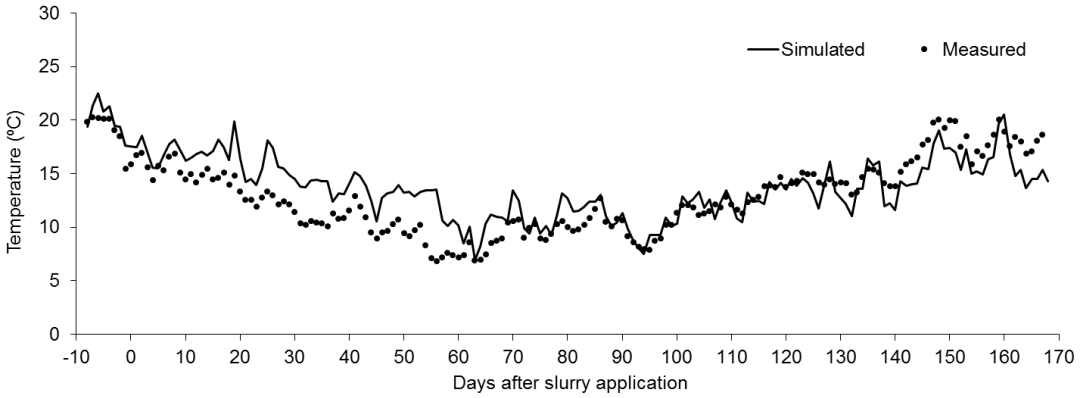

Figure 4.3 - Simulated versus measured values for the soil temperature at the depth of 25 cm. Sandy soil, 2014-2015 crop season (calibration).

4.1.1.2 Nitrogen related variables

As presented in section 3.2.2, the expected N mineralization for the sandy soil during the simulation period of the 2014-2015 season, should be around 7.9 kg ha^{-1}. For the model to predict this mineralization, the partition of the measured soil OM among the different pools was performed by the “wizard assistant” without being necessary to calibrate the default interpool coefficients, as shown in Table 4.2. This Table also shows the parameters regulating the N transformations, which were calibrated using N emission fluxes as control variables. These new values for the parameters will increase the potential both for nitrification and denitrification as shown by the model process based equations (section 2.71). Thus, depending upon the

soil moisture conditions this can result in higher NO_3^- and N_2O emissions (higher N_2O fraction from nitrification process) as compared to the use of the default parameters. The NH_3 volatilization constant was not changed by the calibration process.

Table 4.2- Initial and calibrated values for the OM partitioning and for N related parameters. Sandy soil, 2014-2015 crop season (calibration)

Parameter	Initial value	Calibrated value	Parameter	Initial value	Calibrated value
OM partitioning coefficients			N transformation parameters		
SR IH	0.3	0.3	NH_3 volatilization constant	1000	1000
FR FH	0.6	0.6	Nitrification rate	1.00E-09	2.00E-09
FH IH	0.6	0.6	Nitrification N_2O fraction	0.0016	0.0026
IH SH	0.7	0.7	Denitrification rate	1.00E-13	2.00E-13

where SR IH is the slow residue pool to intermediate soil humus pool coefficient, FR FH is the fast residue to fast humus coefficient, FH IH is the fast humus to intermediate humus coefficient and IH SH is the intermediate humus to slow humus coefficient, all these coefficients are decimal fractions.

Figure 4.4 shows the temporal series of the NO_3^- leaching flux (φNO_3^-) at the depth of 70 cm and N_2O emission flux (φN_2O) from the soil surface after calibration of the parameters in Table 4.2. The water filled pore space (WFPS) was added to this Figure in order to help interpreting the results.

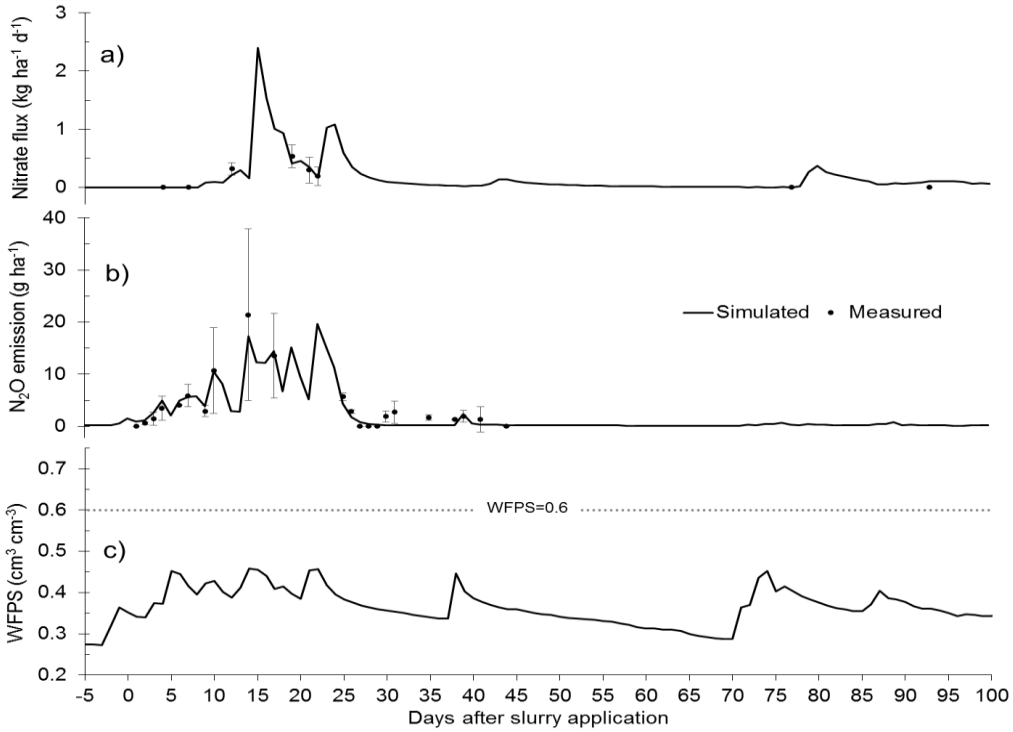

Figure 4.4 - Simulated versus measured values of: a) NO_3^- flux at the depth of 70 cm; b) N_2O emissions at soil surface. c) Water filled pore space. Sandy soil, 2014-2015 crop season (calibration).

The φNO_3^- follows the tendency of D (Fig 4.2.b) showing the importance of convection as a solute transport process in these conditions (winter rainy season). The φN_2O, which represents

N_2O losses to the atmosphere, occurred until approximately one month after slurry applications, showing values of low/medium magnitude, varying between 0 and 20 g ha^{-1}. The percentage of WFPS during the simulation period is always below 0.6 (Fig 4.2.c) due to the high conductivity for water and consequent low retention capacity. This means that there are no especially favourable conditions for the denitrification process (Dobbie *et al*. 1999), suggesting that most of the N_2O is a "by-product" from the nitrification process.

A good fit between the simulated and measured values is observed for both N fluxes in Figure 4.4 that shows an overall agreement both in the emission peaks and the temporal tendencies.

4.1.1.3 Goodness of fit evaluation

Soil water content, drainage and temperature:

Complementing the graphical analysis, the goodness of the calibration was quantified through the calculation of statistical indicators (section 3.2.4). Table 4.3 shows the results for SWC, D and T during 2014-2015 crop season.

Table 4.3 shows that after model parameterization, the statistical indicators presented values far from the pretended (see Section 3.2.4). The simulations yielded considerably high RMSE values, in comparison with the MSD of the observations. EF presented poor values for SWC and T, even negative value for SWC, indicating that the measurements mean was a better estimator than the model itself (Wilcox *et al*., 1990). After calibrating the model, an overall improvement of the indicators is observed, especially for RMSE, EF and R^2. However, for T the indicators barely changed due to the fact that a direct calibration of the soil heat parameters is not possible at the moment. Both SWC and D fulfil the condition presented in Section 3.2.4, as RMSE is either lower or very similar to MSD, and the respective values of EF and R^2 meet the minimum advised for soil water simulations (Ma *et al*., 2011). The results in Table 4.3 are similar to the ones presented by Cameira *et al*. (2014) and Ma *et al*. (2012).

Table 4.3 - Goodness of fit analysis for the soil water content at 25 cm, water drainage at 100 cm depth and soil temperature at 25 cm depth, before (BC) and after (AC) model calibration. Sandy soil (2014-2015)

	SWC (cm^3 cm^{-3})		D (mm d^{-1})		T (ºC)	
Indicators	BC	AC	BC	AC	BC	AC
Number of samples	174		12		177	
$\overline{O}$	0.15		1.45		12.94	
MSD	0.01		0.43		-	
$\overline{S}$	0.11	0.14	1.40	1.70	13.77	13.87
RMSE	0.04	0.01	1.49	0.76	2.49	2.46
RMSE/$\overline{O}$ (%)	30	7	103	52	19	19

EF (%)	-106	86	78	94	58	60
R^2	0.75	0.88	0.87	0.99	0.59	0.61

where SWC is the soil water content, D is the soil water drainage, T is the soil temperature, $\overline{O}$ is the measured mean, MSD is the mean standard deviation, $\overline{S}$ is the simulated mean, RMSE is the root mean squared error, EF is the model efficiency and R^2 is the determination coefficient (dim.).

Figure 4.5 shows the correlation between the measured and simulated values and the correspondent coefficients of determination (R^2).

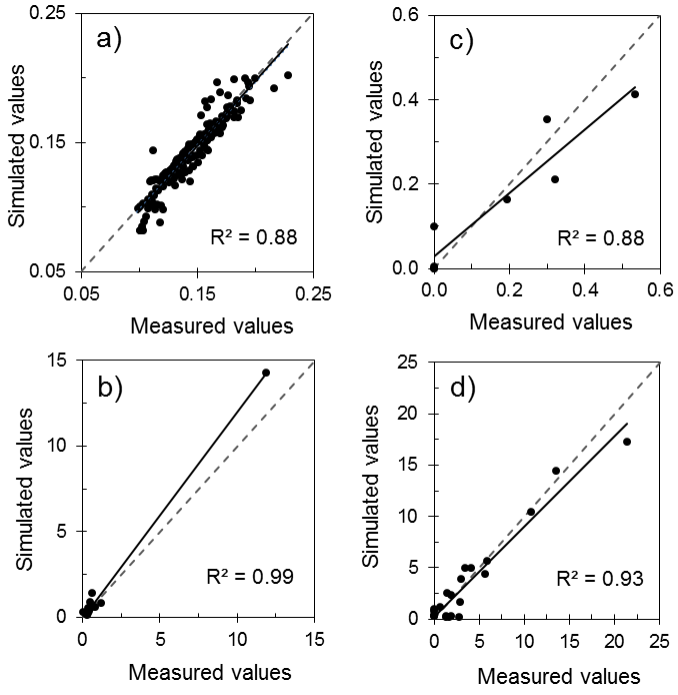

Figure 4.5 - Simulated versus measured values correlation comparison for: a) soil water content; b) drainage; c) nitrate leaching and d) N_2O flux to the atmosphere. Sandy soil, 2014-2015 (calibration).

The 1:1 line is also shown (dashed line), indicating that the model has a slight tendency to underestimate both N fluxes. In the case of the SWC, the model tends to underestimate the smaller values and overestimate the larger ones.

Based both upon the graphical display of simulations versus measurements and on the results from the goodness of fit analysis for the 2014-2015 crop season, it is possible to conclude that the model is estimating the soil-water related processes within the desired range of accuracy, thus the calibrated parameters were used to proceed the calibration process, now focusing on the OM and N related parameters.

Nitrogen component

Table 4.4 shows the goodness of fit indicators for the simulation of φNO_3^- at the depth of 70 cm, and for the estimation of the φN_2O to the atmosphere. Overall, the calibrated model yielded good results for these indicators. For both φNO_3^- and φN_2O, RMSE is lower the average

standard deviation of the measured data which is considered as an excellent result for N related processes (Cameira *et al*, 2000). The correspondent values of EF and R^2 meet the minimum required for N-related simulations (Ma *et al*., 2011). Similar results were obtained by Fang *et al*. (2012) and Cameira *et al*. (2007).

Based in the above and the analysis of Figure 4.4, it is possible to conclude that the model is estimating the N related processes within the desired range of accuracy, thus the calibrated soil water and N parameters are kept for the validation phase.

Table 4.4 - Goodness of fit analysis for NO_3^- and N_2O emissions after model calibration. Sandy soil (2014-2015).

Indicator	φNO_3^- (kg ha^{-1})	φN_2O (g ha^{-1})	Indicator	φNO_3^- (kg ha^{-1})	φN_2O (g ha^{-1})
Number of samples	8	22	RMSE	0.06	1.39
$\overline{O}$	0.17	3.80	RMSE/$\overline{O}$ (%)	37	37
MSD	0.09	2.20	EF (%)	89	93
$\overline{S}$	0.14	3.54	R^2	0.93	0.93

where φNO_3^- is the nitrate flux, φN_2O is the nitrous oxide emission, $\overline{O}$ is the measured mean, MSD is the mean standard deviation, $\overline{S}$ is the simulated mean, RMSE is the root mean squared error, EF is the model efficiency and R^2 is the determination coefficient (dim.).

4.1.2 Sandy loam soil

4.1.2.1 Soil water content, drainage and soil temperature

Table 4.5 shows the initial and calibrated values of saturated hydraulic conductivity (K_{sat}) and soil moisture at field capacity (θ_{10}). Unlike what happened with the sandy soil, here the calibration process did not result in significant variation in K_{sat} and θ_{10}. Only a 13% increase of the water retention at field capacity was produced for the bottom soil layer. This means that the measurements and the Brooks and Corey estimation procedure used in the model, were able to describe well the soil hydraulic properties. The correspondent Brooks and Corey functions for soil water retention and hydraulic conductivity are presented in Figure 4.6.

Table 4.5 - Initial and calibrated values of the selected soil hydraulic parameters, for the sandy soil loam soil

Parameter	Layer (cm)	Initial value	Calibrated value	Variation (%)
K_{sat}	0-50	2.59	2.59	0
θ_{10}		0.263	0.296	13
K_{sat}	50-100	2.59	2.59	0
θ_{10}		0.263	0.264	0

where K_{sat} is the saturated hydraulic conductivity in cm.hr^{-1}; and $\theta_{1/10}$ is the field capacity at 10 kPa in cm^3.cm^{-3}.

Figure 4.6 shows the typical hydraulic behaviour of a sandy loam soil, which is low/medium saturated conductivity and overall high water retention capacity with a slow decrease, as

pressure head increases. After calibration the 50-100 cm layer presents an increase in water retention curve when compared to the original parameterization.

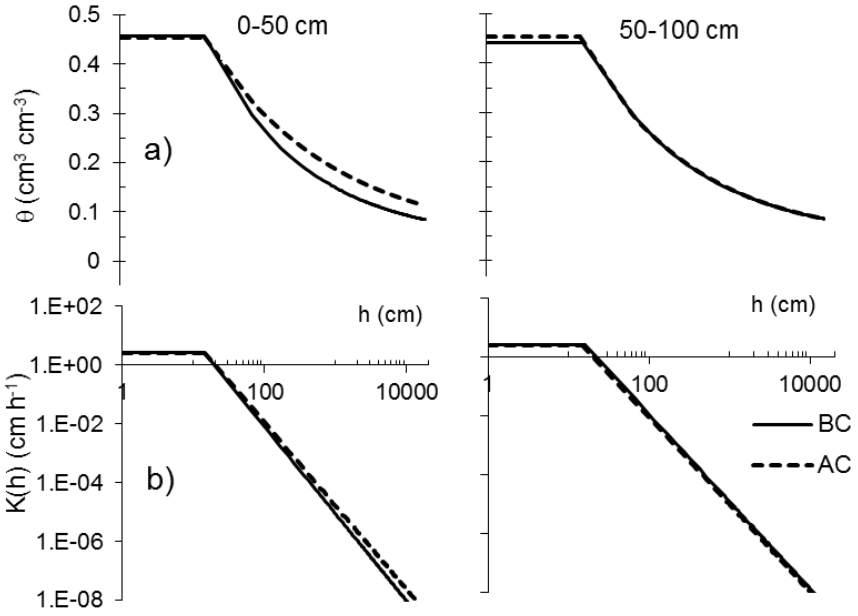

Figure 4.6 - Hydraulic properties of the sandy loam soil described by the Brooks and Corey functions before (BC) and after (AC) calibration: a) Water retention; b) Saturated hydraulic conductivity.

Figure 4.7 shows the SWC at the depth of 20 cm, and the D at the bottom of the profile (100 cm) after the calibration of the soil hydraulic properties. P during the simulation period in 2014-2015 crop season is also shown. The X-axis represents the number of days after slurry application, starting 10 days prior to the application (X = -10).

The sandy loam soil shows considerably higher SWC values (0.25 to 0.4 $cm^3.cm^{-3}$), as compared to the sandy soil, being in the optimum range for N mineralization (Campbell & Biederbeck, 1982) and nitrification, except from 70 days after application onwards (Haynes et al., 1986). The response to the precipitation inputs is smoother when compared to the sandy soil (Fig 4.7.a). The SWC at the depth of 20 cm is often bellow field capacity and the number of days with D to the underlying soil and eventually out of the profile is less. The D flux follows the P pattern as in the sandy soil although in the present case the two peaks are 30 % lower (Fig 4.7.b). Like in the sandy soil, the period with the higher occurrence of D is the one between 10 and 30 days after slurry application, where the potential for NO_3^- leaching is higher.

A good fit between simulated and measured values is shown both for the SWC at the depth of 20 cm and D at the depth of 100 cm. The model closely reproduced the variations of soil moisture as a result of precipitation and crop uptake, in both wetting and drying periods. Regarding D at 100 cm, the model closely predicted the lower D peak in day 25 as compared to the sandy soil.

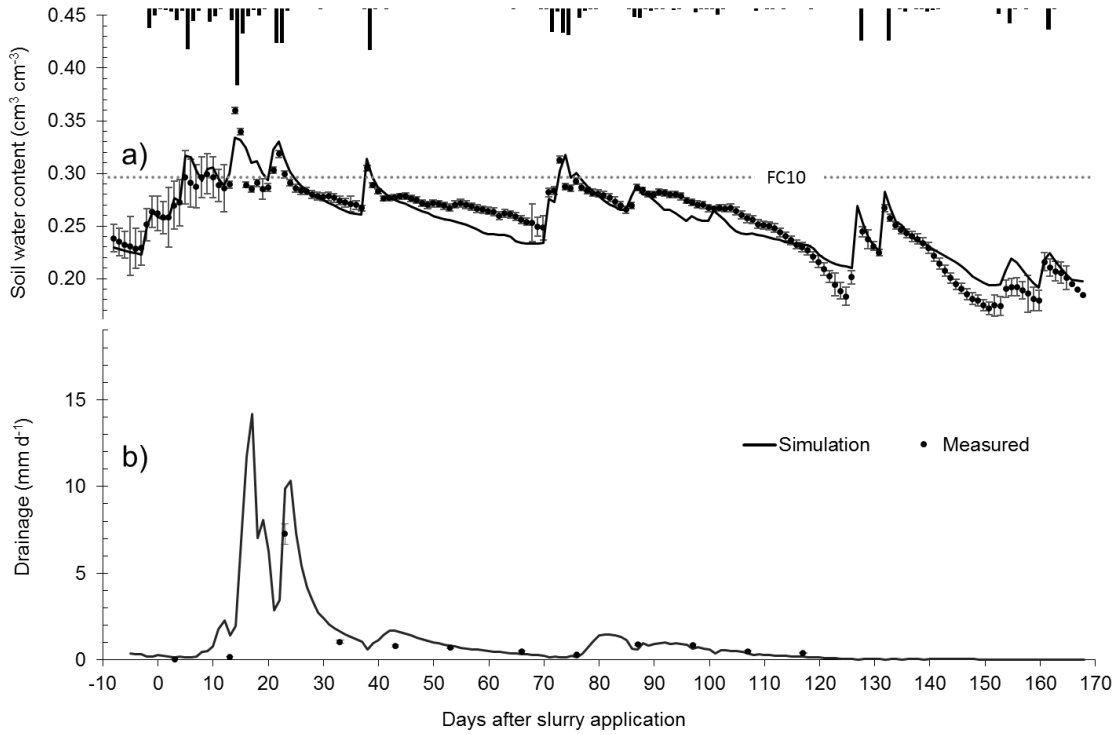

Figure 4.7 - Simulated versus measured values for: a) soil water content at 20 cm and b) drainage at 100 cm. Sandy loam soil, 2014-2015 crop season (calibration). (FC10 is the soil water content at field capacity at 10 kPa.)

Figure 4.8 shows the simulated and measured values for T, after calibration of the soil water in the SLS during the 2014-2015 crop season. No significant differences between the temporal series of T is observed between SS and SLS, meaning that this temperature range is favourable for N mineralization (Stanford *et al*., 1973), NH_3 volatilization (Sommer *et al*., 1991) and denitrification (Dobbie & Smith, 2001), but less for nitrification (Haynes *et al*., 1986). Like for the SS a good fit is observed, with the highest deviations occurring during the period from 10 to 80 days after slurry application. However the magnitude of the deviations is smaller than in SL due to the more accurate simulations of SWC during this period. The T simulation is also better at the end on the studied period than in the SS

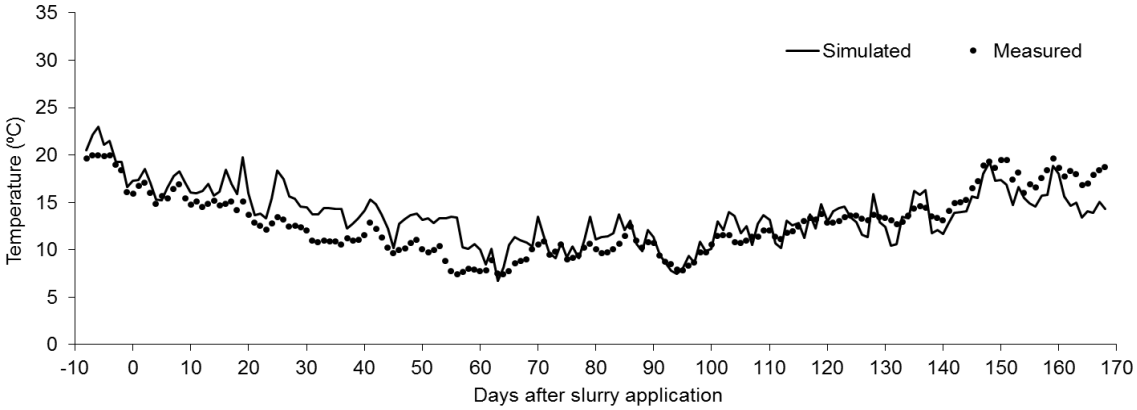

Figure 4.8 - Simulated versus measured values for the soil temperature at the depth of 25 cm. Sandy loam soil, 2014-2015 crop season (calibration).

4.1.2.2 Nitrogen related variables

Based in Scheppers & Mosier (1991), the expected N mineralization for the SLS during the simulation period of the 2014-2015 crop season is around 14.3 kg ha^{-1}. This was achieved with the values of OM partitioning coefficients presented in Table 4.6. In this case it was necessary to decrease the coefficients responsible for the transformation between the fast decomposing and the slow decomposing pools. This means that there is, during time, a higher amount of fast and medium fast decomposing OM in this soil than in the sandy soil. As to the parameters that influence the N transformations, the calibration led to an increase in the NH_3 volatilization constant and in the denitrification coefficient. This is probably associated to the fact that after the precipitation events, this soil presents wetter conditions during larger periods than the sandy soil. Thus, after calibration the model will predict higher NH_3 volatilization and denitrification activity, resulting in a higher N loss through gaseous emission to the atmosphere, when compared to the default parameters based predictions.

Table 4.6 - Initial and calibrated values for the OM partitioning and for N related parameters. Sandy loam soil, 2014-2015 crop season (calibration)

Parameter	Initial value	Calibrated value	Parameter	Initial value	Calibrated value
OM partitioning coefficients			N transformation parameters		
SR IH	0.3	0.3	NH_3 volatilization constant	1000	2000
FR FH	0.6	0.6	Nitrification rate	1.00E-09	1.00E-09
FH IH	0.6	0.1	Nitrification N_2O fraction	0.0016	0.0016
IH SH	0.7	0.3	Denitrification rate	1.00E-13	1.50E-13

where SR IH is the slow residue pool to intermediate soil humus pool coefficient, FR FH is the fast residue to fast humus coefficient, FH IH is the fast humus to intermediate humus coefficient and IH SH is the intermediate humus to slow humus coefficient, all these coefficients are decimal fractions.

Figure 4.9 shows the temporal series of the φNO_3^- at the depth of 70 cm and the φN_2O from the soil surface into the atmosphere. WFPS was added to this Figure in order to help interpreting the results.

Like in the sandy soil, the φNO_3^- follows the D pattern, showing the importance of convection as a solute transport process in these conditions. However, the leaching pecks are considerably lower in this case. Concerning φN_2O it can be verified that they started after slurry application and stopped a few days sooner than in the sandy soil. The flux varied between 0 to 75 g ha^{-1}. The period of larger N_2O emissions (0 to 25 days after slurry application) coincides with the period where WFPS is above 0.6, meaning that in this case, unlike what happened in the SS, there were favourable conditions for the denitrification process to occur (Dobbie et al. 1999). This indicates that N_2O is a “by-product” from the nitrification process and also a result of the denitrification process, thus yielding larger values of φN_2O than in the sandy soil. This is

in accordance to the low conductivity for water of this soil and consequently its higher water retention capacity, when compared to the sandy soil, and thus, allowing anaerobic conditions during larger periods.

A good fit between the simulated and measured values is observed in Figure 4.9 for both N fluxes, where and overall agreement concerning both value peaks and temporal distributions is observed. Nevertheless, it appears that the model started to simulate N_2O emissions to the atmosphere earlier than what is shown by the lysimeter measurements.

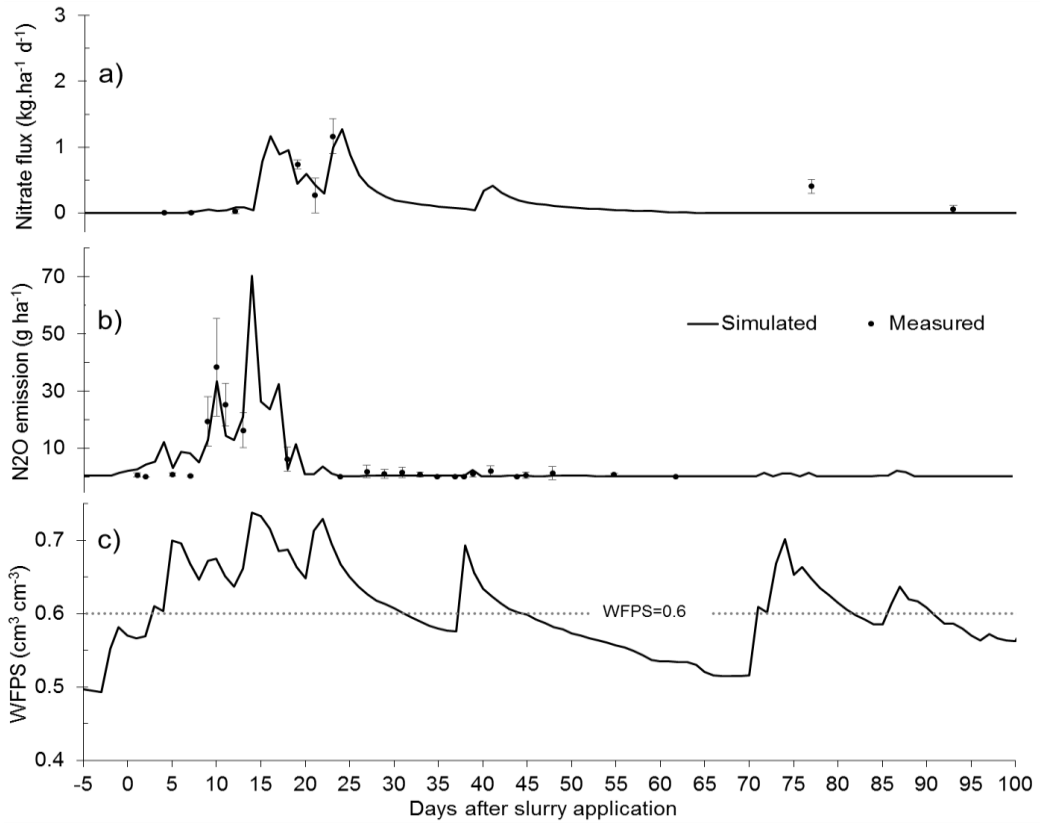

Figure 4.9 - Simulated versus measured values of: a) NO_3^- flux at the depth of 70 cm; b) N_2O emissions at soil surface. c) Water filled pore space. Sandy loam soil, 2014-2015 crop season (calibration).

4.1.2.3 Goodness of fit evaluation

Soil water content, drainage and temperature

Complementing the graphical analysis, the goodness of the calibration was quantified through the calculation of statistical indicators. Table 4.7 shows the results for SWC, D and T during 2014-2015 crop season.

Table 4.7 shows that that the uncalibrated model yielded poor results for the indicators, far from the pretended values presented in section 3.2.4. High values of RMSE were obtained, when compared to MSD, additionally EF and R^2 yielded poor values for SWC and T (D had a reasonable EF and R^2).

Table 4.7 - Goodness of fit analysis for the soil water content at 25 cm, water drainage at 100 cm depth and soil temperature at 25 cm depth, before (BC) and after (AC) model calibration. Sandy loam soil (2014-2015)

	SWC ($cm^3\ cm^{-3}$)		D ($mm\ d^{-1}$)		T (ºC)	
Indicator	BC	AC	BC	AC	BC	AC
Number of samples	175		12		177	
$\overline{O}$	0.26		1.13		12.92	
MSD	0.01		0.09		-	
$\overline{S}$	0.23	0.25	1.67	1.28	13.94	13.71
RMSE	0.03	0.01	0.95	0.49	2.10	2.07
RMSE/$\overline{O}$ (%)	13	5	84	44	16	16
EF (%)	16	87	79	94	61	62
R^2	0.56	0.81	0.88	0.94	0.69	0.68

where SWC is the soil water content, D is the soil water drainage, T is the soil temperature, $\overline{O}$ is the measured mean, MSD is the mean standard deviation, $\overline{S}$ is the simulated mean, RMSE is the root mean squared error, EF is the model efficiency and R^2 is the determination coefficient (dim.).

After calibration, an overall improvement of the statistical indicators is observed, especially for RMSE, EF and R^2. However, this was only observed for SWC and D, as T indicators barely change due to the fact that a direct calibration of the soil heat parameters is not possible at the time. Both SWC and D fulfil the condition of RMSE being very similar to MSD, and the respective values of EF and R^2 meet the minimum advisable for soil water and N-related calibrated simulations (Ma *et al*., 2011). The results in Table 4.7 are similar to the ones obtained by Cameira *et al*. (2014) and Ma *et al*. (2012).

Figure 4.10 shows the correlation plot between the measured and simulated values and the R^2 for all variables. In relation with the SS, for this case the values show a larger dispersion when compared to the regression lines, which in turn are always very close to the 1:1 line.

For this soil, the model shows a tendency to very slightly overestimate the N emissions. In fact, the SS calibration of the soil water component yielded slightly better results when compared to the SLS, confirming that it is easier to simulate the coarser soils. Nonetheless, based on the results from the goodness of fit analysis of the calibrated model for the 2014-2015 crop season, in the sandy loam soil, it is possible to conclude that the model is estimating the soil-water related processes within the desired range of accuracy, thus the calibrated parameters were kept for the calibration of the OM and N related parameters.

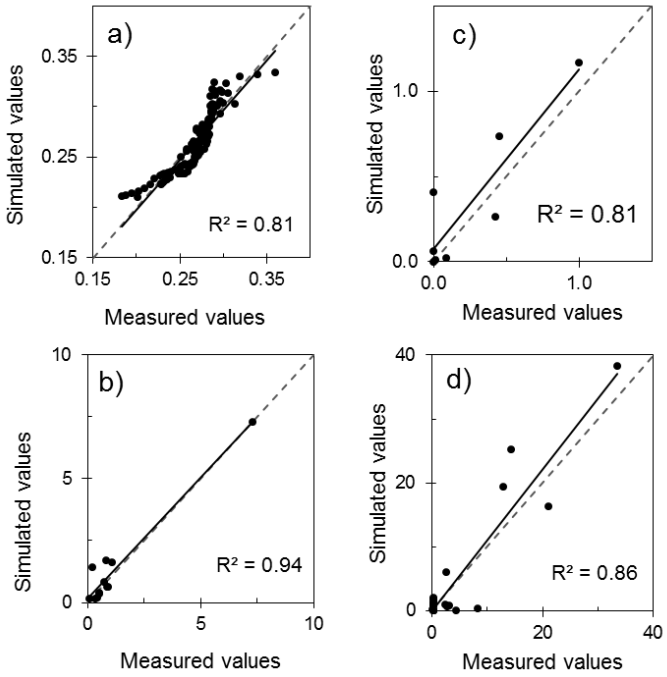

Figure 4.10 - Simulated versus measured values correlation comparison for: a) soil water content; b) drainage; c) nitrate leaching and d) N2O flux to the atmosphere. Sandy loam soil, 2014-2015 (calibration).

Nitrogen component

Table 4.8 shows the goodness of fit indicators for the φNO_3^- in the soil at the depth of 70 cm, and the φN_2O to the atmosphere.

Table 4.8 - Goodness of fit analysis for NO_3^- and N_2O emissions after calibration. Sandy loam soil (2014-2015).

Indicator	φNO_3^- (kg.ha^{-1})	φN_2O (g.ha^{-1})	Indicator	φNO_3^- (kg.ha^{-1})	φN_2O (g.ha^{-1})
Number of samples	8	24	RMSE	0.20	3.66
$\overline{O}$	0.33	4.95	RMSE/$\overline{O}$ (%)	59	74
MSD	0.10	2.45	EF (%)	76	85
$\overline{S}$	0.25	4.60	R^2	0.81	0.86
RMSE	0.20	3.66			

where φNO_3^- is the nitrate flux, φN_2O is the nitrous oxide emission, $\overline{O}$ is the measured mean, MSD is the mean standard deviation, $\overline{S}$ is the simulated mean, RMSE is the root mean squared error, EF is the model efficiency and R^2 is the determination coefficient (dim.).

Unlike what happened for the SS, the RMSE of the N simulation is not smaller than the MSD. Nevertheless, they are very close, which is considered very good for the simulation of N related processes given the big dynamics of this element in the soil-plant system. Furthermore, the respective values of EF and R^2 meet the minimum advisable for the N-related calibrated simulations (Ma et al, 2011). Similar results were obtained by Fang *et al*. (2012) and Cameira *et al*. (2007). Based in what was exposed above, and the graphical analysis of the Figure 4.8,

it is possible to conclude that the model is estimating the N related processes within the desired range of accuracy, thus the calibrated parameters are kept for the validation phase.

4.2 Model validation

This section shows the results of running the model for datasets independent of the previous ones that is, using different slurry and climatic data sets. Also the soil, water and N related parameters that resulted from the calibration process were kept unchanged.

4.2.1 Sandy soil

4.2.1.1 Soil water content, drainage and soil temperature

Experimental data regarding SWC, D and T were used to validate the model for the period between 15 of November 2015 and 13 of March 2016. Slurry was applied on 23 of November 2015, corresponding to day 0 in x-axis. Figure 4.11 shows simulated and measured values for the SWC at the depth of 25 cm, the D at the bottom of the profile (100 cm). A good fit between simulated and measured values is shown for both SWC at the depth of 25 cm and D at the bottom of the profile.

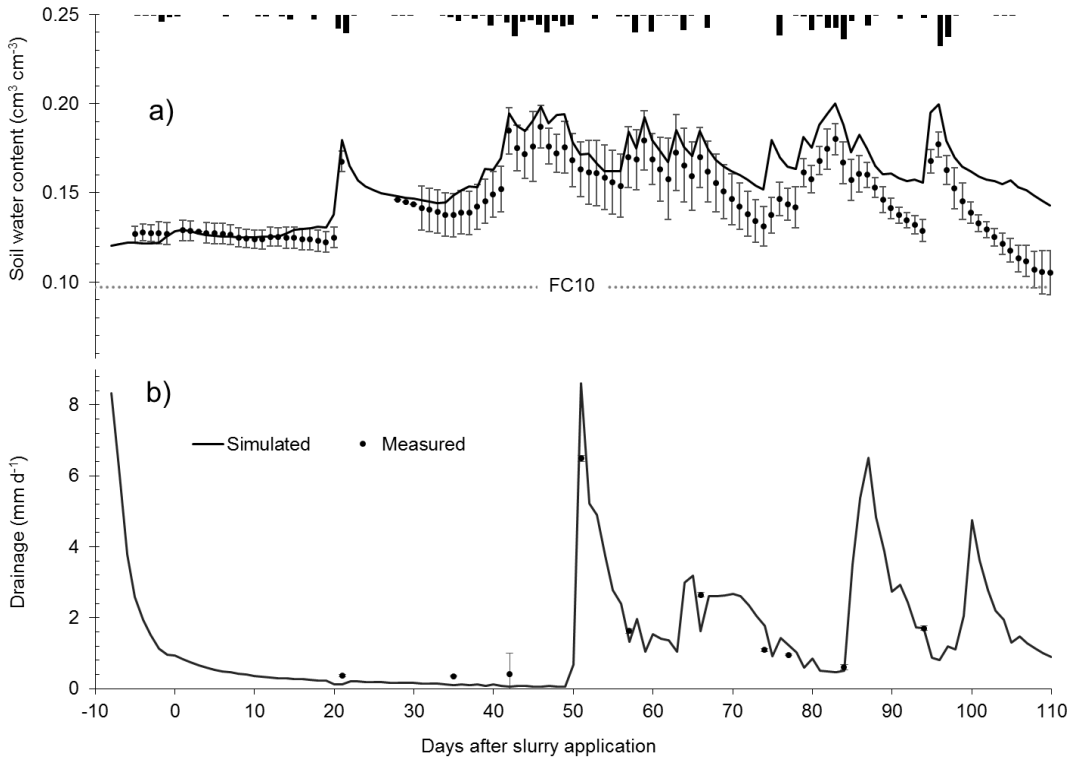

Figure 4.11 - Simulated versus measured values for: a) soil water content at 25 cm and b) drainage at 100 cm. Sandy soil, 2015-2016 crop season (validation). (FC10 is the soil water content at field capacity at 10 kPa.)

The model reproduced closely the variations of SWC as a result of P and crop uptake, in both wetting and drying periods. However, from 90 days after slurry applications to the end, larger deviation occurs between simulated and measured values. Since the other variables

depending upon soil water did not reflect this deviation, we can assume that there was some error with the SWC measurement probe. Regarding D at 100 cm, the model closely predicted the peak in day 55 and the lower values in the remaining days where D was measured at the bottom of the lysimeters.

Figure 4.12 shows the simulated and measured values of T at the depth of 25 cm, in the soil water validation during the 2015-2016 crop season. The T range is slightly smaller when compared to the SS calibration during 2014-2015 (approximately 10-16 ºC), maintaining the same effects on the N transformation processes in the soil as shown in SS calibration. A reasonably good fit is observed, with the highest deviations occurring from 80 days after slurry application onwards, coinciding with the large deviations in SWC period (Figure 4.11).

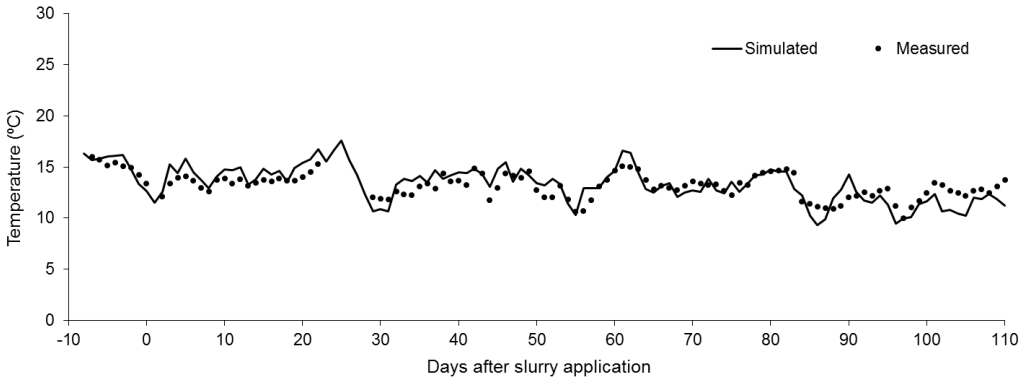

Figure 4.12 - Simulated versus measured values for the soil temperature at the depth of 25 cm. Sandy soil, 2015-2016 crop season (validation).

4.2.1.2 Nitrogen related variables

Experimental data regarding the N fluxes was available for two crop seasons, corresponding to the periods from 5 of November 2012 to 13 of March 2013 (2012-2013 season) and 12 of November 2013 to 7 of April 2014 (2013-2014 season), no data from 2015-2016 season was available for N fluxes. Figure 4.13 shows the temporal series of φNO_3^- at the depth of 70 cm and φN_2O, for both crop seasons, where WFPS was added to this in order to help interpreting the results.

For 2012-2013, simulated φNO_3^- follows the tendency the measure values. Concerning φN_2O, as during the calibration crop season, for both the validation seasons the WFPS never exceeds 0.6, it can be verified that, for the present conditions, it occurred until approximately 40 days after slurry application, where the values were of low/average magnitude, varying between 0 and 30 g ha^{-1}. In the 2013-2014 season the fluxes only start increasing (from zero) at 40 days after slurry application, much later than the previous crop season. The magnitude for both variables is also lower than in 2012-2013. The difference in the N emission patterns between the validation seasons is most likely due to the P during the initial period (-10 to 40 days after

slurry application), with moderate amount of rainfall for 2012-2013 and almost none to very low amounts of P inputs for 2013-2014, affecting both SWC and D during this period.

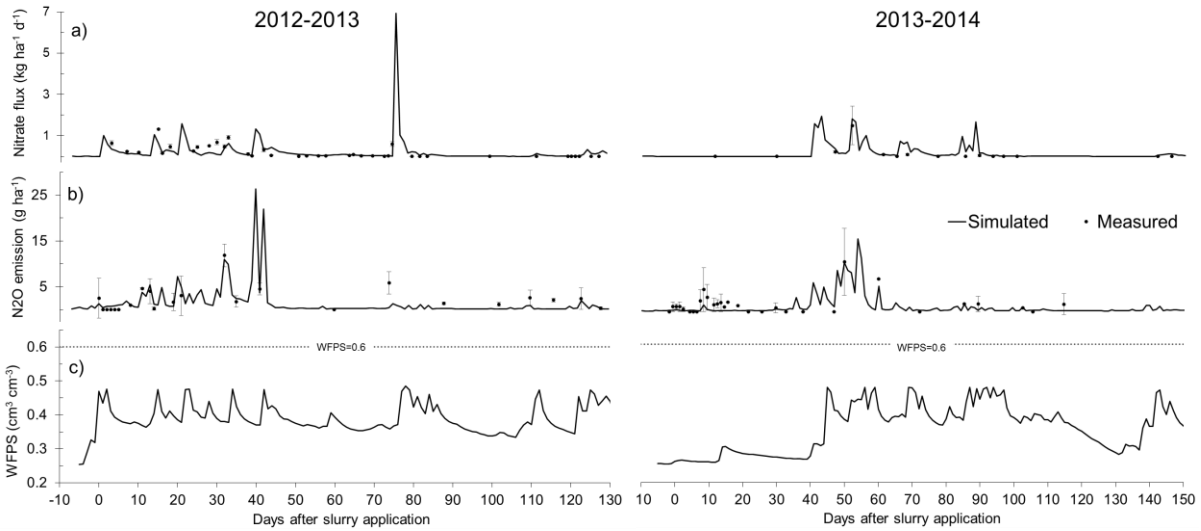

Figure 4.13 - Simulated versus measured values of: a) NO_3^- flux at the depth of 70 cm; b) N_2O emissions at soil surface. c) Water filled pore space. Sandy loam soil, 2012-2013 and 2013-2014 crop seasons (validation).

Like for the soil water component variables, a reasonable fit is observed for these validation datasets, being the statistical indicators lower than the ones obtained for the calibration. However, this is an expected and accepted by the scientific community fact since for the validation procedure the parameters are not changed.

4.2.1.3 Goodness of fit evaluation

Table 4.9 shows the statistics for SWC, D and T, during 2015-2016 crop season; and φNO_3^- and φN_2O, during 2012-2013 and 2013-2014 crop seasons. The Table shows lower values than the calibration for EF for all variables.

Table 4.9 - Goodness of fit analysis for the validation of WWC at 25 cm, D at 100 cm depth and T at 25 cm (2015-2016) and the NO_3^- flux and N_2O emission flux (2012-2013 and 2013-2014). Sandy soil.

	2015-2016			2012-2013		2013-2014	
Validation	SWC	D	T	φNO_3^-	φN_2O	φNO_3^-	φN_2O
	$cm^3\ cm^{-3}$	$mm\ d^{-1}$	ºC	$kg\ ha^{-1}$	$g\ ha^{-1}$	$kg\ ha^{-1}$	$g\ ha^{-1}$
Number of samples	112	10	111	39	22	15	31
RMSE	0.02	0.79	1.04	0.27	1.58	0.20	1.21
EF (%)	23	89	25	57	66	72	72

where SWC is the soil water content, D is the soil water drainage, T is the soil temperature, φNO_3^- is the nitrate flux, φN_2O is the nitrous oxide emission, , RMSE is the root mean squared error, EF is the model efficiency (%),

The extremely low modelling efficiency of the SWC is due to the overestimation at the end of the simulation period already discussed. All the other indicators present expected values for

validation. As both φNO_3^- and φN_2O are to some extent dependant of SWC and D, and the fact that both SWC and D were simulated and validated as reasonably good, at least reasonable results were expected for both φNO_3^- and φN_2O during the validation. Both variables obtained good results for the considered indicators, during both 2012-2013 and 2013-2014 crop seasons datasets. Similar results as the ones in Table 4.9 were described by Cameira et al. (2014), Fang et al. (2012) and Ahmed et al. (2007).

This means that the model was able to reproduce the soil water and N related variables, for the different precipitation and other climatic patterns occurring through the validation years as well as for different properties of the slurry applied during the same period, realistically.

4.2.2 Sandy loam soil

4.2.2.1 Soil water content, drainage and soil temperature

Like in the SS, experimental data regarding SWC, D and T were used to validate the model for the period between 15 of November 2015 and 13 of March 2016. Slurry was applied on 23 of November 2015, corresponding to day 0 in x-axis. Figure 4.14 show SWC at the depth of 20 cm and the D at the bottom of the profile (100 cm).

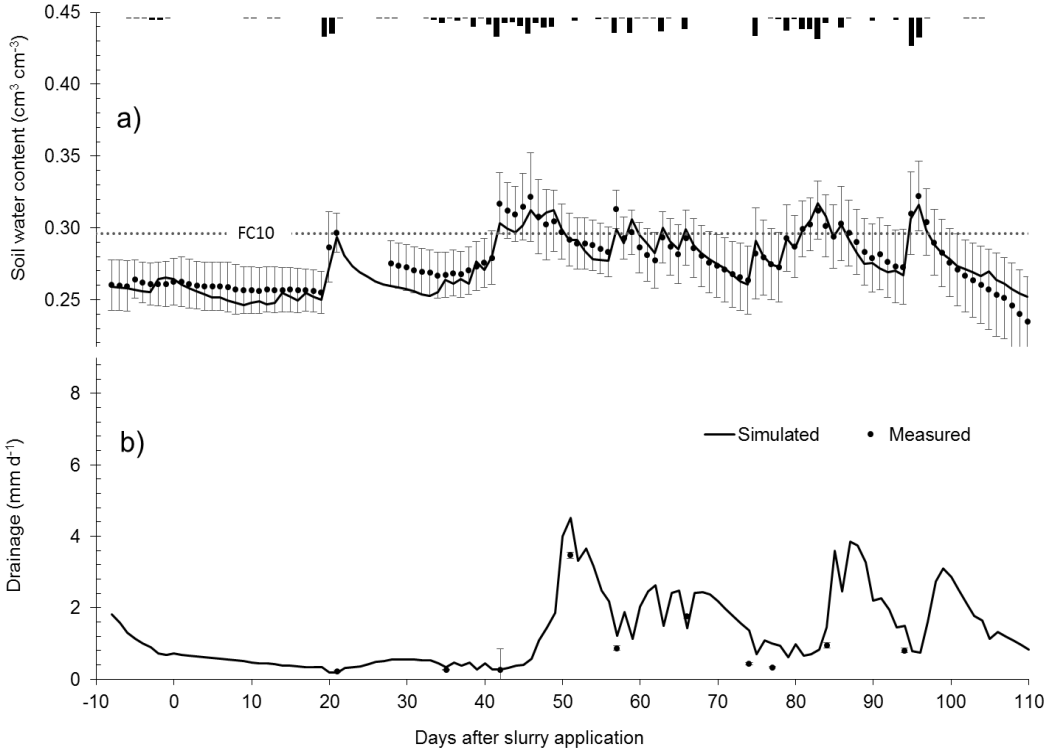

Figure 4.14 - Simulated versus measured values for: a) soil water content at 20 cm and b) drainage at 100 cm. Sandy loam soil, 2015-2016 crop season (validation). (FC10 is the soil water content at field capacity at 10 kPa).

Like in the sandy soil, a good fit between simulated and measured values is shown for both SWC at the depth of 20 cm and D at the bottom of the profile. It is possible to verify that the model was able to reproduce firmly the variations of SWC caused by P and crop uptake, during

both wetting and drying period. Unlike the sandy soil, no significant deviation between predicted and measured values is observed, resulting in a very good fit for the SWC. Concerning D, the model was able to simulate closely the various peaks in and the lower values in the remaining days where D was measured at the bottom of the lysimeters.

Figure 4.15 shows the simulated and measured values of T at the depth of 20 cm, in the soil water validation during the 2015-2016 crop season. The T range is similar when compared to the SS validation for T (approximately 10-16 ºC), maintaining the same effects on the N transformation processes in the soil as shown in SS calibration. A reasonably good fit is also observed, with the highest deviations occurring from 85 days after slurry application onwards.

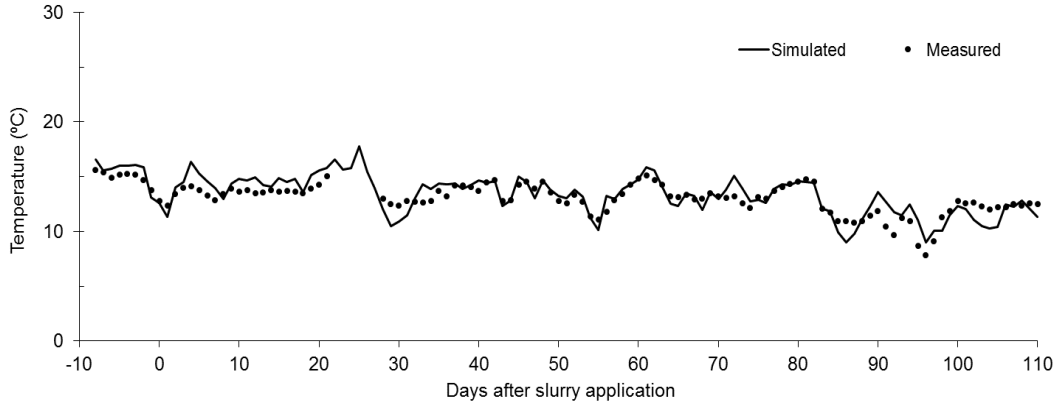

Figure 4.15 - Simulated versus measured values for the soil temperature at the depth of 20 cm. Sandy loam soil, 2015-2016 crop season (validation).

4.2.2.2 Nitrogen related variables

Figure 4.16 shows the temporal series of φNO_3^- at the depth of 70 cm and φN_2O, for both 2012-2013 and 2013-2014 crop seasons.

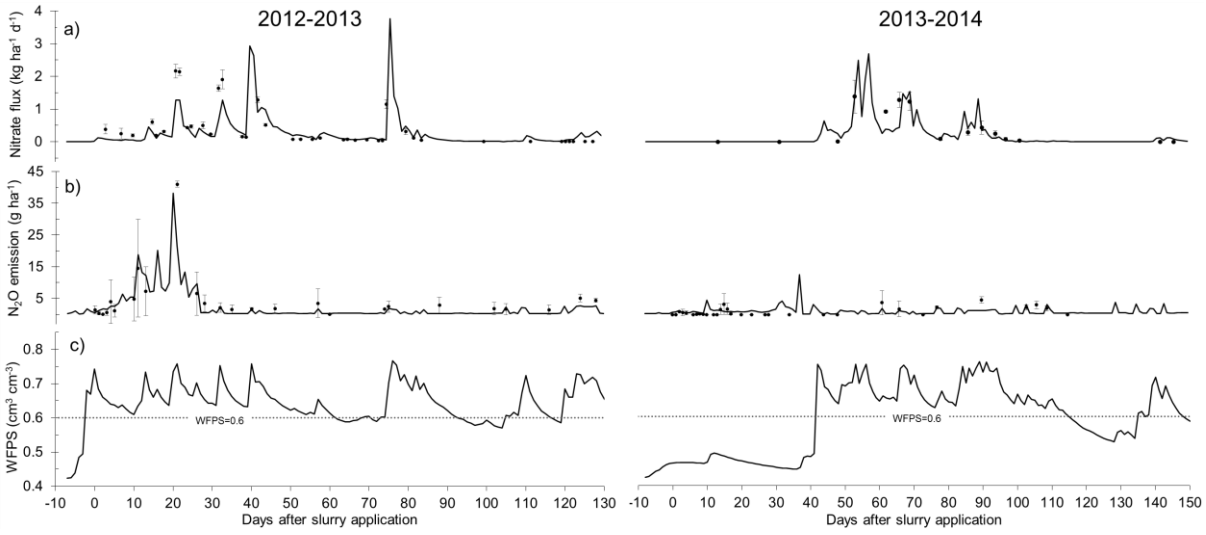

Figure 4.16 - Simulated versus measured values of: a) NO_3^- flux at the depth of 70 cm; b) N_2O emissions at soil surface. c) Water filled pore space. Sandy loam soil, 2012-2013 and 2013-2014 crop seasons (validation).

During 2012-2013, once again it is possible to verify that φNO_3^- follows the tendency of the measured values. Unlike the sandy soil, for the sandy loam soil, it is possible to observe that WFPS exceed 0.6, on most days of the validation seasons, meaning that a higher amount of φN_2O is expected for this type of soil. In fact, it can be verified that φN_2O, for the present conditions, occurred until approximately one month after slurry application where the values were of average magnitude, varying between 0 and 40 g ha^{-1}. For 2013-2014, it is possible to observe the same delay of the sandy soil, in flux increasing concerning φNO_3^-, also possibly due to the P distribution on this season, nonetheless, these values are almost identical to the results from sandy soil for the same crop season, possibly due to the higher mineralization gain in this soil. Regarding φN_2O, both predicted and simulated values are unexpectedly low with low variability, with the simulated values most likely due to the high values of φNO_3^-, which implies a lack of N availability in the soil, susceptible to being lost through denitrification.

Like for the soil water component variables, a reasonable fit is observed between predicted and measured (validation dataset) values, however these are still worse when compared to the fit observed for the calibration (Figure 4.9) which is expected considering that for the validation procedure, the parameters are not changed in order to yield good results, like for the calibration. However the validation for the soil water component yielded better fit than its calibration counterpart.

4.2.2.3 Goodness of fit evaluation

Complementing the graphical analysis, the goodness of the calibration was quantified through the calculation of statistics. Table 4.10 shows the statistics for SWC, D and T, during 2015-2016 crop season; φNO_3^- and φN_2O, during 2012-2013 and 2013-2014 crop seasons.

Table 4.10 - Goodness of fit analysis for the validation of soil water content, water drainage at 100 cm depth and temperature (2015-2016 crop season) and the NO_3^- flux and N_2O emission flux (2012-2013 and 2013-2014 crop seasons). Sandy loam soil

Indicators	2015-2016			2012-2013		2013-2014	
	SWC	D	T	φNO_3^-	φN_2O	φNO_3^-	φN_2O
	$cm^3\ cm^{-3}$	$mm\ d^{-1}$	ºC	$kg\ ha^{-1}$	$g\ ha^{-1}$	$kg\ ha^{-1}$	$g\ ha^{-1}$
Number of samples	112	10	111	43	26	15	32
RMSE	0.01	0.56	0.98	0.28	4.25	0.29	1.46
EF (%)	84	79	51	77	71	68	-28

where SWC is the soil water content, D is the soil water drainage, T is the soil temperature, φNO_3^- is the nitrate flux, φN_2O is the nitrous oxide emission, , RMSE is the root mean squared error, EF is the model efficiency (%).

Table 4.10 presents reasonably good values for RMSE and EF in the validation procedure, for all variables, except φN_2O for 2013-2014 dataset. For both SWC and D fairly good results of

RMSE and EF were obtained, which is in accordance to what is observed in Figure 4.14. Nonetheless, T obtained average results, which was already justified earlier. Considering that both φNO_3^- and φN_2O are dependant of SWC and D to some extent, directly or indirectly, and the fact that both SWC and D were simulated and validated yielding good results, a good simulation was expected for both φNO_3^- and φN_2O during the validation. Unsurprisingly, both variables obtained good results for considered indicators, during both 2012-2013 and 2013-2014 crop seasons datasets. The only exception being φN_2O for 2013-2014, with a negative EF, suggesting that the prediction error is higher than the variability of measurements, possibly caused by the low variability of the measured data during this crop season (thus low deviation from the measurements mean), which is common in agricultural systems according to Cameira *et al*. (2014), Fang *et al*. (2012) and Youssef *et al*. (2006). Similar results as the ones in Table 4.10 were described by Cameira *et al*. (2014), Fang *et al*. (2012) and Ahmed *et al*. (2007).

Considering the graphical analysis and what was exposed above, it is possible to conclude that the results are within the desired range of accuracy, thus the model was validated with the tested calibrated parameters, and ready for further applications. Furthermore, better results were obtained for the sandy loam soil using the 2015-2016 and 2012-2013 validation datasets, while for the sandy soil the best results were achieved with the 2013-2014 validation dataset.

4.3 Model applications

With the RZWQM2 calibrated and validated, that is, simulating the water and N related processes for the winter oat systems with the desired accuracy, the model was used to make predictions of the water and N budgets for six different scenarios. The objective was to investigate the influence of soil water and T upon the N path losses in this production system. Four scenarios consist in different hydrological years and the last two present an increase in air temperature as estimated in the scope of the climate changes (see section 3.3.1).The balances were calculated for the soil layer from the surface to the depth of one meter.

The scenarios (Sc) are summarized below and are based in the actual agricultural practices

Sc VDy: Precipitation from the very dry year obtained from a 30 years' data series;

Sc Dy: Precipitation from the dry year obtained from a 30 years' data series;

Sc M: Precipitation from the average year obtained from a 30 years' data series;

Sc W: Precipitation from the wet year obtained from a 30 years' data series;

Sc B1: Sc M and average temperature increase of 1.8 ºC;

Sc AF1: Sc M and average temperature increase of 4 ºC.

4.3.1 Water and N balances

Table 4.11 shows the soil water balance terms, for both sandy and sandy loam soils, for different precipitation regime scenarios.

Table 4.11 – Soil water balance for the precipitation scenarios. Sandy and sandy loam soils (04/11 to 22/04),

Precipitation scenario	Si	Sf	ΔS		P	AET		D	
	mm	mm	mm	(%)	mm	mm	(% P)	mm	(% P)
Sandy soil									
VDy	111	121	10	4	284	108	38	165	58
Dy		129	18	5	348	112	32	219	63
M		143	32	7	464	116	27	316	73
W		148	37	6	600	119	21	444	79
Sandy loam soil									
VDy	215	201	-14	-5	284	155	55	143	50
Dy		206	-9	-2	348	161	46	196	56
M		215	0	0	464	170	37	294	63
W		223	8	1	600	179	30	413	70

where VDy is very dry, Dy is dry, M is medium, W is wet, Si is the initial water stored in the soil, Sf is the final water stored in the soil, ΔS is the variation of the water stored in the soil, P is the total precipitation, AET is the total actual evapotranspiration and D is the total water drainage.

Table 4.11 shows that in term of soil water balance the model in coherent in predicting the contribution of the precipitation inputs for both AET and D. The average contribution of the precipitation to evapotranspiration is 42 % higher for the SLS than for the SS. D as a part of precipitation is 12.5 % lower for the SLS. The difference between soils is higher for the very dry and dry scenarios. For high amounts of precipitation both soils behave similarly in term of water loss out of the system. Thus, the model yields conceptually correct results, where it is worth noting that P is able to mask, to some extent, the difference between SS and SLS hydraulic properties.

Table 4.12 shows the N balance terms, for both sandy and sandy loam soils. For the very dry scenario, it is possible to observe a large accumulation of N in both soils, possibly due to the very low input of water through P. A higher rate of N mineralization (N_{min}) occurs for the SLS, when compared to the SS, in association with the higher endogenous OM content, and soil moisture content retention for the SLS, as mineralization increase with wetness of the soil (Killham *et al*., 1993). N_{uptk} is similar for both soils, decreasing 27 and 23 % for the SS and the SLS respectively from scenario VDy to W. This similarity is most likely due to the fact of the slurry being applied on the day before sowing, meaning that most of the N will either be

accumulated in parts of the soil that the crop is unable to extract, or that it is lost from the crop-soil system. Concerning N leaching SS yielded higher values than SLS, which is expected considering both soils hydraulic properties. The contribution of leaching increases for both soils from the VDy to the W scenario while for the gas losses the opposite is verified. The average contribution of N_{leach} is 84 and 68 % for the SS and the SLS respectively, showing the SLS more sensitivity to the type of hydrological year.

Table 4.12 – Nitrogen balance for precipitation scenarios. Sandy and sandy loam soils, 2013-2014 crop season

Scenario	Si_N	Sf_N	ΔS_N	N_{fert}	N_{min}	N_{uptk}	N_{leach}	N_{gas}
	kg ha^{-1}						(%)*	
Sandy soil								
VDy	10	41	31	105	12	33	78	22
Dy		30	19	105	12	30	82	18
M		17	7	105	12	26	87	13
W		9	-1	105	13	24	88	12
Sandy loam soil								
VDy	8	82	73	105	23	31	46	54
Dy		70	62	105	23	29	65	35
M		52	43	105	23	27	79	21
W		36	28	105	23	24	84	16

where VDy is very dry, Dy is dry, M is medium, W is wet, S_i is the initial stored mineral N in the soil, S_f is the final stored mineral N in the soil, ΔS is the variation of the mineral N stored in the soil, N_{fert} is the total N input from fertilization, N_{min} is the N mineralization, N_{uptk} is the N uptake by the plant, N_{leach} is the N lost from drainage and N_{gas} is the N lost in the gaseous from volatilization, denitrification and nitrification.
* Percentage of the total N emissions.

Figure 4.17 shows the N output comparison (N_{leach} vs N_{gas}) for both soils, during the different hydrological years. Figure 4.17 shows that once again the differences between soil types in terms of N losses are higher for the VDy and Dy scenarios. For both soils, it is possible to verify pollution swapping between N_{leach} and N_{gas} as the scenario gets wetter where a decrease of N_{gas}, accompanied with an increase in N_{leach}, is observed. This is possibly due to the increasing amount of water input as it goes from a) to d), which most likely will leach most of the soluble N in the soil, and thus not allow it to be used for the denitrification process, additionally, the increasing wetness in the soil slows the nitrification rate (Monaghan & Barroclough, 1992), meaning that there will be less NO_3^- in the soil to fuel the denitrification process. Nonetheless, it displays expected N_{leach} and N_{gas} differences between soils, higher N_{leach} for SS and higher N_{gas} for SLS.

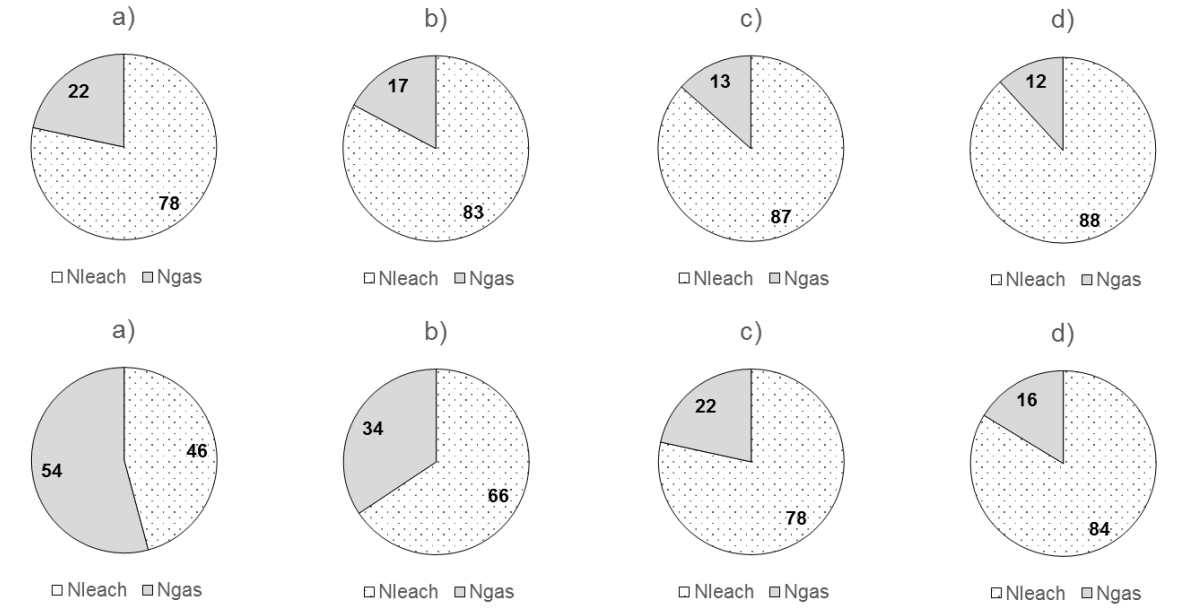

Figure 4.17 - N output from crop-soil system comparison for sandy soil (top) and sandy loam soil (bottom), in the different precipitation scenarios: a) very dry; b) dry; c) medium and d) wet.

Figure 4.18 shows the variation of N_2O and NH_3 emissions between VDy with the remaining hydrological years, for both soils. It is possible to verify that N_2O emissions are much more sensitive to wetness variations, it decreases significantly as the scenario gets wetter (in comparison to VDy), for both soils, however it is more significant for the SS than the SLS. The same is not observed for the NH_3 volatilization, as only small variations are verified, as the increasing wetness in the soil slows the volatilization down (Al-Kanani *et al*., 1991).

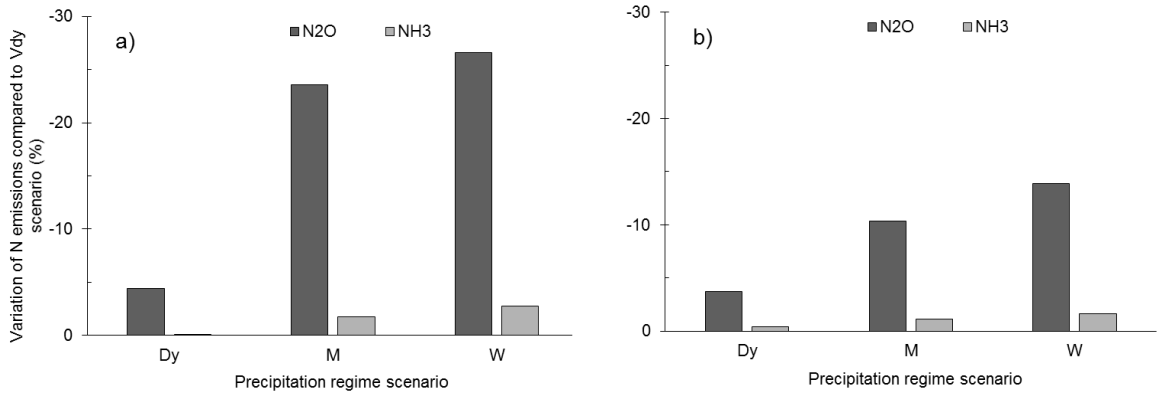

Figure 4.18 – N_2O and NH_3 variation for all hydrological years, in comparison with Vdy in the a) sandy soil and b) sandy loam soil (VDy – very dry; Dy – dry; M – medium; W – wet; N2O – N_2O emission losses; NH3 – NH_3 volatilization losses).

Figure 4.19 shows the contribution of the nitrification and denitrification processes to the N_2O emission for the different scenarios. It shows a tendency of the nitrification contribution to N_2O emission to increase as the hydrological year is wetter, for both soils. The effect of anaerobic conditions is visible only for the sandy soil due to the higher retention capacity and low conductivity for water in comparison with the sandy soil. For denitrification to occur is

necessary to have long periods of soil near saturation (Moisier *et al*., 1986) which does not happens on the sandy soil which is very permeable to water.

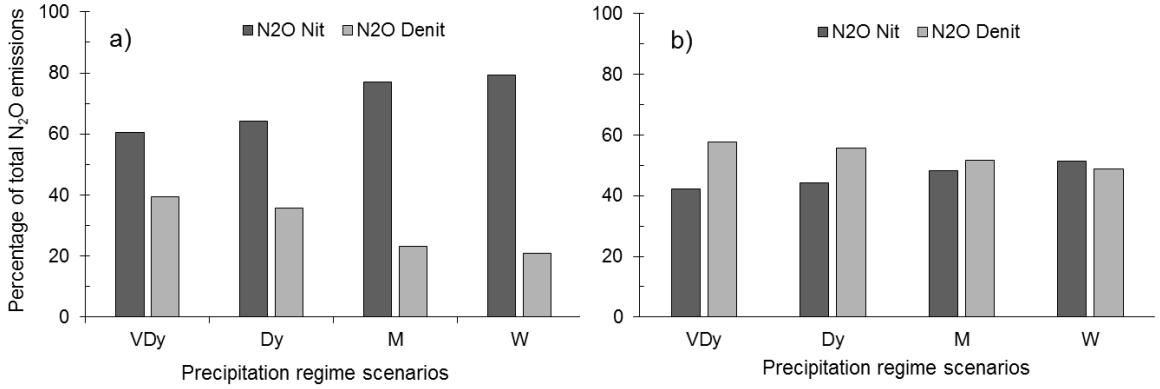

Figure 4.19 – Contribution of nitrification and denitrification for the total N_2O emission for: a) sandy soil and b) sandy loam soil. (VDy – very dry; Dy – dry; M – medium; W – wet; N2O Nit - N_2O resulting from nitrification process and N2O Denit - N_2O resulting from denitrification process).

Figure 4.20 shows the variation in N gas losses for the climate change temperature scenarios B1 and A1F1, which predict an increase of 1.8 and 4.0 ºC to the average annual temperature, respectively. The base for comparison is the scenario M (Medium) already presented before, so the hydrological conditions do not change among Scenarios.

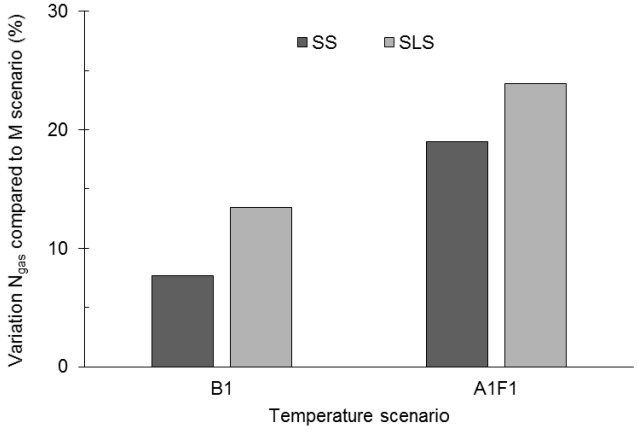

Figure 4.20 – Variation in N_{gas} losses during the temperature scenarios. Sandy and sandy loam soils.

The contribution of gas losses to the total N losses increases from the M to the warmer scenarios. This increase is gradual for both soils. The results show that for this type of production systems the most unfavourable climate change scenario (temperature increase of 4 ºC) may produce an increase of 25 % and 18 % in the N gas loss contributions for the SLS and the SS respectively. Some factors may explain this increase:

- N_{min} increases as the temperature increases, for both soils, considering that N mineralization rate is higher with higher temperatures so the N available for losses increase;

- Volatilization and denitrification rate also increases with the temperature (Black et al., 1985a; Ryden, 1986), thus explaining the increase of N_{gas} for the warmer scenarios B1 and A1F1, when compared to the normal scenario;
- As the N in the soil is more prone to be lost through gaseous emissions, a slight decrease in N_{leach} is expected and observed since the hydrological conditions did not change in this analysis;

Figure 4.21 shows the ammonia volatilization variation for the climate change temperature scenarios, compared to the M scenario, reinforcing the factors presented above, as it is possible to observe a clear influence of temperature increase in the NH_3 volatilization, where it increases for both soil, however SS has a larger increase with temperature than SLS. The highest variations/increases were observed for the A1F1 scenario, where a 4ºC increase in average annual temperature is projected.

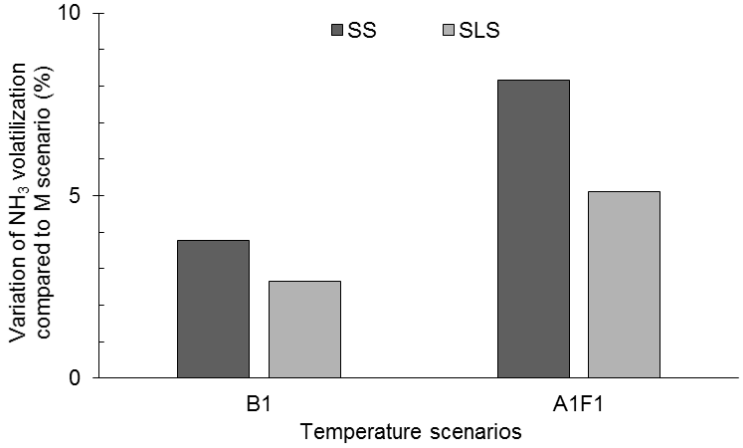

Figure 4.21 – Variation of NH_3 volatilization during the temperature scenarios, in comparison with M scenario. Sandy and sandy loam soils.

Figure 4.22 –shows the comparison between the contribution of the nitrification and denitrification processes in the N_2O emission.

Like in Figure 4.19, it is possible to verify that denitrification contributes more toward N_2O emission in the SLS, while nitrification contributes more for the SS. The increase in yearly average temperature for both B1 and A1F1 does not seem to affect greatly the different processes contribution to the N_2O emission, although there is indeed a (very small) influence. As the temperature increases, denitrification intensifies, emitting more N_2O, as shown in Figure 4.21.

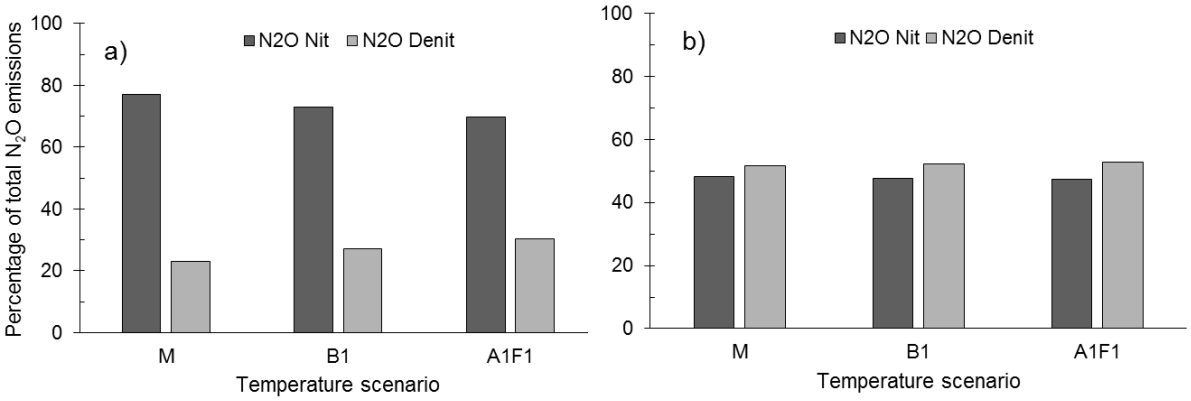

Figure 4.22 – Contribution of nitrification and denitrification for the total N_2O emission for: a) sandy soil and b) sandy loam soil. (N2O Nit - N_2O resulting from nitrification and N2O Denit - N_2O resulting from denitrification).

Figure 4.23 shows the N output comparison (N_{leach} vs N_{gas}) for both soils, during the different temperature scenarios plus Medium scenario. It is possible to verify clearly the effect of temperature on N_{leach} and N_{gas}, where N_{gas} increases steadily as the temperature increase and N_{leach} decreases, a prime example of pollution swapping. Like in Figure 4.17, expected N_{leach} and N_{gas} differences between SS and SLS, i.e. higher N_{leach} for SS and higher N_{gas} for SLS, are observed in this case.

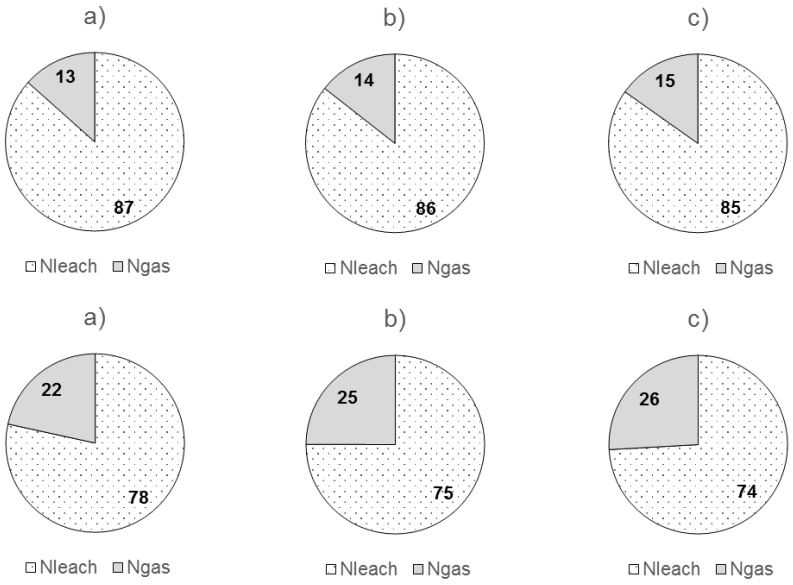

Figure 4.23 - N output from crop-soil system comparison for sandy soil (top) and sandy loam soil (bottom), in the different temperature scenarios: a) M; b) B1 and c) A1F1.

4.3.2 Nitrate leaching fluxes

For better interpretation of the NO_3^- leaching statistical results, Figure 4.24 shows the D fluxes, in the SS, for the same crop seasons which are responsible for the convective transport of NO_3^- in the soil, that is, NO_3^- leaching.

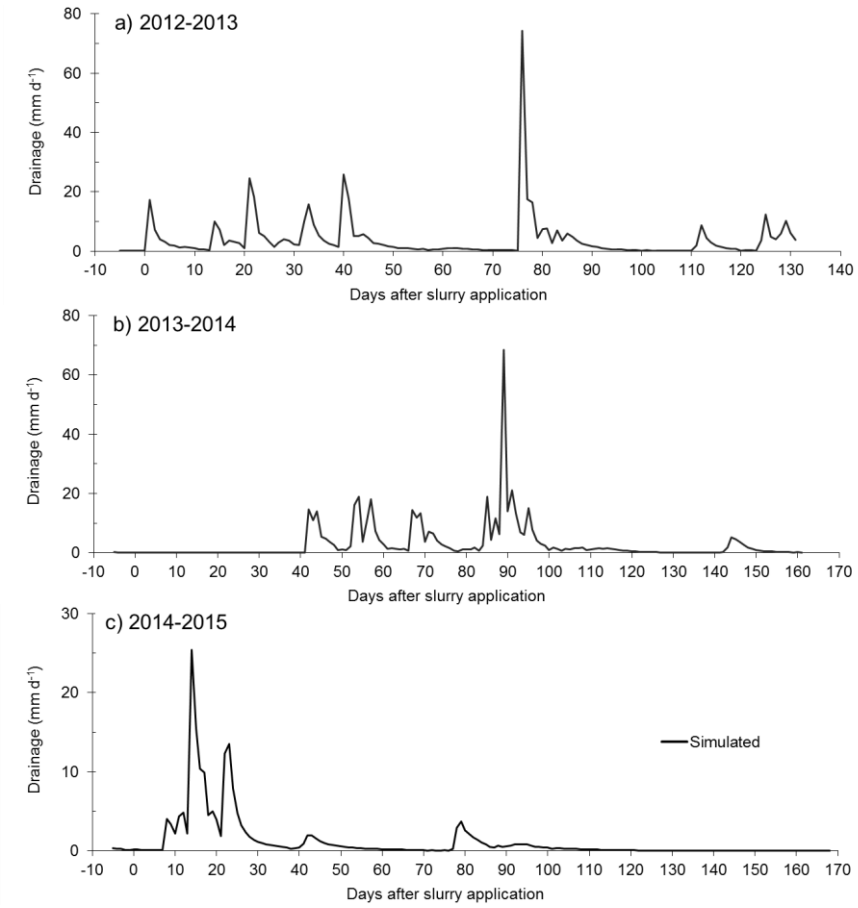

Figure 4.24 – Drainage fluxes at 70 cm depth, average for all slurry treatment in the SS.

Figure 4.25 shows the φNO_3^- means comparison between slurry treatments for the sandy soil. The treatments are: CTR, control, where no slurry was applied for control purposes; WSI, whole slurry injection, with the whole slurry being injected in the soil; WSM, whole slurry mobilization where the whole slurry was applied and incorporated in the soil; AWSM, acidified whole slurry mobilization, the whole slurry was subject of an acidification treatment prior to its application in the lysimeter, where it was incorporated; AWSS, acidified whole slurry surface, where the whole slurry was subject of an acidification treatment prior to its superficial application in the lysimeter. The tables containing the average means for each date and slurry treatment during all crop seasons for both SS and SLS is shown in Appendix 2.

Analysing the φNO_3^- means comparison between treatments, it is possible to verify the following points:

2012-2013

- 3 days after slurry application, a low leaching flux is observed for all treatments when compared to the remaining days. Considering that soil solution is sampled at a depth of 70 cm, most likely the NO_3^- that was produced after application didn't reach this depth at this time.

Even so, the whole slurry treatments (WS) show statistically high fluxes than the rest of the treatments, except for the acidified whole slurry with surface broadcast (AWSS);

- 21 days after application, the same behaviour as the previous run is observed, however with higher leaching losses. At this time, the processes leading to the NO_3^- production, namely the nitrification, of the more available ammonia, had time to occur. In the meantime there was enough travel time for the NO_3^- to reach the 70 cm depth, as shown by the water D at 70 cm in Figure 4.24a. In this date the acidified treatments (AS) produced significantly lower fluxes than the WS (except AWSS) and from the control. This is possibly a result of the acidification treatment, which delays the nitrification process (Chadwick et al., 2011);
- 30 days after application, we observe an overall decrease in φNO_3^-, possibly attributed to the φNO_3^- that happened before that leached most of NO_3^-. Low φNO_3^- is to be expected as only a small time lapse occurred since the previous run, which is hardly enough to produce and transport (considering the low water D on this day) NO_3^- to the depth of 70 cm;
- 41 days after application, the leaching fluxes are again higher. It seems that a considerable amount of the NO_3^- produced since 21 days after application, which was able to reach the depth of 70 cm, reinforce with the fact that it is possible to observe a significant D on this date. The whole slurry injection (WSI) treatment is the one presenting the most significantly high leaching losses, which is expectable considering that the injection of slurry in the soil, will promote and advance in the NO_3^- position in soil in comparison to the other application methods;
- 77 days after application, right after the largest D peak during this crop season, all treatment are significantly different. AWSS shows the highest φNO_3^-, possibly due to nitrification delay associated with as the acidification.

<u>2013-2014</u>

It is worth noting that the samples for NO_3^- concentration for this crop season only started 13 days after slurry application, with the next sampling being done only 31 days after application, and the third sample for this crop season being 48 days after application.

- 48 days after application, it is possible to verify a low leaching flux and no significant differences between all treatments. As 48 days have already passed since slurry application, these results are not unexpected, no substantial D was verified until 40 days after application (Figure 4.24b), meaning that any NO_3^- in the soil still had not reached 70 cm depth;
- 56 days after application, a large increase of leaching flux is observed, in fact the highest peak when compared to the other dates, taking into account the high water flux on this date. The fact that the AS have equal or higher NO_3^- fluxes than the WSI might be explained

by the effects of acidification on N dynamics in the soil, including higher content of NH_4^+ and delayed nitrification. Nonetheless, these differences are not significant, between AS and WS;

- 62 days after application, we observe the same pattern as we did in the previous run, albeit at much lower values of φNO_3^-, due to the low water fluxes at this time, where no differences are verified between AS and WS, except between AWSS and WSM;
- 70 days after, we observe the same pattern as we did in the previous run of 56 days after application, but with much lower leaching flux, as unlike 56 days after application, this date had a low D. No significant differences are observed between AS and WS;
- 90 days after application there are no significantly differences between treatments, where we are able to verify, once again, low values of φNO_3^-, possibly meaning that most of it was leached beforehand, which is reinforce with the largest D peak occurring before this sample date (Figure 4.24b).

2014-2015

- There are no significant differences between treatments for all tested runs/days;
- φNO_3^- variation over time is noticeable, with it increasing steadily from 10 to 14 days after application, followed by a large increase and peak at 17 days after application, which is immediately succeeded with a low φNO_3^- day (22 days after application), showing that leaching flux follows the tendency of D, as shown in Figure 4.24c;
- A time skip in terms of sampling is also observed, from 22 to 78 days after application, meaning that, most likely, a loss of relevant information regarding the NO_3^- at 70 cm depth in-between these dates occurred, especially during the peaking periods (22-26, 40-45 and 78-86).

It is possible to observe a increasing in number of days where there is not significant differences in NO_3^- fluxes means between treatments (0 days in 2012-2013, 2 days in 2013-2014 and 5 days for 2014-2015) and the decreasing in φNO_3^- magnitude as we advance in crop season, possibly and mostly due to the decreasing precipitation and consequent decrease in water flux, which reflects in the NO_3^- flux. This allows a possible NO_3^- accumulation in the soil, susceptible to being converted into N_2O, increasing the emissions of this N form, for the crop seasons with lower precipitations, and thus causing pollution swapping.

Higher fluxes for treatments that inject slurry into the soil (WSI), while the other treatments a lower flux was expected, however it is possible to verify constantly, that AWSS has larger φNO_3^- than WSI during 2013-2014 and 2014-2015, which is unexpected considering that the former is a superficial application and the latter an injected one. However this might be explained by the effects of acidification on N dynamics in the soil, including higher content of

NH_4^+ and delayed nitrification. Summarizing, concerning the sandy soil, the slurry acidification treatments did not present significant differences from the whole slurry injection treatment in 12 out of 15 dates.

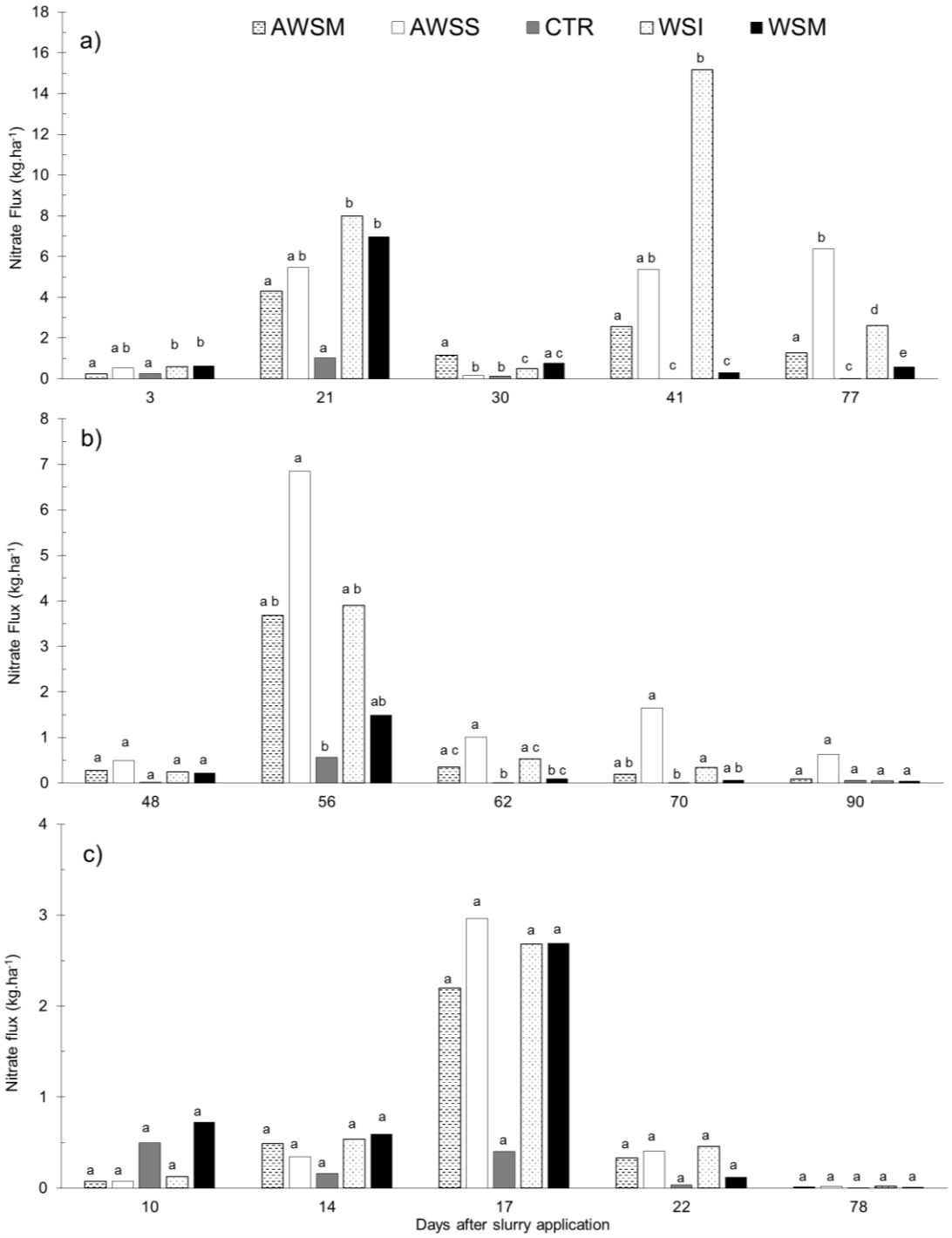

Figure 4.25 - Nitrate flux means comparison between slurry treatments of the sandy soil, for the (a) 2012-2013, (b) 2013-2014 and (c) 2014-2015 crop seasons.

Figure 4.26 shows the D fluxes, while Figure 4.27 shows the φNO_3^- means comparison between slurry treatments for the sandy loam soil

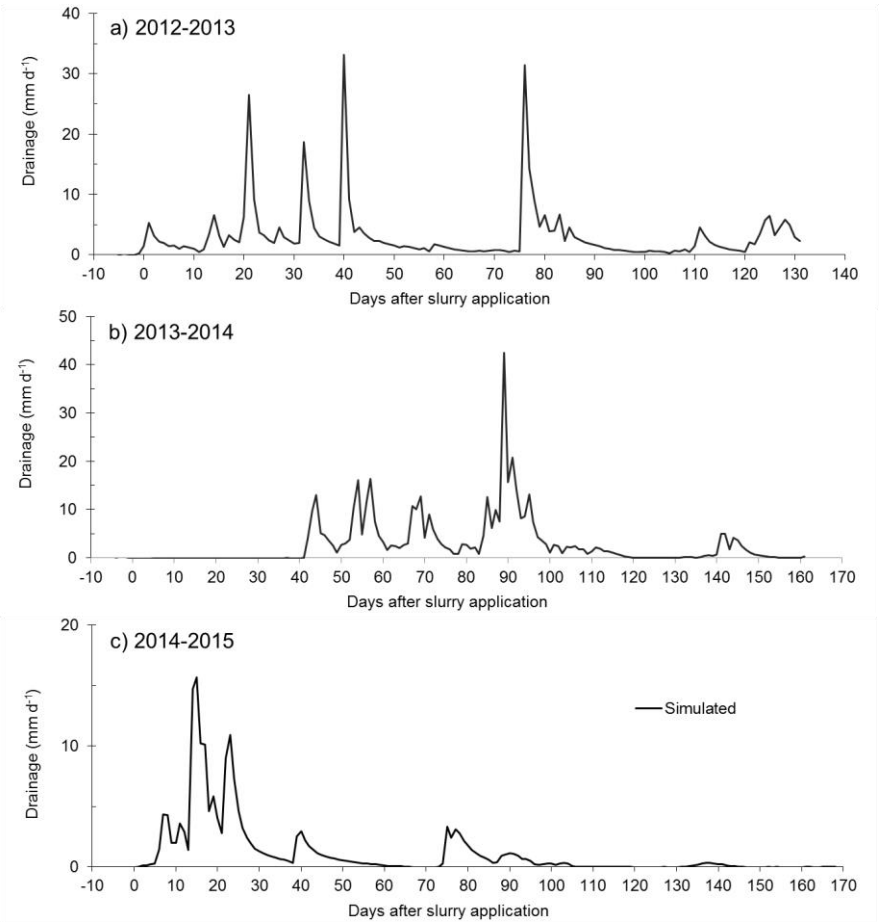

Figure 4.26 - Drainage fluxes at 70 cm depth, average for all slurry treatment in the SLS.

Analysing Figure 4.27, it is possible to verify the following points:

2012-2013

It is worth noting the difference in maximum peak values between SS and SLS, where SLS has much lower values when compared to SS.

- 3 days after application, low φNO_3^- values are observed. Most likely, the NO_3^- that was produced after application still has not reached the depth of 70 cm, which is reinforced with the low D values shown in Figure 4.26a. A statistical difference between WS and AS is verified (both acidified treatments yielded significantly higher leaching values than WSI), except for WSM;
- 21 days after application, like in the previous date, low leaching values are observed, even when a large D peak occurs during this date, possibly indicating that NO_3^- was depleted by denitrification process, higher probability of WFPS exceeding 0.6 in SLS, meaning higher intensity of denitrification process which consumes NO_3^- (Dobbie et al. 1999). Total difference between AS and WS is verified, with AWSS being significantly higher than the WS and CTR;

- 30 days after application, a slight decrease in φNO_3^- is observed, which like for the SS during the same date, is possibly due to low D for this date in conjunction with the little time lapse since the previous date, hardly any NO_3^- is produced and transported to the 70 cm depth;
- 41 days after application, an increase in φNO_3^- is detected, meaning that there is finally NO_3^- reaching the capsules at 70 cm depth (See Figure 4.26a), in particular for WSI. However, WSI has no significant differences to AWSS;
- 77 days after application, right after the largest D peak during this crop season, basically the same pattern observed during the previous run is verified again, except the fact that there are no significant difference between AS and WS.

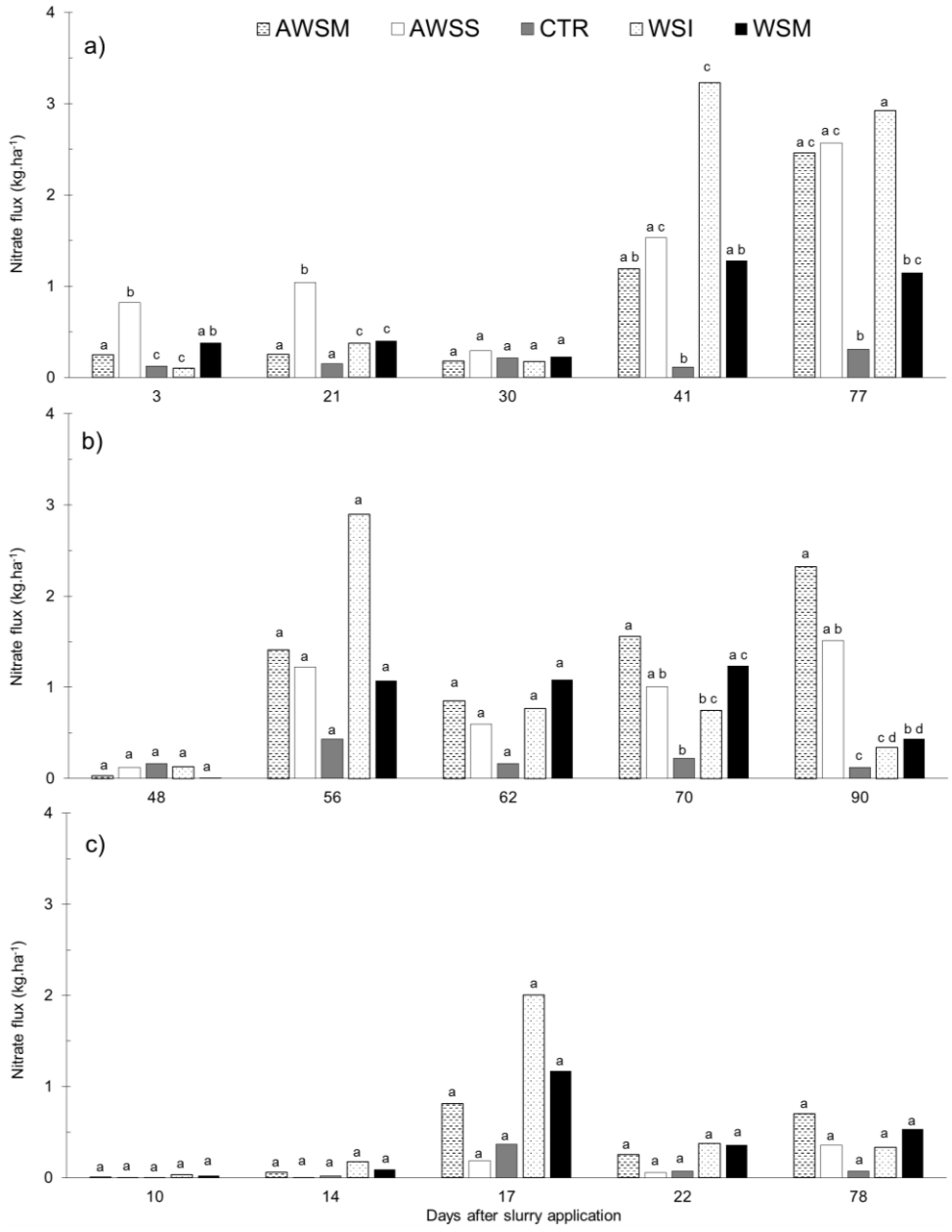

Figure 4.27 - Nitrate flux means comparison between slurry treatments of the SLS, for the (a) 2012-2013, (b) 2013-2014 and (c) 2014-2015 crop seasons.

2013-2014

During this crop season, and for the SLS, the same sampling methodology described for the SS is also applicable.

- 48 days after application, it is possible to verify a low leaching flux and no significant differences between all treatments. As 48 days have already passed since slurry application, these results are not unexpected, no substantial D was verified until 40 days after application (Figure 4.26), meaning that any NO_3^- in the soil still had not reached 70 cm depth, being accumulated in the soil;
- 56 days after application, there are no significant differences between treatments, however an increase of φNO_3^- in comparison to the previous run is observed, with WSI having the highest peak;
- 62 days after application, a small decrease in NO_3^- leaching is observed, in comparison to the previous date, possibly associated with the low D on this date. There are no significant differences between treatments;
- 70 days after application, now a slight increase in leaching flux is detected, as this date has a higher D compared to the previous date. Only AWSS is similar to WSI;
- 90 days after application, the values of φNO_3^- for each treatment are quite similar to the previous run, with AS having higher fluxes and WS having lower. The fact that the AS have significantly higher NO_3^- fluxes than the WSI might be explained by the effects of acidification on N dynamics in the soil, including higher content of NH_4^+ and delayed nitrification.

2014-2015

- No significant differences detected for all dates:
- Like in the SS, we observe a variation of φNO_3^- over time, with low fluxes at the start (10 and 14 days after application), peaking at 17 days and immediately dropping to low values at 22 days after application onwards showing that leaching flux follows the tendency of D, as shown in Figure 4.26c;
- A time skip in terms of sampling is observed, from 22 to 78 after application, meaning that, most likely, a loss of information regarding the NO_3^- at 70 cm depth in-between these dates occurred.

It is possible to observe different behaviour between crop seasons, as we did for the SS, like the increasing in number of days where there is not significant differences in φNO_3^- means between treatments (1 days in 2012-2013, 3 days in 2013-2014 and 5 days for 2014-2015) and a slight decreasing in φNO_3^- magnitude as we advance in crop season, possibly and mostly due to the decreasing precipitation and consequent decrease in water flux, which affect the

φNO_3^-. This allows a possible NO_3^- accumulation in the soil, susceptible to being converted into N_2O, increasing the emissions of this N form, for the crop seasons with lower precipitations, and thus causing pollution swapping.

Higher flux values were expected for WSI, in comparison to the other treatments, however, like in SS, it is possible to observe some instances where AS have larger fluxes than WSI, this might be explained by the effects of acidification on N dynamics in the soil, including higher content of NH_4^+ and delayed nitrification and/or denitrification.

Summarizing, for sandy loam soil, AS did not present significant differences from the WSI in 11 out of 15 dates. A difference in φNO_3^- values was detected between soils, with SS yielding higher values of φNO_3^- when compared to the SLS, most likely due to the differences in D due to each soils hydraulic properties.

5. Conclusions

The main conclusions of the work are presented next:

(a) Regarding the calibration and validation of the RZWQM2 model for both soils:

The RZWQM2 was calibrated against measured data regarding soil water content, drainage, soil temperature, nitrate flux and nitrous oxide emissions from the 2014-2015 wet season. The parameters soil water content at 10 kPa (field capacity), saturated hydraulic conductivity, organic matter partitioning coefficients and nitrogen transformation parameters where chosen for calibration. Posteriorly, the model was validated using independent data, measured during the wet seasons of 2012-2013, 2013-2014 (nitrate and nitrous oxide fluxes) and 2015-2016 (soil water content, drainage and soil temperature), being considered fit for further applications.

For the winter oats in the sandy soil system, the model predicted soil water content and drainage with efficiencies of 86 and 94 % respectively, while for temperature the modelling efficiency (EF) was 60 %. The modelling efficiency for nitrate fluxes below the root zone and nitrous oxide emissions to the atmosphere was 89 and 93% respectively. Additionally the root mean squared error (RMSE) of the simulations was lower than the average standard deviation of the measured values (MSD), as required. For the sandy loam system the calibrated model yielded EF values of 87, 94, 62, 76 and 85%, for the control variables soil water content, drainage, soil temperature, nitrate fluxes and nitrous oxide emissions, respectively. The RMSE of the simulations was always very close to MSD. The validation results were not as good as for the calibration due to the nature of the process itself. These results are in agreement with the ones obtained by other authors, concerning the soil water and N related processes modelling. The quality of the calibration and validation processes was similar for both soils regarding the water retention and movement, while for the N related processes was slightly higher for the sandy soil than for the sandy loam soil.

(b) Regarding the comparative analysis between both soils with respect to both path losses for NO_3^- leaching and N_2O emissions to the atmosphere and its relation with the soil water regimes and temperatures:

The resulting N emissions, φNO_3^- and φN_2O, for both soil systems were conceptually correct, as the magnitude of each flux was in accordance with the physical properties and water regimes of each soil.

With the sandy soil yielding larger values of φNO_3^- than sandy loam soil, considering the coarser nature and consequent higher values of drainage of the sandy soil and N leaching rate; while the sandy loam soil yielded higher φN_2O, which is expected if one takes into account the finer texture of this soil, having a higher chance of creating anaerobic conditions in the sandy

loam soil under water input events, and thus higher denitrification rate. The simulated T was quite similar between soils, which might intensified denitrification while slowing nitrification process.

(c) Regarding the scenario analysis for the prediction of the N losses under different hydrological years and a climatic change perspective using a 30 years' data series:

Averaging the four scenarios, from the very dry to the wet hydrological year, the contribution of the precipitation to evapotranspiration is 42 % higher for the SLS than for the SS. Drainage as a part of precipitation is 12.5 % lower for the SLS. The difference between soils is higher for the very dry and dry scenarios. For high amounts of precipitation both soils behave similarly in term of water loss out of the system, as if the increasing precipitation for the different scenarios was able to mask to some extent, the different hydraulic properties differences between both soils.

For the very dry scenario, there was a large accumulation of N in both soils, in association with to the low precipitation. Concerning N leaching, the sandy soil yielded higher values than the sandy loam, which is in agreement the hydraulic properties. The contribution of leaching increases for both soils from the very dry to the wet scenario while for the gas losses the opposite is verified. The average (for the 4 hydrological years) contribution of N leaching to the total losses is 84 and 68 % for the sandy soil and the sandy loam soil respectively, showing the SLS soil more sensitivity to the type of hydrological year.

A case of pollution swapping is observed as the scenario does from very dry to wet with the decrease of the N lost through gaseous emissions. These showed to be greatly affected by the differences in precipitation, which was compensated with the increases in the N losses through leaching. Also the contribution of the nitrification process to the N_2O emissions seems to increase as wetness increases, as denitrification originated N_2O decreases.

Overall, higher variations in the water and N balances were found for the sandy loam soil in association with the different hydrological years.

As to the scenarios using the projected values of average temperature increase released by IPCC, the results show that for this type of production systems the most unfavourable climate change scenario (temperature increase of 4 ºC) may produce an increase of 25 % and 18 % in the N gas loss contributions for the sandy loam soil and the sandy soil respectively. The increase in temperature intensified the process of NH_3 volatilization for both soils (more for SS) and of denitrification (more for SLS), while slowing nitrification process.

An example of pollution swapping is also observed for the climate change scenarios, with a decrease of N leaching, that is compensated by the increase of gaseous N emissions, due to the intensification of the processes responsible for these emissions.

(d) Regarding the nitrate fluxes determination for different slurry treatments:

NO_3^- leaching fluxes were also calculated for four different slurry management scenarios by combining predicted drainage fluxes and measures nitrate concentrations in the soil solution. The results were subject of a statistical analysis, namely an analysis of variance (KW test), with higher fluxes being observed for the SS when compared to SLS. The amount of precipitation for a give crop season appears to influence the differences between treatments, increasing the differences as the amount of rainfall increases.

Final conclusions

The model proved to be capable of being applied to the Portuguese reality, regarding the climate, soils and agricultural practices, for the analysis range of potential best management practices, aiming to comply with the existing EU policies. Nonetheless, the model is not a tool developed to be used directly by the farmers, as it is necessary for the researcher to work together with a technician, who will approach the farmers.

Although processes-based models like RZWQM2 can describe reality with a high level of accuracy, these models need calibration and validation, meaning that field data is always needed to test the model. However, after calibrating and validating the model, the posterior scenarios analysis no longer needs field work

Future study needs and perspectives

After doing this work, the necessity to improve the following model aspects remains:

- Make the soil thermal module more accessible to the user, in order to calibrate the soil thermal properties;
- Improve the plant parameterization in the Quickplant model;
- In-depth study of the N_2O emissions sub-model;

After that work it would be interesting to calibrate and validate the model for various typical production systems in Portugal and estimate the associated N emission factors.

References

Agostini, F., Tei, F., Silgram, M., Farneselli, M., Benincasa, P., & Aller, M. F. 2010. Decreasing nitrate leaching in vegetable crops with better N management. In Genetic Engineering, Biofertilisation, Soil Quality and Organic Farming (pp. 147-200). Springer Netherlands.

Ahmed, I., Rudra, R., McKague, K., Gharabaghi, B., & Ogilvie, J. 2007. Evaluation of the root zone water quality model (RZWQM) for Southern Ontario: Part I. Sensitivity analysis, calibration, and validation. Water Qual. Res. J. Canada, 42(3), 202-218.

Ahuja, L. R., K. E. Johnsen, and K. W. Rojas. 2000b. Water and chemical transport in soil matrix and macropores. In The Root Zone Water Quality Model, 13-50. L. R. Ahuja, K. W. Rojas, J. D. Hanson, M. J. Shaffer, and L. Ma, eds. Highlands Ranch, Colo.: Water Resources Publications.

Ahuja, L. R., K. W. Rojas, J. D. Hanson, M. J. Shaffer, and L. Ma, eds. 2000a. The Root Zone Water Quality Model. Highlands Ranch, Colo.: Water Resources Publications.

Ahuja, L. R., Naney, J. W., & Williams, R. D. 1985. Estimating soil water characteristics from simpler properties or limited data. Soil Science Society of America Journal, 49(5), 1100-1105.

Ahuja, L., Rojas, K., Hanson, J., Shaffer, M., & Ma, L. 2000. Modelling management effects on water quality and crop production. Colorado: Water Resources Publications, LLC.

Ahuja, L., Rojas, K., Hanson, J., Shaffer, M., Ma, L. (Eds.), 1999. RZWQM Modeling Management Effects on Water Quality and Crop Production. Water Resources Publications, LLC, CO, USA.

Al-Kanani T., MacKenzie A.F., Barthakur N.N. 1991 Soil water and ammonia volatilization relationships with surface-applied nitrogen fertilizer solutions. Soil Science Society of America Journal, 55, 1761–1766.

Amaro, S., Ribeiro, L., Paralta, E., & Cardoso Pinto, F. 2006. Aplicação de Efluentes de Suiniculturas como Fertilizantes na Agricultura: Impacto na Qualidade dos Meios Hídricos (Um caso de estudo em Santiago do Cacém, Alentejo). 8ª congresso da água. Figueira da Foz: Associação Portuguesa dos Recursos Hídricos.

Appel, T., & Mengel, K. 1990. Importance of organic nitrogen fractions in sandy soils, obtained by electro-ultrafiltration or CaCl2 extraction, for nitrogen mineralization and nitrogen uptake of rape. Biology and Fertility of Soils, 10(2), 97-101.

Bakhsh, A., Kanwar, R.S., & Karlen, D. 2005. Effects of liquid swine manure applications on NO3-N leaching losses to subsurface drainage water from loamy soils in Iowa. Agriculture, Ecosystems and Environment 109, pp. 118-128.

Ball, R., Keeney, D. R., Thoebald, P. W., & Nes, P. 1979. Nitrogen balance in urine-affected areas of a New Zealand pasture. Agronomy journal, 71(2), 309-314.

Bateman, E. J., & Baggs, E. M. 2005. Contributions of nitrification and denitrification to N2O emissions from soils at different water-filled pore space.Biology and Fertility of Soils, 41(6), 379-388.

Belnap, J. 2001. Factors influencing nitrogen fixation and nitrogen release in biological soil crusts. In Biological soil crusts: structure, function, and management (pp. 241-261). Springer Berlin Heidelberg.

Bengtsson, G., Bengtson, P., & Månsson, K. F. 2003. Gross nitrogen mineralization-, immobilization-, and nitrification rates as a function of soil C/N ratio and microbial activity. Soil Biology and Biochemistry, 35(1), 143-154.

Bicudo, J.R. 1999. A exploração leiteira compatível com o ambiente. Holstein 15:56-62.

Bishop, P. and Manning, M., 2010. Urea volatilisation: the risk management and mitigation strategies. Palmerston North, New Zealand: Fertilizer and Lime Research Centre, Massey University.

Black A.S., Sherlock R.R., Cameron K.C., Smith N.P., Goh K.M. 1985a Comparison of three field methods for measuring ammonia volatilization from urea granules broadcast on to pasture. Journal of Soil Science, 36, 271–280.

Black A.S., Sherlock R.R., Smith N.P. 1987 Effect of timing of simulated rainfall on ammonia volatilization from urea, applied to soil of varying moisture content. Journal of Soil Science, 38, 679–687.

Black A.S., Sherlock R.R., Smith N.P., Cameron K.C., Goh K.M. 1985b Effects of form of nitrogen, season, and urea application rate on ammonia volatilisation from pastures. New Zealand Journal of Agricultural Research, 28, 469–474.

Bouwman, A. F., Van der Hoek, K. W., & Olivier, J. G. J. 1995. Uncertainties in the global source distribution of nitrous oxide. Journal of Geophysical Research: Atmospheres, 100(D2), 2785-2800.

Boyer E.W. and Howarth R.H. (eds) 2002. The Nitrogen Cycles at Regional to Global Scales. Kluwer, New York.

Brooks, R. H., and A. T. Corey. 1964. Hydraulic properties of porous media. Hydrology Paper No. 3. Fort Collins, Colo.: Colorado State University.

Burford, J. R., & Bremner, J. M. 1975. Relationships between the denitrification capacities of soils and total, water-soluble and readily decomposable soil organic matter. Soil biology and biochemistry, 7(6), 389-394.

Bussink, D. W., Huijsmans, J. F. M., & Ketelaars, J. J. M. H. 1994. Ammonia volatilization from nitric-acid-treated cattle slurry surface applied to grassland.Netherlands Journal of Agricultural Science (Netherlands).

Cameira M.R., Pereira, A., Ahuja, L., Ma. L..2014 Sustainability and environmental assessment of fertigation in an intensive olive grove under Mediterranean conditions

Cameira, M., Fernando, R. A., & Pereira, L. 2005. Simulating the fate of water in field soil–crop environment. J. Hydrol. 315, 1-24.

Cameira, M.R. & Mota, M. 2016. Nitrogen related diffuse pollution from Horticulture Production. Horticulturae. In press

Cameira, M.R., Fernando, R.M., Ahuja, L.R., Ma, L., 2007. Using RZWQM to simulatethe fate of nitrogen in field soil–crop environment in the Mediterranean region.Agric. Water Manage. 90 (1), 121–136.

Cameron, K. C., Di, H. J., & Moir, J. L. 2013. Nitrogen losses from the soil/plant system: a review. Annals of Applied Biology, 162(2), 145-173.

Campbell, C. A., & Biederbeck, V. O. 1982. Changes in mineral N and numbers of bacteria and actinomycetes during two years under wheat-fallow in southwestern Saskatchewan. Canadian Journal of Soil Science, 62(1), 125-137.

Campbell, G. S. (1974). A simple method for determining unsaturated conductivity from moisture retention data. Soil science, 117(6), 311-314.

Carneiro, J., Coutinho, J., & Trindade, H. 2012. Nitrate leaching from a maize×oats double-cropping forage system fertilized with organic residues under Mediterranean conditions. Agriculture, Ecosystems and Environment, 29-39.

Carpenter, S. R. 2008. Phosphorus control is critical to mitigating eutrophication. Proceedings of the National Academy of Sciences, 105 (32), 11039-11040.

Carranca, C. 2000. Principais processos do ciclo do azoto numa agricultura sustentável. Avaliação através do marcador N, 15.

Celia, M. A., E. T. Bouloutaas, and R. L. Zarba. 1990. A general mass-conservative numerical solution for the unsaturated flow equation. Water Resources Res. 26(7): 1483-1496.

Chadwick, D., Sommer, S., Thorman, R., Fangueiro, D., Cardenas, L., Amon, B., & Misselbrook, T. 2011. Manure management: Implications for greenhouse gas emissions. Animal Feed Science and Technology 166-167, pp. 514-531.

Chen, X., Cui, Z., Fan, M., Vitousek, P., Zhao, M., Ma, W., ... & Deng, X. 2014. Producing more grain with lower environmental costs. Nature, 514(7523), 486-489.

Cordovil, C. 2004. Dinâmica do azoto na reciclagem de resíduos orgânicos aplicados ao solo. Alfragide: Instituto do Ambiente.

Coutinho-Mendes, J. F. 1989. A análise de terra. Limitações, correlação, calibração e interpretação dos resultados. UTAD, Vila Real, 51 p

Coutinho-Mendes, J. F. 1989. A análise de terra. Limitações, correlação, calibração e interpretação dos resultados. UTAD, Vila Real.

Crohn, D. 2004. Nitrogen mineralization and its importance in organic waste recycling. In Proceedings, National Alfalfa Symposium (pp. 13-5).

de Klein, C. A. M., & Van Logtestijn, R. S. P. 1996. Denitrification in grassland soils in the Netherlands in relation to irrigation, N-application rate, soil water content and soil temperature. Soil Biology and Biochemistry, 28(2), 231-237.

de Klein, C. A., Sherlock, R. R., Cameron, K. C., & van der Weerden, T. J. 2001. Nitrous oxide emissions from agricultural soils in New Zealand—a review of current knowledge and directions for future research. Journal of the Royal Society of New Zealand, 31(3), 543-574.

De Vries, D.A. 1963. Thermal properties of soils. p. 210–235. In W.R. van Wijk (ed.) Physics of plant environment. North-Holland Publishing Company, Amsterdam.

Del Grosso, S. J., Parton, W. J., Mosier, A. R., Ojima, D. S., Kulmala, A. E., & Phongpan, S. 2000. General model for N2O and N2 gas emissions from soils due to dentrification. Global Biogeochemical Cycles, 14(4), 1045-1060.

Di, H. J., & Cameron, K. C. 2002a. Nitrate leaching in temperate agroecosystems: sources, factors and mitigating strategies. Nutrient cycling in agroecosystems, 64(3), 237-256.

Di, H. J., & Cameron, K. C. 2003. Mitigation of nitrous oxide emissions in spray-irrigated grazed grassland by treating the soil with dicyandiamide, a nitrification inhibitor. Soil use and management, 19(4), 284-290.

Dobbie, K. E., & Smith, K. A. 2001. The effects of temperature, water-filled pore space and land use on N2O emissions from an imperfectly drained gleysol. European Journal of Soil Science, 52(4), 667-673.

Dobbie, K. E., McTaggart, I. P., & Smith, K. A. 1999. Nitrous oxide emissions from intensive agricultural systems: variations between crops and seasons, key driving variables, and mean emission factors. Journal of Geophysical Research: Atmospheres, 104(D21), 26891-26899.

DuBois, J. D., & Kapustka, L. A. 1983. Biological nitrogen influx in an Ohio relict prairie. American Journal of Botany, 8-16.

Erisman, J. W., Domburg, N., de Vries, W., Kros, H., de Haan, B., & Sanders, K. 2005. The Dutch N-cascade in the European perspective. Science in China Series C: Life Sciences, 48(2), 827-842.

Fang, Q.X., Malone, R.W., Ma, L., Jaynes, D.B., Thorp, K.R., Green, T.R., Ahuja, L.R., 2012.Modeling the effects of controlled drainage, N rate and weather on nitrate lossto subsurface drainage. Agric. Water Manage. 103, 150 – 161.

Fangueiro, D., Coutinho, J., Cabral, F., Fidalgo, P., Bol, R., & Trindade, H. 2012a. Nitric oxide and greenhouse gases emissions following the application of different cattle slurry particle size fractions to soil. Atmospheric Environment 47, 373-380.

Fangueiro, D., Ribeiro, H., Coutinho, J., Cardenas, L., Trindade, H., Cunha-Queda, C., Cabral, F. 2010c. Nitrogen mineralization and CO2 and N2O emissions in a sandy soil amended with original or acidified pig slurries or with the relative fractions. Biology and Fertility of Soils 46, pp. 383–391.

Fangueiro, D., Surgy, S., Coutinho, J., & Vasconcelos, E. 2013. Impact of cattle slurry acidification on carbon and nitrogen dynamics during storage and after soil incorporation. Journal of Plant Nutrition and Soil Science.- 000, pp. 1-11.

Flerchinger, G.N., R.M. Aiken, K.W. Rojas, and L.R. Ahuja. 2000. Development of the root zone water quality model (RZWQM) for over-winter conditions. Trans. ASAE 43:59–68.

Galloway, J. N., Cowling, E. B., Seitzinger, S. P., & Socolow, R. H. 2002. Reactive nitrogen: too much of a good thing?. AMBIO: A Journal of the Human Environment, 31(2), 60-63.

Granhall, U., & Selander, H. 1973. Nitrogen fixation in a subarctic mire.Oikos, 8-15.

Green, W. H., & Ampt, G. A. 1911. Studies on Soil Phyics. The Journal of Agricultural Science, 4(01), 1-24.

Grizzetti, B., Bouraoui, F., Billen, G., van Grinsven, H., Cardoso, A. C., Thieu, V., ... & Johnes, P. 2011. Nitrogen as a threat to European water quality.

Harper, L. A., Langdale, G. W., & Giddens, J. E. 1987. Nitrogen cycling in a wheat crop: soil, plant, and aerial nitrogen transport. Agronomy Journal, 79(6), 965-973.

Harris, R. F. 1981. Effect of water potential on microbial growth and activity.Water potential relations in soil microbiology, (waterpotentialr), 23-95.

Haynes R.J., Cameron K.C., Goh K.M., Sherlock R.R. 1986. Mineral Nitrogen in the Plant – Soil System. New York, NY, USA: Academic Press.

Haynes, R. J., & Sherlock, R. R. 1986. Gaseous losses of nitrogen. Mineral nitrogen in the plant-soil system, 242-302.

Honeycutt, H.D. and Metcalf, D.S. 1994. Linking nitrogen mineralization and plant nitrogen demand with thermal units. p. 49–80. In J.L. Havlin and J.S. Jacobsen (Ed.), Soil Testing: Prospects for Improving Nutrient Recommendation. Soil Sci. Soc. Amer., Madison, WI, USA.

Hoogenboom, G., J.W. Jones, P.W. Wilkens, C.H. Porter, W.D. Batchelor, L.A. Hunt, K.J. Boote, U. Singh, O. Uryasev, W.T. Bowen, A.J. Gijsman, A. du Toit, J.W. White, and G.Y. Tsuji. 2004. Decision Support System for Agrotechnology Transfer Version 4.0 [CD-ROM]. Univ. of Hawaii, Honolulu.

Hoogenboom, G., J.W. Jones, P.W. Wilkens, W.D. Batchelor, W.T. Bowen, L.A. Hunt, N.B. Pickering, U. Singh, D.C. Goldwin, B. Baker, K.J. Boote, J.T. Ritchie, and J.W. White. 1994. Crop models. p. 95–129. In G.Y. Tsuji et al. (ed.) DSSAT version 3, Vol. 2. Univ. of Hawaii, Honolulu

IPCC, 1995. Houghton JT et al (eds) Climate Change 1994: Radiative Forcing of Climate Change and an Evaluation of the IPCC IS92 Emission Scenarios. Cambridge Univ. Press, Cambridge.

IPCC, 2000. Special Report on Emissions Scenarios: A Special Report of Working Group III of the Intergovernmental Panel on Climate Change. [Nakicenovic, N., Swart, R. (Eds.)], Cambridge University Press, Cambridge.

IPCC, 2001. Synthesis report 2001: Contribution of Working Groups I, II, and III to the Third Assessment Report of the Intergovernmental Panel on Climate Change. [Watson, R.T., Core Writing Team (Eds.)], Cambridge University Press, Cambridge, 184p.

IPCC, 2007a. Climate Change 2007: The Physical Science Basis. Contribution of Working Group I to the Fourth Assessment Report of the Intergovernmental Panel on Climate Change. [Solomon, S., Qin, D., Manning, M., Chen, Z., Marquis, M., Averyt, K.B., Tignor, M., Miller, H.L. (Eds.)] Cambridge University Press, Cambridge, United Kingdom and New York, NY, USA.

Jenkinson, D. S. 2001. The impact of humans on the nitrogen cycle, with focus on temperate arable agriculture. Plant and Soil, 228(1), 3-15.

Jones, J.W., G. Hoogenboom, C.H. Porter, K.J. Boote, W.D. Batchelor, L.A. Hunt, P.W. Wilkens, U. Singh, A.J. Gijsman, and J.T. Ritchie. 2003. The DSSAT cropping system model. Eur. J. Agron. 18:235–265.

Khalil, W., & Dombre, E. 2004. Modeling, identification and control of robots. Butterworth-Heinemann.

Killham, K., Amato, M., & Ladd, J. N. 1993. Effect of substrate location in soil and soil pore-water regime on carbon turnover. Soil Biology and Biochemistry, 25(1), 57-62

Knobeloch, L., Salna, B., Hogan, A., Postle, J., & Anderson, H. 2000. Blue babies and nitrate-contaminated well water. Environmental Health Perspectives, 108(7), 675.

Kokkonen, A., Esala, M., & Aura, E. 2006. Acceleration of N mineralization by release of enzymes and substrates from soil mineral particles with phosphates. Soil Biology & Biochemistry 38, 504-508.

Kool, D. M., Müller, C., Wrage, N., Oenema, O., & Van Groenigen, J. W. 2009. Oxygen exchange between nitrogen oxides and H 2 O can occur during nitrifier pathways. Soil Biology and Biochemistry, 41(8), 1632-1641.

Kozak, J.A., R. Aiken, G.N. Flerchinger, D.C. Nielsen, L. Ma, and L.R. Ahuja. 2007. Quantifying residue architecture effects on soil temperature and water. Soil Tillage Res. 95:84–96.

Kruskal, W. H., & Wallis, W. A. 1952. Use of ranks in one-criterion variance analysis. Journal of the American statistical Association, 47 (260), 583-621.

Lakanen, E., & Ervio, R. 1971. Comparison of eight extractants for the determination of plant available micronutrients in soils. Acta Agr. Fenn, 123, 223-232.

Laura, R. D. 1977. Salinity and nitrogen mineralization in soil. Soil Biology and Biochemistry, 9(5), 333-336.

Legates, D.R., and G.J. McCabe. 1999. Evaluating the use of “goodness-of-fit” measures in hydrologic and hydroclimatic model validation. Water Resour. Res. 35:233–241.

Loague, K., & Green, R. E. 1991. Statistical and graphical methods for evaluating solute transport models: overview and application. Journal of contaminant hydrology, 7(1), 51-73.

Ma, L., Ahuja, L. R., Saseendran, S. A., Malone, R. W., Green, T. R., Nolan, B. T., & Hoogenboom, G. 2011. A protocol for parameterization and calibration of RZWQM2 in field research . Methods of introducing system models into agricultural research, 1-64.

Ma, L., Ahuja, L.R., Nolan, B.T., Malone, R.W., Trout, T.J., Qi, Z., 2012. Root Zone WaterQuality Model (RZWQM2): model use, calibration and validation. Trans. ASABE55, 1425–1446

Martins, M. 2014. Dinâmica do Azoto em Solos Fertilizados com Chorume de Bovino Tratado. Dissertação de mestrado. Instituto Superior de Agronomia

Melo e Abreu, J. P.; Pereira, L. P. 2010. Impactos e vulnerabilidade da agricultura resultantes das alterações climáticas

Miola, E.C., Rochette, P., Chantigny, M.H., Angers, D.A., Aita, C., Gasser, M.O., Pelster, D.E. and Bertrand, N., 2014. Ammonia volatilization after surface application of laying-hen and broiler-chicken manures. Journal of environmental quality, 43(6), pp.1864-1872.

Monaghan, R. M., & Barraclough, D. 1992. Some chemical and physical factors affecting the rate and dunamics of nitrification in urine-affected soil.Plant and Soil, 143(1), 11-18.

Monteith, J.L., 1965. Evaporation and environment. Symp. Soc. Exp. Biol. 19, 205–234.

Mosier, A. R., Guenzi, W. D., & Schweizer, E. E. 1986. Soil losses of dinitrogen and nitrous oxide from irrigated crops in northeastern Colorado. Soil Science Society of America Journal, 50(2), 344-348.

Mosier, A. R., Syers, J. K., & Freney, J. R., 2004. Nitrogen fertilizer: an essential component of increased food, feed, and fiber production (Vol. 65, pp. 3-15). Island Press. Scientific Committee on Problems of the Environment (SCOPE) Series.

Mosier, A., Kroeze, C., Nevison, C., Oenema, O., Seitzinger, S., & Van Cleemput, O. 1998. Closing the global N2O budget: nitrous oxide emissions through the agricultural nitrogen cycle. Nutrient cycling in Agroecosystems,52(2-3), 225-248.

Mulvaney, R. 1996. Nitrogen: inorganic forms. In Methods of Soil Analysis, Part 3: Chemical Methods (pp. 1129-1139). USA: Soil Science Society of America.

Nacry, P., Bouguyon, E., & Gojon, A. (2013). Nitrogen acquisition by roots: physiological and developmental mechanisms ensuring plant adaptation to a fluctuating resource. Plant and Soil, 370(1-2), 1-29.

Nash III, T. H. 1996. Nitrogen, its metabolism and potential contribution to ecosystems. Lichen biology. Cambridge University Press, Cambridge, 121-135.

Nicolardot, B., Mary, B., Houot, S., & Recous, S. 1997. [Nitrogen dynamics in cultivated soils]. Colloques de l'INRA (France).

Nimah, M., and R. J. Hanks. 1973. Model for estimating soilwater-plant-atmospheric interrelation: I. Description and sensitivity. SSSA Proc. 37(4): 522-527.

Oenema, O., Bleeker, A., Braathen, N. A., Budnakova, M., Bull, K., Cermak, P., ... & Leip, A. 2011. Nitrogen in current European policies.

Parry, M. L., Canziani, O. F., Palutikof, J. P., van der Linden, P. J., & Hanson, C. E. (2007). IPCC, 2007: climate change 2007: impacts, adaptation and vulnerability. Contribution of working group II to the fourth assessment report of the intergovernmental panel on climate change.

Parton, W. J., Holland, E. A., Del Grosso, S. J., Hartman, M. D., Martin, R. E., Mosier, A. R., ... & Schimel, D. S. 2001. Generalized model for NO x and N2O emissions from soils. Journal of Geophysical Research: Atmospheres,106(D15), 17403-17419.

Parton, W. J., Mosier, A. R., Ojima, D. S., Valentine, D. W., Schimel, D. S., Weier, K., & Kulmala, A. E. 1996. Generalized model for N2 and N2O production from nitrification and denitrification. Global biogeochemical cycles,10(3), 401-412.

Pohlert, T. 2014. The pairwise multiple comparison of mean ranks package (PMMR). R package.

Portaria nº 631/2009 de 9 de Junho de 2009 - 1.ª série — N.º 111. MINISTÉRIO DO AMBIENTE, DO ORDENAMENTO DO TERRITÓRIO E DO DESENVOLVIMENTO REGIONAL E DA AGRICULTURA, DO DESENVOLVIMENTO RURAL E DAS PESCAS.

Prosser J.I. 2007. The ecology of nitrifying bacteria. In Biology of the Nitrogen Cycle, pp. 223–244. Eds H. Bothe, S.J. Ferguson andW.E. Newton. Amsterdam, the Netherlands: Elsevier.

Rabot, E., Cousin, I., & Hénault, C. 2015. A modeling approach of the relationship between nitrous oxide fluxes from soils and the water-filled pore space. Biogeochemistry, 122(2-3), 395-408.

Rawls, W.J., D.L. Brakensiek, and K.E. Saxton. 1982. Estimation of soil water properties. Trans. ASAE 25:1316–1320, 1328.

Rhoades, J.D., N.A. Manteghi, P.J. Shouse, W.J. Alves. 1989. Soil electrical conductivity and soil salinity: New formulations and calibrations. Soil Sci. Soc. Am. J., 53:433-439.

Rocha, C. 2007. Desenvolvimento de um sistema integrado de gestão de resíduos de natureza. Dissertação de Mestrado. Universidade de Aveiro.

Ryden, J. C. 1986. Gaseous losses of nitrogen from grassland. Nitrogen fluxes in intensive grassland systems, 59-73.

Sadeghpour, A., Hashemi, M., Weis, S.A., Spargo, J.T., Mehrvarz, S. and Herbert, S.J., 2015. Assessing tillage systems for reducing ammonia volatilization from spring-applied slurry manure. Communications in Soil Science and Plant Analysis, 46(6), pp.724-735

Schepers, J. S., & Mosier, A. R. 1991. Accounting for nitrogen in nonequilibrium soil-crop systems. Managing nitrogen for groundwater quality and farm profitability, (managingnitroge), 125-138.

Schlesinger, W. H. 1991. Biogeochemistry: an analysis of global change. Academic Press, San Diego, California, USA.

Scholefield, D., Tyson, K. C., Garwood, E. A., Armstrong, A. C., Hawkins, J., & Stone, A. C. 1993. Nitrate leaching from grazed grassland lysimeters: effects of fertilizer input, field drainage, age of sward and patterns of weather.Journal of Soil Science, 44(4), 601-613.

Shaffer, M. J., K. W. Rojas, D. G. DeCoursey, and C. S. Hebson. 2000a. Nutrient chemistry processes: OMNI. In The Root Zone Water Quality Model, 119-144. L. R. Ahuja, K. W. Rojas, J. D. Hanson, M. J. Shaffer, and L. Ma, eds. Highlands Ranch, Colo.: Water Resources Publications.

Shaffer, M. J., K. W. Rojas, D. G. DeCoursey, and C. S. Hebson. 2000a. Nutrient chemistry processes: OMNI. In The Root Zone Water Quality Model, 119-144. L. R. Ahuja, K. W. Rojas, J. D. Hanson, M. J. Shaffer, and L. Ma, eds. Highlands Ranch, Colo.: Water Resources Publications.

Shaffer, M.J., K.W. Rojas, D.G. DeCoursey, and C.S. Hebsen. 2000. Nutrient chemistry processes–OMNI. p. 119–144. In L.R. Ahuja et al. (ed.) The Root Zone Water Quality Model. Water Resources Publ., Highlands Ranch, CO.

Shaffer, M.J., K.W. Rojas, D.G. DeCoursey, and C.S. Hebsen. 2000. Nutrient chemistry processes–OMNI. p. 119–144. In L.R. Ahuja et al. (ed.) The Root Zone Water Quality Model. Water Resources Publ., Highlands Ranch, CO.

Shuttleworth, W.J., Wallace, J.S., 1985. Evaporation from sparse crops—an energy combination approach. Q. J. R. Meterol. Soc.111, 839–855.

Smil, V. 2000. Feeding the World Challenge for the 21st Century The MIT Press, Cambridge, MA.

Smil, V., 2001. Enriching the Earth Fritz Haber, Carl Bosch and the Transformation of World Agriculture The MIT Press, Cambridge, MA.

Smith K.A., McTaggart I.P., Tsuruta H., Smith K. 1997. Emissions of N2O and NO associated with nitrogen fertilization in intensive agriculture, and the potential for mitigation. Soil Use and Management, 13, 296–304.

Smith, V. H., & Schindler, D. W. 2009. Eutrophication science: where do we go from here?. Trends in Ecology & Evolution, 24(4), 201-207.

Sommer S.G., Schjoerring J.K., Denmead O.T. 2004. Ammonia emission from mineral fertilizers and fertilized crops. Advances in Agronomy, 82, 558–622.

Sommer, S. G., & Olesen, J. E. 1991. Effects of dry matter content and temperature on ammonia loss from surface-applied cattle slurry. Journal of Environmental Quality, 20(3), 679-683.

Sommer, S. G., Schjoerring, J. K., & Denmead, O. T. 2004. Ammonia emission from mineral fertilizers and fertilized crops. Advances in agronomy,82, 557-622.

Stanford, G., Frere, M. H., & Schwaninger, D. H. 1973. Temperature coefficient of soil nitrogen mineralization. Soil Science, 115(4), 321-323.

Stevens, C. J., & Quinton, J. N. 2009. Diffuse pollution swapping in arable agricultural systems. Critical Reviews in Environmental Science and Technology, 39(6), 478-520.

Stevenson, F. J. 1982. Organic forms of soil nitrogen. Nitrogen in agricultural soils, (nitrogeninagrics), 67-122.

Tedesco, S., 2013. Avaliação das práticas de gestão da rega e da fertilização nas hortas urbanas de Lisboa: Experimentação e modelação. Contributo para uma agricultura urbana ambientalmente sustentável. Dissertação de mestrado. Instituto Superior de Agronomia

Thomson A.J., Giannopoulos G., Pretty J., Baggs E.M., Richardson D.J. 2012. Biological sources and sinks of nitrous oxide and strategies to mitigate emissions. Philosophical Transactions of the Royal Society of London. Series B, Biological Sciences, 367, 1157-1168.

Tisdale, S. L., Nelson, W. L., & Beaton, J. D. 1985. Soil fertility and fertilizers. Collier Macmillan Publishers.

Velthof, G., & Oenema, O. 1993. Nitrous oxide flux from nitric-acid treated cattle slurry applied to grassland under semi-controled conditions. Netherlands Journal of Agricultural Science 41, pp. 81-93.

Warrick, A. W., Mullen, G. J., & Nielsen, D. R. 1977. Scaling field-measured soil hydraulic properties using a similar media concept. Water Resources Research, 13(2), 355-362.

Whitehead D.C., Raistrick N. 1990. Ammonia volatilization from five nitrogen compounds used as fertilizers following surface application to soils. Journal of Soil Science, 41, 387–394.

Wilcox, B. P., Rawls, W. J., Brakensiek, D. L., & Wight, J. R. 1990. Predicting runoff from rangeland catchments: a comparison of two models.Water Resources Research, 26(10), 2401-2410.

Wild, A., & Cameron, K. C. 1980. Nitrate leaching through soils and environmental considerations with special reference to recent work in the United Kingdom. In Soil nitrogen as fertilizer or pollutant.

WMO, 2013. Planning water quality monitoring systems. World meteorological organization, Switzerland.

Youssef, M.A., Skaggs, R.W., Chescheir, G.M., Gilliam, J.W., 2006. Field evaluation ofa model for predicting nitrogen losses from drained lands. J. Environ. Qual. 35(6), 2026–2042.

Zak, D. R., Holmes, W. E., MacDonald, N. W., & Pregitzer, K. S. 1999. Soil temperature, matric potential, and the kinetics of microbial respiration and nitrogen mineralization. Soil Science Society of America Journal, 63(3), 575-584.

Zaman, M., Saggar, S., Blennerhassett, J. D., & Singh, J. 2009. Effect of urease and nitrification inhibitors on N transformation, gaseous emissions of ammonia and nitrous oxide, pasture yield and N uptake in grazed pasture system. Soil Biology and Biochemistry, 41(6), 1270-1280.

Appendices

Appendix 1

Nitrogen cascade model (from UNEP, 2004)

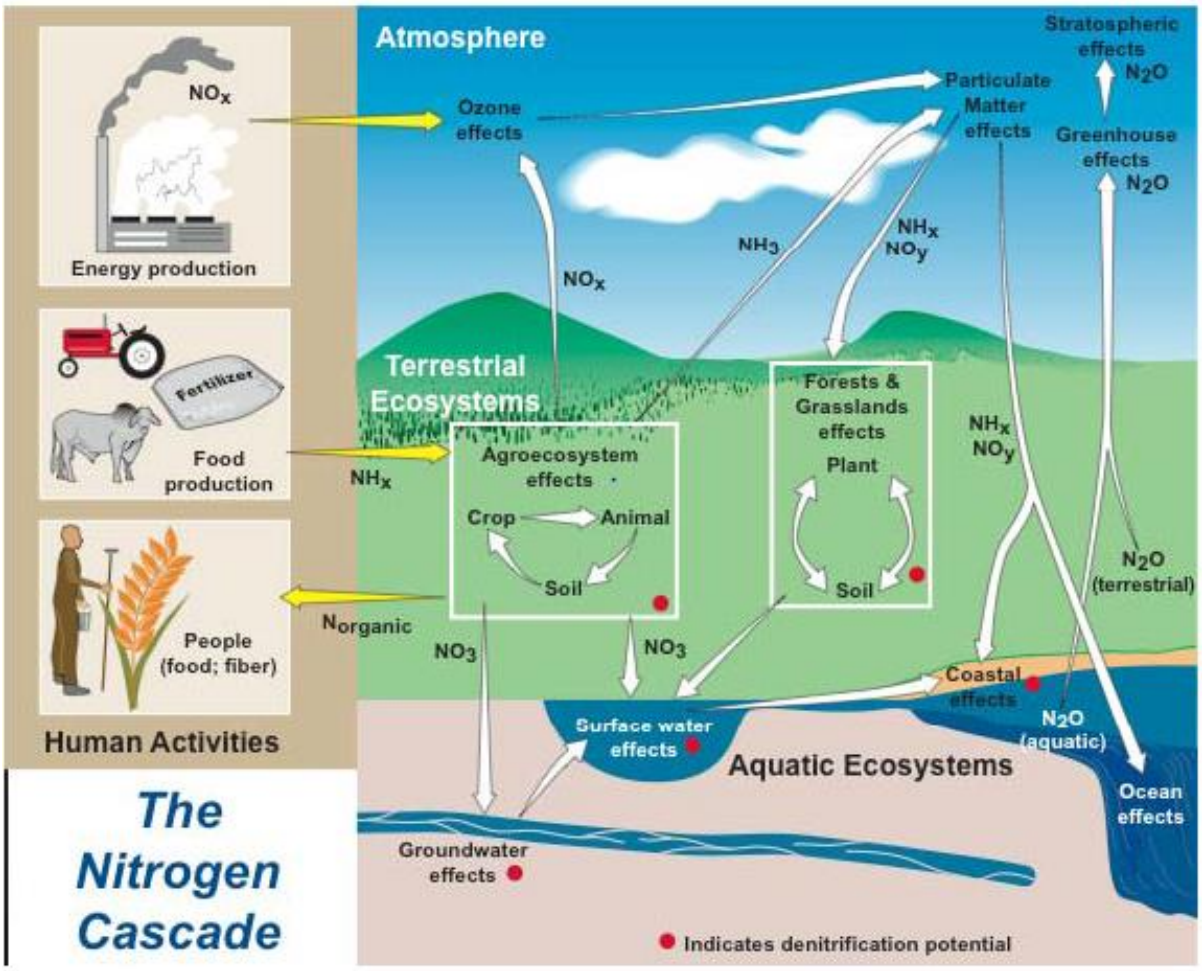

Appendix 2

Nitrate flux means comparison tables for sandy and sandy loam soil

2012-2013

DOY	Days after slurry application	Sandy soil					Sandy loam soil				
		AWSM	AWSS	CTR	WSI	WSM	AWSM	AWSS	CTR	WSI	WSM
312	3	0.23 a	0.54 a b	0.24 a	0.59 b	0.64 b	0.25 a	0.82 b	0.12 c	0.1 c	0.38 a b
330	21	4.31 a	5.47 a b	1.02 a	7.98 b	6.97 b	0.25 a	1.04 b	0.15 a	0.37 c	0.4 c
339	30	1.15 a	0.16 b	0.14 b	0.49 c	0.79 a c	0.18 a	0.29 a	0.22 a	0.18 a	0.23 a
350	41	2.55 a	5.36 a b	0 c	15.17 b	0.31 c	1.19 a b	1.53 a c	0.12 b	3.23 c	1.28 a b
386	77	1.26 a	6.38 b	0.01 c	2.6 d	0.59 e	2.46 a c	2.57 a c	0.31 b	2.92 a	1.15 b c

2013-2014

DOY	Days after slurry application	Sandy soil					Sandy loam soil				
		AWSM	AWSS	CTR	WSI	WSM	AWSM	AWSS	CTR	WSI	WSM
364	48	0.28 a	0.49 a	0.02 a	0.24 a	0.22 a	0.03 a	0.12 a	0.16 a	0.13 a	0.01 a
372	56	3.68 a b	6.85 a	0.57 b	3.9 a b	1.49 a b	1.41 a	1.22 a	0.43 a	2.9 a	1.08 a
378	62	0.35 a c	1.01 a	0 b	0.53 a c	0.09 b c	0.85 a	0.59 a	0.16 a	0.77 a	1.09 a
386	70	0.19 a b	1.65 a	0.01 b	0.34 a	0.06 a b	1.56 a	1.01 a b	0.22 b	0.74 b c	1.24 a c
406	90	0.09 a	0.62 a	0.06 a	0.05 a	0.04 a	2.32 a	1.51 a b	0.12 c	0.34 c d	0.44 b d

DOY	Days after slurry application	2014-2015									
		Sandy soil					**Sandy loam soil**				
		AWSM	AWSS	CTR	WSI	WSM	AWSM	AWSS	CTR	WSI	WSM
318	10	0.07 a	0.08 a	0.5 a	0.12 a	0.73 a	0 a	0 a	0 a	0.03 a	0.02 a
322	14	0.49 a	0.34 a	0.16 a	0.54 a	0.6 a	0.06 a	0 a	0.02 a	0.02 a	0.18 a
325	17	2.2 a	2.96 a	0.4 a	2.68 a	2.69 a	0.81 a	0.19 a	0.37 a	2.01 a	1.17 a
330	22	0.33 a	0.41 a	0.03 a	0.46 a	0.12 a	0.26 a	0.06 a	0.07 a	0.38 a	0.36 a
386	78	0.01 a	0.02 a	0 a	0.02 a	0.01 a	0.7 a	0.36 a	0.07 a	0.34 a	0.53 a